Antiferroelectric liquid crystals: Interplay of simplicity and complexity

Hideo Takezoe*

Department of Organic and Polymeric Materials, Tokyo Institute of Technology, O-okayama, Meguro-ku, Tokyo 152-8552, Japan

Ewa Gorecka†

Department of Chemistry, Warsaw University, Al. Zwirki i Wigury 101, 02-089 Warsaw, Poland

Mojca Čepič‡

Jozef Stefan Institute, Jamova 39, 1000 Ljubljana, Slovenia and Faculty of Education, University of Ljubljana, Kardeljeva pl 16, 1000 Ljubljana, Slovenia

(Published 23 March 2010)

This paper reviews nearly 20 years of research related to antiferroelectric liquid crystals and gives a short overview of possible applications. "Antiferroelectric liquid crystals" is the common name for smectic liquid crystals formed of chiral elongated molecules that exhibit a number of smectic (Sm) tilted structures with variation of the strong-tilt azimuthal direction from layer to layer (i.e., nonsynclinic structures). The phases have varying crystallographic unit periodicity from a few (SmC^*_α), four (SmC^*_{FI2}), three (SmC^*_{FI1}), and two (SmC^*_A) smectic layers and all of the phases possess liquidlike order inside the layer. The review describes the discovery of these phases and various methods used for their identification and to determine their structures and their properties. A theoretical description of these systems is also given; one of the models—the discrete phenomenological model—of antiferroelectric liquid crystals is discussed in detail as this model allows for an explanation of phase structures and observed phase sequences under changes of temperature or external fields that is most consistent with experimental results.

DOI: 10.1103/RevModPhys.82.897 PACS number(s): 61.30.Dk, 42.70.Df, 42.79.Kr

CONTENTS

*takezoe.h.aa@m.titech.ac.jp
†gorecka@chem.uw.edu.pl
‡mojca.cepic@ijs.si

I. INTRODUCTION

Liquid crystals are now indispensable materials for flat panel displays. However, the discovery of this class of materials was made only 120 years ago (Kelker, 1988). Since then, a variety of phases has been discovered, and even recently new phases have been found and charac-

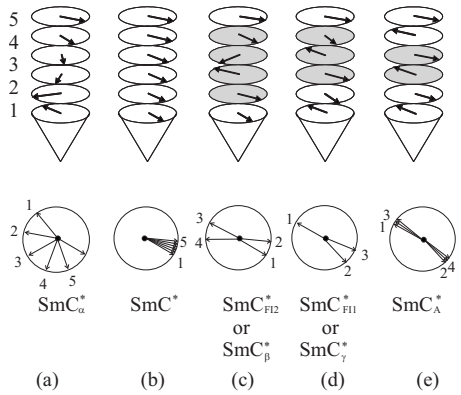

FIG. 1. Schematic illustration of molecular ordering in structures of (a) SmC^*_α, (b) SmC*, (c) SmC^*_{FI2}, (d) SmC^*_{FI1}, and (e) SmC^*_A phases, which emerge as temperature decreases.

terized. Thus, liquid crystals are not only useful for practical application but also a rich source for the study of physics and chemistry of soft matter.

The formation of liquid crystalline structures, particularly the nematic phase, is naively explained by an electrostatic attractive force, i.e., the van der Waals interaction, and a repulsive force, i.e., the excluded volume effect (Chandrasekhar, 1977; de Gennes and Prost, 1993). For rodlike or disklike molecules, these interactions lead to the nematic phase, where the long axes of the rodlike molecules and the disk normal of the disklike molecules orient on average toward a particular direction called the *director*. However, one cannot describe the antiferroelectric (AF) and ferrielectric phases, in which molecules form layered structures with complex director changes from layer to layer, by these basic interactions only. The structures that we discuss are shown in Fig. 1. As the temperature is lowered, the phases usually observed are (a) the SmC^*_α phase which has a short pitch, (b) the conventional ferroelectric SmC* phase, (c) the SmC^*_{FI2} and (d) the SmC^*_{FI1} phases with unit cells of four and three layers, respectively, and (e) the antiferroelectric SmC^*_A phase. The purpose of this review is to summarize the current knowledge about the antiferroelectric and ferrielectric phases, describing how these structures are experimentally identified and how the formation of and transitions between these structures are theoretically explained.

For the system to be ferroelectric it is necessary to have sufficiently low symmetry at least C_n or C_{nv} (see Fig. 2). Why? If the symmetry is $C_{\infty h}$ as for the nonpolar SmA phase, the uniaxial molecules, described as simple rods (Fig. 2, upper right), are free to rotate around their long axes. This rotation does not allow for polar order of dipoles in the smectic plane (transverse polarization). Moreover, the horizontal mirror plane symmetry, if it exists in the system, does not allow for polar order of dipoles in the direction perpendicular to the smectic plane (longitudinal polarization). Therefore such systems cannot be polar. Polar properties cannot appear even in a system of biaxial lathlike molecules, which reduces the symmetry to C_{2h} (Fig. 2, top middle), because

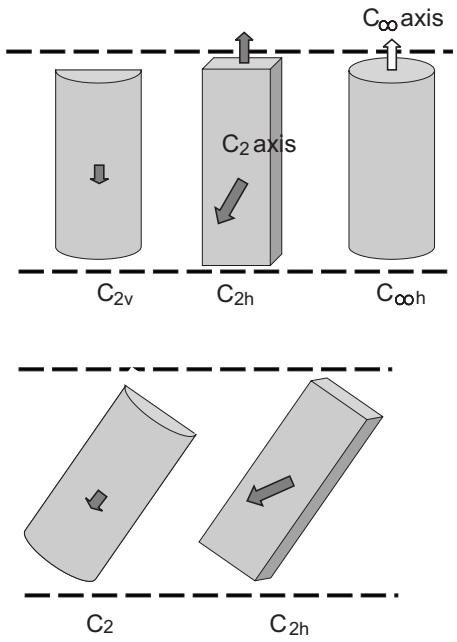

FIG. 2. Simple illustration of realization of C_n and C_{nv} symmetries necessary for polar systems in nontilted (top) and tilted (bottom) smectic phases.

the orientation of transverse molecular dipole moments is symmetrically distributed around the C_2 axis. However, the phase structure can be macroscopically polar if it has C_{2v} symmetry. This can be realized, for example, in a smectic formed of nontilted "half rods" (Fig. 2, left) or in a smectic with C_2 symmetry if half rods are additionally tilted from the layer normal. In both cases the C_2 axis prevents longitudinal polarization but transverse (in-plane) polarization can exist. In liquid crystals, reduction of the symmetry is necessary to obtain polar properties—C_{2v} symmetry is obtained in a nontilted smectic made of bent-core molecules (Niori *et al.*, 1996) and C_2 symmetry is realized if a SmC phase is formed of chiral molecules since chirality removes the mirror plane in the system (Meyer *et al.*, 1975). The actual value of the electric polarization depends on the hindrance of rotation around the long molecular axis.

Polar properties can be found in other systems as well. Even in diskotic columnar phases, the introduction of chirality works in a similar way as in the tilted chiral smectic phases. Scherowsky and Chen (1994) and Bock and Helfrich (1995) obtained a helical diskotic columnar phase and found a ferroelectric switching between two states with uniformly tilted disks with respect to the direction of the column. The second possibility of introducing polar properties by changing the shape of the molecules from disklike to conical was also studied (Gorecka *et al.*, 2004; Kishikawa *et al.*, 2005; Takezoe *et al.*, 2006). Bent-core liquid crystals are also typical examples of systems with low symmetry. In many bent-core smectic phases, the bent core lowers the symmetry of the system to C_{2v} by preventing free rotation about the long axis (Niori *et al.*, 1996). It is worth mentioning that for these systems formed of molecules with bent

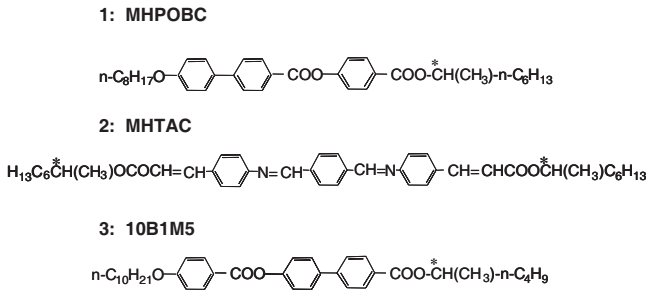

FIG. 3. Chemical structures of important compounds in which the antiferroelectric phase was identified early.

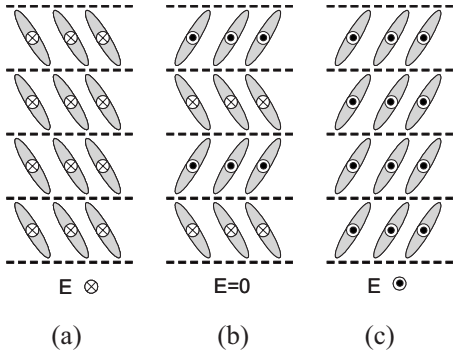

FIG. 4. The local molecular arrangements of (b) the antiferroelectric phase and (a) the positive and (c) negative electric-field-induced ferroelectric phases.

cores, phases with C_1 symmetry are also possible; for these, polarization is not constrained to any specific direction (Jákli *et al.*, 2001; Bailey and Jákli, 2007; Gorecka *et al.*, 2008).

In the above examples of smectic phases, the polarization direction is perpendicular to the molecular long axis, except in the phases with local C_1 symmetry. In the uniaxial nematic phase, however, the polar direction must be parallel to the director because of the free rotation of molecules about their long axis. Therefore, it is much more difficult to realize polar order in the nematic phase. Two examples have been reported so far, i.e., polypeptides (Yen *et al.*, 2006) and aromatic polyesters (Koike *et al.*, 2007). In both cases, the dipole-dipole interaction between rigid organizations of sequential dipoles seems to be the origin of the polar order (Terentjev *et al.*, 1994). In this sense, these ferronematic phases are proper ferroelectrics, for which spontaneous polarization appears as a consequence of dipole-dipole interactions and which have never been realized in other liquid crystalline phases.

II. DISCOVERY OF ANTIFERROELECTRIC AND FERRIELECTRIC LIQUID CRYSTAL PHASES

A. Toward the discovery of the antiferroelectric phase

The ferroelectric SmC* phase was discovered by Meyer (Meyer *et al.*, 1975; Meyer, 1977) on the basis of elegant symmetry considerations. Because of the possible application to fast displays, extensive studies have been conducted from the physics, chemistry, and engineering viewpoints. During this course of studies, at least three groups noticed peculiar behaviors in their individual materials. However, it has taken a long time to understand that these peculiarities can be attributed to in the antiferroelectric phase. This was probably because of a common wisdom for liquid crystals, namely, "molecules in liquid crystal tend to align parallel to each other."

The materials in which the three groups found the antiferroelectric phase are listed in Fig. 3: 4-(1-methylheptyloxycalbonyl)phenyl 4′-octyloxybiphenyl-4-carboxylate (MHPOBC) (Inukai *et al.*, 1985), 1-methylheptyl-terephthalidene-bis-aminocinnamate (MHTAC) (Levelut *et al.*, 1983), and (R)- and (S)-1-methylpentyl 4′-(4″-*n*-decyloxybenzoyloxy) biphenyl-4-carboxylates (Goodby and Chin, 1988). All these compounds were synthesized rather a long time ago before the identification of the antiferroelectric phase structure and were recognized as new ferroelectric liquid crystal (FLC) materials. The MHPOBC compound was first reported in 1985 by Inukai *et al.* (1985). In the first international conference on ferroelectric liquid crystals (FLC87) in Arcachon, France, two groups pointed out unusual behaviors in this compound. Hiji *et al.* (1988) reported a third stable state exhibiting a dark view between crossed polarizers when one of the polarizers is parallel to the smectic layer. Furukawa *et al.* (1988) reported a very small dielectric constant and a threshold behavior in the electro-optic response in the lower-temperature region of SmC*, suggesting a new phase SmY*. It is now clear that these experimental facts unambiguously indicated the structure called the herringbone or antiferroelectric structure, where molecules in neighboring layers are tilted in opposite directions. In this phase the antiparallel or *anticlinic* molecular tilt in adjacent layers results in the structure showing light extinction between crossed polarizers along the layer normal and an electric-field-induced transition to the ferroelectric structure with a threshold and extinction direction inclined from the layer normal, as shown in Fig. 4.

An MHTAC analog was first synthesized in 1976, and MHTAC first appeared in the literature in 1983 (Levelut *et al.*, 1983). Phase identification was attempted based on texture observation (mainly), miscibility tests, and x-ray analysis. Detailed experiments gave many hints of the antiferroelectric structure. For instance, some observed many 1/2 disclination defects, which were later recognized as characteristic for an antiferroelectric structure. Unfortunately, they could not establish the phase structure. The antiferroelectric structure of this material was first reported at the Second International Conference on FLCs (1989, Göteborg) (Galerne and Liebert, 1989). At the same conference, Takezoe *et al.* also reported the antiferroelectricity of MHPOBC (Takezoe, Chandani, Gorecka, *et al.*, 1989; Takezoe, Chandani, Lee, *et al.*, (1989).

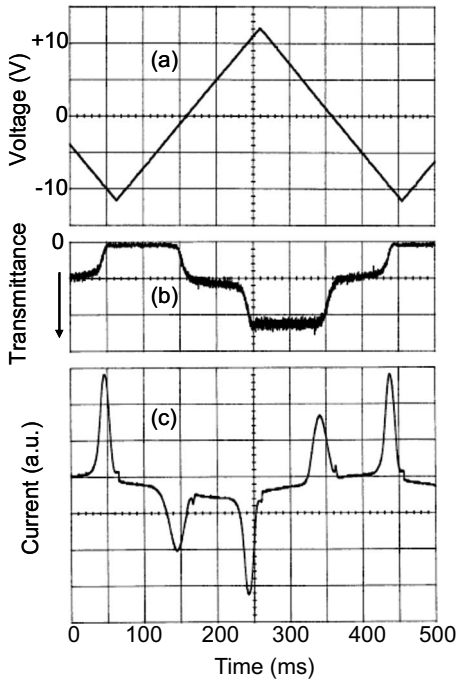

FIG. 5. Transmittance change and switching current observed by applying a triangular-wave voltage to MHPOBC. Note that two changes in the transmittance and two current peaks are observed at the same voltages. From Chandani *et al.*, 1988.

Goodby and Chin (1988) synthesized (R)- and (S)-1-methylpentyl 4′-(4″-*n*-decyloxybenzoyloxy)biphenyl-4-carboxylates in 1988 and reported the phase behavior without noticing the existence of the antiferroelectric phase in these compounds. They actually found two distinct phases below the ferroelectric SmC* phase and noted the influence of racemization on the phase sequence. They suggested several phase structures such as SmI*-like or SmF*-like, depending on optical purity, and simply SmC* phases with different senses of the helical modulation. Finally they reported that these two phases are actually ferrielectric and antiferroelectric (SmC^*_A) phases (Goodby *et al.*, 1992).

The proposal for the application of antiferroelectric liquid crystals in display devices was made in 1988 before the phase identification, because of their tristable switching with a sharp threshold and double hysteresis (Chandani *et al.*, 1988). The tristable switching is observable by two methods: the electro-optic effect and switching current measurements. These results are shown in Fig. 5 (Chandani *et al.*, 1988). The transmittance showed three stable states under the application of a triangular-wave voltage, and two switching current peaks appeared when sharp transmittance changes occurred between the tristable states. Figure 6 shows the apparent tilt angle as a function of a dc electric field (Chandani *et al.*, 1988). The apparent tilt angle is zero in the absence of the field and shows sharp changes to finite positive and negative angles with thresholds and hysteresis, as reported at the First International FLC Conference in 1987 by Hiji *et al.* (1988) and Furukawa *et al.* (1988). Clearly, a switching device could be made by utilizing the threshold and the

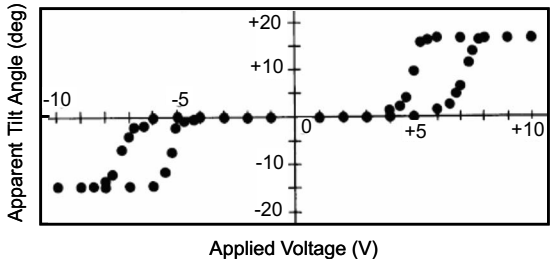

FIG. 6. Apparent tilt angle in MHPOBC under the application of dc electric voltages. Double hysteresis loop is observed. From Chandani *et al.*, 1988.

hysteresis. Actually, Chandani *et al.* demonstrated the electro-optic performance: transmittance changes on application of positive and negative pulses superposed on a biased voltage, as shown in Fig. 7 (Chandani *et al.*, 1988). This is the essential principle of the tristable antiferroelectric display (Yamamoto *et al.*, 1992). Despite the observation of the double hysteresis loop (Fig. 6) characteristic of the antiferroelectric phase the identification of the antiferroelectric phase was not made at this stage. It was another year before it was clarified that the electro-optic switching appeared due to the electric-field-induced antiferroelectric-ferroelectric transition.

B. Identification of the antiferroelectric phase structure

As mentioned, two groups presented the antiferroelectric structure shown in Figs. 1(e) and 4(b) at the

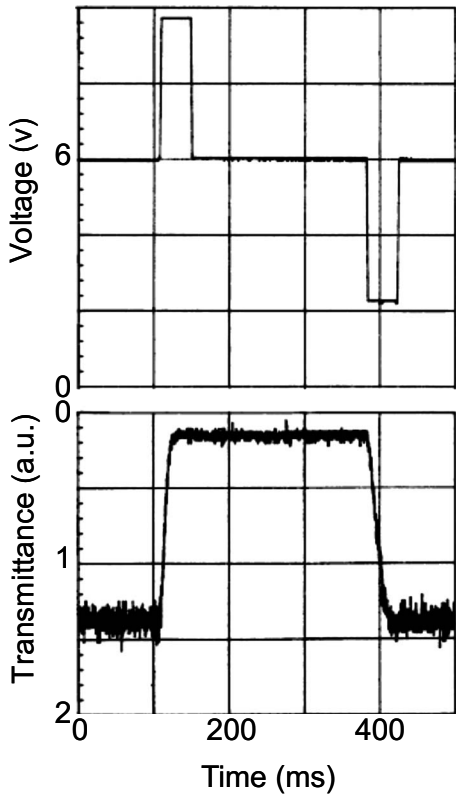

FIG. 7. Electro-optic response of MHPOBC obtained by application of positive and negative electric pulses in addition to a bias voltage of 6 V. From Chandani *et al.*, 1988.

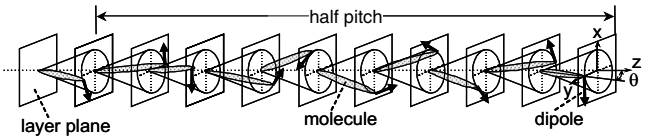

FIG. 8. Helical structure of the SmC^*_A phase.

same conference in 1989 (Galerne and Liebert, 1989; Takezoe, Chandani, Gorecka, *et al.*, 1989; Takezoe, Chandani, Lee, *et al.*, 1989). They used the different materials and methods to identify the phase structure. We now introduce four methods used to identify the antiferroelectric phase, some of which are still the most convenient and decisive methods for identification even now.

Chandani, Gorecka, *et al.* (1989) proposed a double helical structure shown in Fig. 8 for the new phase and designated it SmC^*_A, where A stands for antiferroelectric with respect to polar organization or anticlinic with respect to the tilt interlayer structure. They used selective reflection at oblique incidence to a thick sample cell, in which the helical structure shown in Fig. 8 is formed with the helical axis perpendicular to the substrate surfaces. Imagine a cholesteric (chiral nematic, N*) liquid crystal with helical modulation of the director. The length in which the local director (optical indicatrix) turns by 2π is one pitch. However, the actual periodicity is only half of the pitch because of the head-tail equivalence of the director (Fig. 9). Therefore, the first-order Bragg reflection (selective reflection) emerges at the wavelength corresponding to one optical pitch (the actual periodicity multiplied by the average refractive index). The situation is the same for the SmC^* and SmC^*_A phases for normal incidence of light. If the incident light is oblique with respect to the axis of the helical modulation, a periodical structure with one full pitch must be observed in the SmC^* structure (Fig. 9). If one measures the selective reflection using obliquely incident light, the reflected wavelength still indicates half of the pitch length in the N* and SmC^*_A structures. This fact makes the obliquely incident reflection spectra in the SmC^* and SmC^*_A structures different; i.e., a full-pitch band emerges in the SmC^* structure (Hori, 1983; Ouchi *et al.*, 1984) but not in the SmC^*_A structures, as shown in Fig. 10. The first

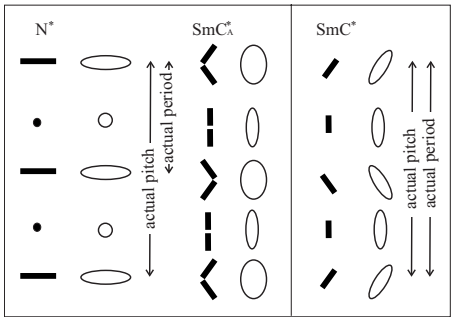

FIG. 9. Schematic structure and corresponding variation of indicatrix along the helical axis in the N*, SmC^*_A, and SmC^* phases. Note that the helices in the N* and SmC^*_A phases are optically the same, but that in the SmC^* phase is different.

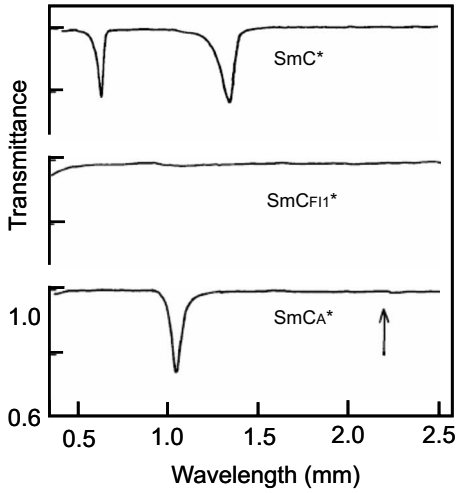

FIG. 10. Transmittance spectra at oblique incidence in the SmC^*, SmC^*_{FI1} (or SmC^*_γ), and SmC^*_A phases of MHPOBC. Note that no transmittance loss is observed at the wavelength indicated by an arrow in the SmC^*_A phase, as explained. No transmittance loss is observed in SmC^*_{FI1} because of the long pitch. From Chandani, Gorecka, *et al.*, 1989.

identification of the SmC^*_A helical structure by Chandani, Gorecka, *et al.* (1989) was thus made. They confirmed that the tilted smectic phase has a helical structure similar to that of the choleresteric N* phase. Strictly speaking, however, they did not experimentally show the layer-by-layer anticlinic structure.

A compatible result with the selective reflection experiment was obtained by Muševič *et al.* (1993) using quasielastic backward light scattering. Gapless phason dispersion was obtained in the SmC^*_A phase of MHPOBC, showing a minimum at $q=2q_c$, where q_c is the wave vector of the unperturbed helical structure, as shown in Fig. 11. This result is consistent with an alternating-tilt molecular orientational structure. It should be noted that the molecular fluctuation, the amplitude (soft) mode, and the phase (sometimes incor-

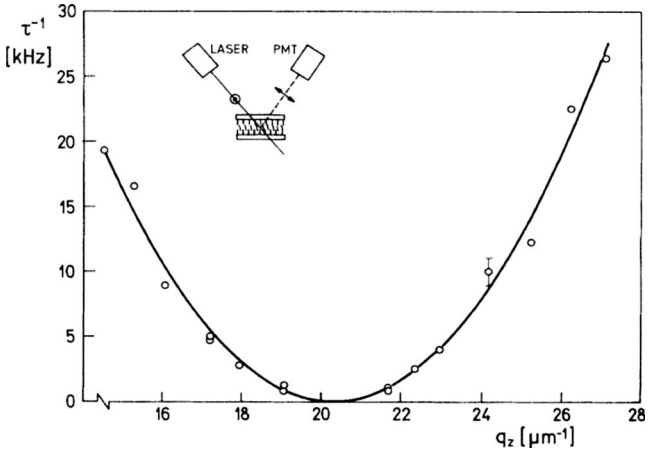

FIG. 11. Gapless antiferroelectric phason in the SmC^*_A phase measured by the photocorrelation technique. From Muševič *et al.*, 1993.

rectly named the Goldstone) mode are not easy to detect by dielectric measurements because the macroscopic dipole moment nearly vanishes. In this sense, the photon correlation technique is useful for detecting such fluctuation modes in the SmC_A^* phase (Muševič *et al.*, 1993).

Galerne and Liebert (1990) first showed the layer-by-layer anticlinic structure. They called the novel phase the SmO* phase, which was later identified to be identical to the SmC_A^* phase (Cladis and Brand, 1993; Heppke *et al.*, 1993; Takanishi *et al.*, 1993). They prepared the SmO* film on the free surface of the isotropic MHTAC droplets by precise control of the temperature. Under definite layer numbers, they applied an in-plane electric field to measure the polarization direction and found that the polarization direction alters from layer to layer, as shown in Fig. 4(b). However, it should be noted that in thin films of the SmC_A^* phase, in order to properly describe the electric-field response we must take into account not only the polarization perpendicular to the tilt plane but also the layer-boundary polarization parallel to the tilt plane, which inevitably exists because the up-down symmetry of molecular distribution is broken at surface layers. Therefore the surface layers must have polarization along the long molecular axes as well (Link *et al.*, 1996, 2001). The former is zero for even-layered structures, whereas the latter is zero for odd-layered structures.

Another experiment to confirm the layer-by-layer alternation of polarization and tilt was conducted by Bahr and Fliegner (1993a, 1993b) using free-standing films. They used transmission ellipsometry with obliquely incident light. They measured the retardation Δ_+ and Δ_- under opposite electric fields perpendicular to the incidence plane. Figure 12 shows the results for (a) three- and (b) four-layer free-standing films. A large difference in the retardations in the SmC* phase is observed in both films because of the tilt of the optical axis either away from or toward the incoming laser beam. However, the SmC_A^* phase is distinctly different in odd- and even-layered films. In the four-layer film, the retardation does not depend on the field direction, as shown in Fig. 12(b). In the three-layered film, a smaller retardation difference for opposite field directions is shown than in the SmC* phase, as shown in Fig. 12(a). These measurements were performed using two-, three-, and four-layer films and verified the layer-by-layer alternation of the polarization and tilt. They also performed the same experiments in the SmCγ^* phase and showed the three-layered repeating unit structure of this phase (Bahr *et al.*, 1994).

A very simple method for the identification of the SmC_A^* phase was proposed by Takanishi, Takezoe, Fukuda, Komura, and Watanabe (1992) and Takanishi, Takezoe, Fukuda, and Watanabe (1992). The method is based on schlieren texture observation. It is known that nematic cells exhibit two- and four-brush disclination. Analogous four-brush disclination is possible for SmC*, although two-brush disclination is prohibited because a defect plane with opposite tilts is inevitably introduced

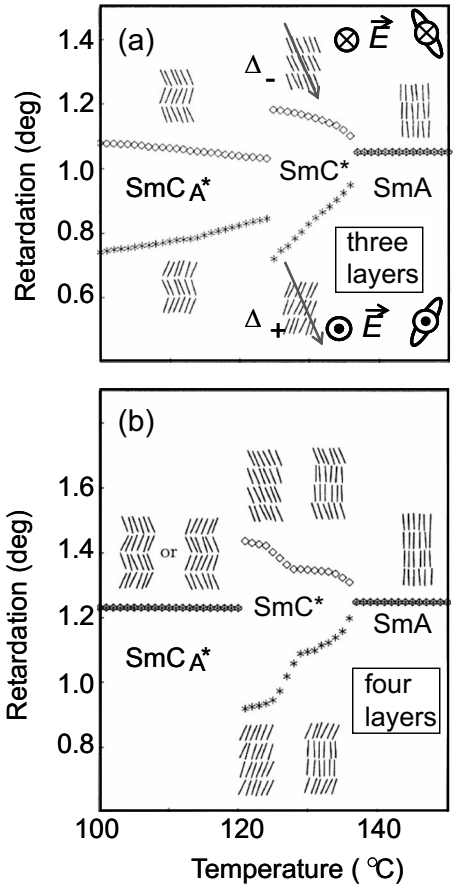

FIG. 12. Phase retardation of (a) three- and (b) four-layer free-standing films of MHPOBC by the oblique incidence of light under the application of positive and negative fields perpendicular to the optical plane. From Bahr *et al.*, 1994.

[Figs. 13(a), 13(b), and 14(a)]. Takanishi *et al.* suggested that the plane defect could be removed in the SmC_A^* phase if screw dislocations exist [Fig. 13(c)]. Actually they showed the existence of two-brush defects [Fig. 14(b)] and attributed this structure to dispiration, which had been theoretically predicted (Harris, 1970) without clear experimental observations. Since this method is simple and applicable even to the racemic SmC_A phase, it is widely used for the identification of the SmC_A^* phase.

The SmC_A^* phase can also be easily identified by direct birefringence measurements in the helix-unwound state. Because of the anticlinic structure, the birefringence becomes small. The difference of the birefringence between the unwound SmC* and the unwound SmC_A^* phases is usually easily seen when planar textures are observed. In the particular case where the tilt angle is 45°, the birefringence becomes zero. This optical characteristic provides an attractive display device even without the necessity of rubbing treatment and good alignment (D'Have, Dahlgren, *et al.*, 2000; D'Have, Rudquist, *et al.*, 2000).

Another important technique for identifying the SmC_A^* and ferrielectric phases, resonant x-ray diffraction, is discussed later.

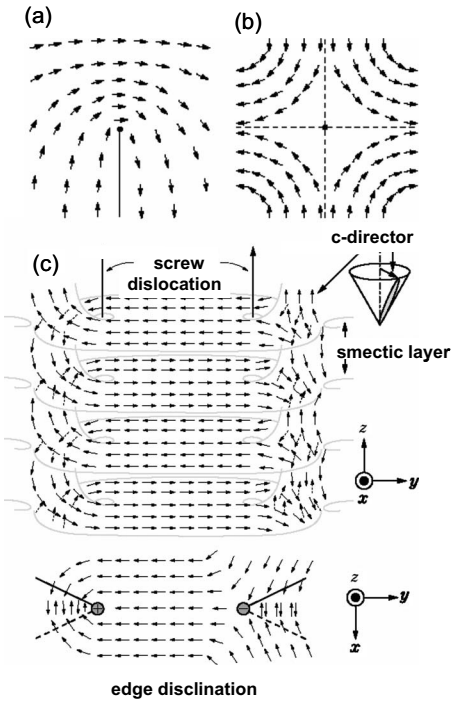

FIG. 13. *C*-director maps (a), (b) in the SmC* phase and (c) the SmC^*_A phase with screw dislocation lines. Note that four-brush defects are possible in the SmC* phase but two-brush defects cannot exist because of a defect plane with discontinuous *C*-director change [solid line in (a)]. Two-brush defects can possibly be introduced in the SmC^*_A phase by screw dislocations. From Takanishi, Takezoe, Fukuda, and Watanabe, 1992.

Today we know hundreds of materials having the SmC_A phase; most of them are chiral compounds.

C. Discovery of the SmC^*_α and intermediate phases

Unambiguously identified subphases so far are the SmC^*_α, the SmC^*_{FI1} (or SmC^*_γ), the SmC^*_{FI2} (or AF or SmC^*_{AF}) in addition to SmC* (or the SmC^*_β), and the SmC^*_A phases, the structures of which are summarized in Fig. 15. Here MHPOBC-family compounds together with some other important compounds are drawn in the order of stronger ferroelectricity or weaker antiferroelectricity. The material at the top (CF278) has the ferroelectric SmC* phase only (strong ferroelectric nature) and the material at the bottom, TFMHPOCBC, has only the antiferroelectric SmC^*_A (strong antiferroelectric nature). From the top to the bottom, additional phases such as SmC^*_α, SmC^*_{FI1}, and SmC^*_{FI2} emerge and disappear one by one. In MHPOBC, the SmC* and SmC^*_A phases coexist and, in MHPBC, the SmC* phase disappears. Fukui *et al.* (1989) first found some distinct phases in a small temperature range of MHPOBC. Chandani, Ouchi, *et al.* (1989) also found the same phase sequence and designated the phases as the SmC^*_α phase, the SmC^*_β phase, and the SmC^*_γ phase in this order from high temperature to the SmC^*_A phase as the lowest-temperature phase. They assigned the SmC^*_β as the SmC* phase (Takezoe, Lee, Chandani, *et al.*, 1991). Later, however, some reported that the SmC^*_β phase has antiferroelectric nature (Li *et al.*, 1996; Sako *et al.*, 1996; Jakli, 1999) and it was finally shown that it is actually the SmC^*_{FI2} phase (Gorecka *et al.*, 2002) in optically very pure materials, but the SmC* phase emerges when the optical purity is slightly decreased (Gorecka *et al.*, 2002). Hence MHPOBC, the first antiferroelectric liquid crystal, has all subphases of the tilted SmC* family.

As shown in Fig. 1, the repeating units of the SmC*, SmC^*_A, SmC^*_{FI1}, and SmC^*_{FI2} phases have one, two, three, and four layers, respectively. All of these phases are chiral, and every subphase has the helical structure. The SmC^*_α phase was initially mysterious but was finally assigned as a tilted phase with extremely short pitch.

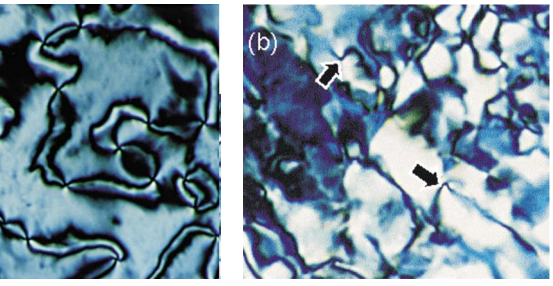

FIG. 14. (Color online) Schlieren textures in (a) the SmC and (b) SmC_A phases. Note that only four-brush defects are observed in the SmC phase, but two-brush defects are also present in the SmC_A phase, as indicated by arrows.

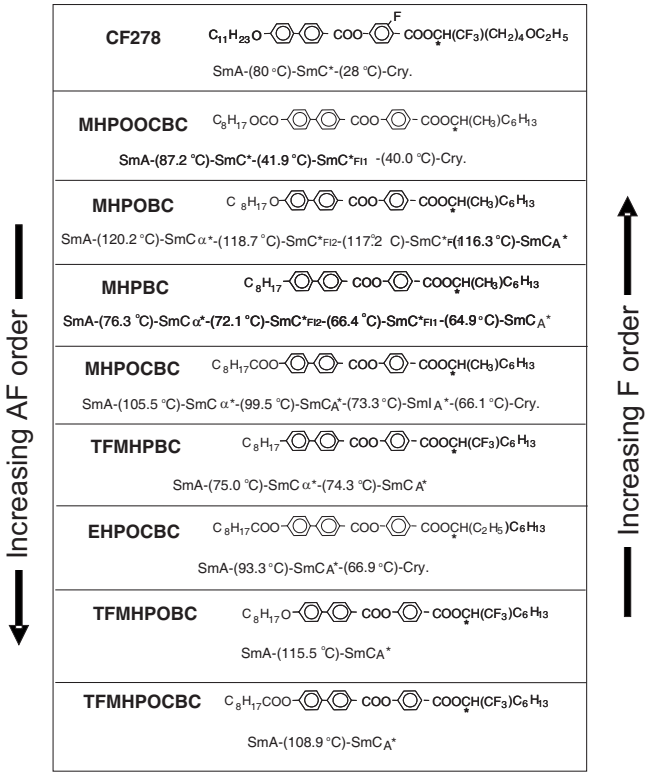

FIG. 15. Compounds that show SmC^*_A and subphases. MHPOBC-family compounds are listed in the order of stronger ferroelectricity or weaker antiferroelectricity.

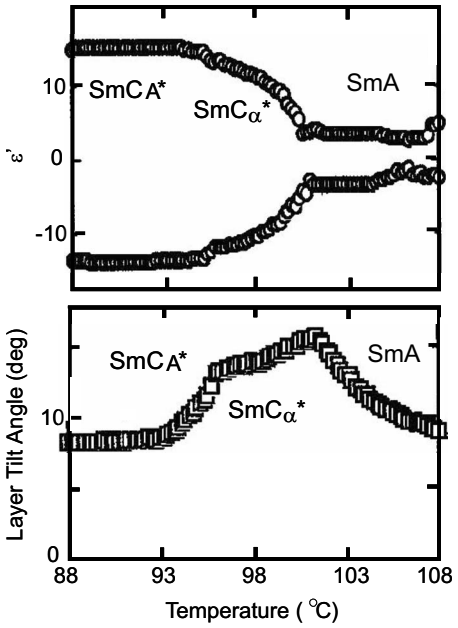

FIG. 16. Simultaneous measurements of dielectric constant and chevron angles. Two measurements clearly identify the phase transitions SmA-SmC$^*_\alpha$-SmC$^*_A$ and indicate that SmC$^*_\alpha$ is a tilted phase. From Isozaki, Hiraoka, *et al.*, 1992.

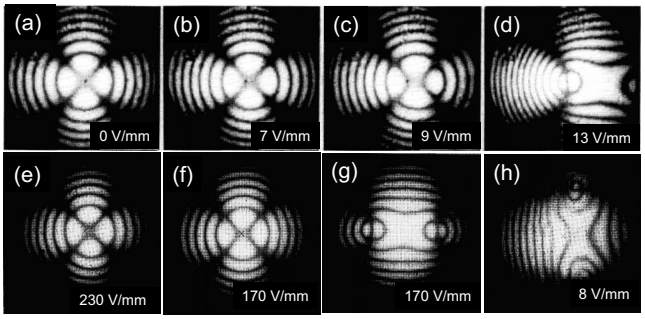

FIG. 17. Conoscopic figures in the (a)–(d) SmC*, (e) SmC$^*_\alpha$, (f) SmC$^*_A$, (g) SmC$^*_{FI2}$, and (h) SmC$^*_{FI1}$ phases. The SmC$^*_{FI2}$ and SmC$^*_A$ phases under the same field are shown. They show essentially the same pattern, suggesting that SmC$^*_{FI2}$ has more or less an antiferroelectric nature, but the threshold fields for the molecular reorientation are totally different. Note also the characteristic conoscopic image in the SmC$^*_{FI1}$ phase.

As mentioned, the SmC$^*_\alpha$ phase was found early. As temperature decreases the SmC$^*_\alpha$ phase usually appears between the nontilted SmA phase and one of the subphases, the SmC* or the SmC$^*_A$ phase. Soon after the discovery of this phase in 1989, a detailed investigation was launched. The SmC$^*_\alpha$ phase cannot be distinguished from the SmA phase by texture observation. Other measurements, however, can easily detect the SmA-SmC$^*_\alpha$ phase transition. (1) The smectic layer starts to shrink at the transition, suggesting that the SmC$^*_\alpha$ phase is a tilted phase (Takanishi *et al.*, 1991; Isozaki, Hiraoka, *et al.*, 1992). Isozaki, Hiraoka, *et al.* (1992) used MHPOCBC with a phase sequence of Iso-SmA-SmC$^*_\alpha$-SmC$^*_A$ and a wide temperature range (6 °C) of the SmC$^*_\alpha$ phase to observe the transition from or to SmA and SmC$^*_\alpha$ by the temperature dependence of the chevron angle (layer-tilt angle) together with dielectric measurements, as shown in Fig. 16. (2) Switching current peaks start to appear on application of a triangular-wave field to a MHPOBC cell. Their number, shape, and position change within a narrow temperature range of the phase, and finally a single switching current peak is observed when the transition to SmC* occurs (Takanishi *et al.*, 1991). These behaviors suggest complicated structural change with change in applied field and temperature. (3) Pretransitional effects are observed in the SmA phase: the dielectric constant (Fukui *et al.*, 1990; Hiraoka, Chandani, *et al.*, 1990; Hiraoka, Taguchi, *et al.*, 1990; Hiraoka *et al.*, 1992; Isozaki, Hiraoka, *et al.*, 1992) and induced circular dichroism (Lee, Ouchi, *et al.*, 1990) increase with decreasing temperature, and inflection points are clearly seen at the transition point. The above observations suggest that SmC$^*_\alpha$ is a SmC*-like phase. Because it is a chiral phase, a helical structure was expected. After extensive effort to measure the period of this structure, the pitch was found to be extremely short, depending on temperature and sample thermal history, i.e., 60–250 nm (Laux *et al.*, 1996), as theoretically predicted by Čepič and Žekš (1995) and Roy and Madhusudana (1996). More detailed pitch measurements in the SmC$^*_\alpha$ phase were made later by Cady *et al.* (2002) and Hirst *et al.* (2002) using resonant x-ray diffraction (see Sec. III.B).

The three- and four-layer periodicities in SmC$^*_{FI1}$ and SmC$^*_{FI2}$, respectively, were suggested in the early stage of their discovery. For the phase determination, conoscopy was adequate (Gorecka *et al.*, 1990). We now summarize the conoscopic data in the SmC$^*_\alpha$, SmC*, SmC$^*_{FI2}$, SmC$^*_{FI1}$, and SmC$^*_A$ phases, some of them presented in Fig. 17. In all cases, the applied field is along the vertical direction. In a sufficiently strong electric field the conoscopic figures will be the same as for the unwound SmC* phase for all phases, although a strong enough field is not always accessible experimentally. In Figs. 17(a)–17(d) the field dependence of the conoscopic figures in SmC* is shown (Gorecka *et al.*, 1990). In the absence of an electric field, a uniaxial figure almost the same as the one in SmA and SmC$^*_\alpha$ is observed, although the center of the isogyre is not dark. This is because of the optical rotatory power due to the helical structure. With increasing field, the center shifts in a direction perpendicular to the electric field and biaxiality emerges, indicating unwinding of the helix and a consequent apparent tilt, i.e., of the average molecular direction over the layers [Figs. 17(c) and 17(d)]. The optical plane is defined by a plane containing two optical axes, the one with the largest and the one with the smallest refractive indices, respectively. The optical plane is perpendicular to the field direction, indicating that the axis of the minimal refractive index is perpendicular to the field and the molecular long axis.

The SmC$^*_\alpha$ phase looks only slightly distorted under an electric field, as shown in Fig. 17(e), which means that under applied field the helix is not completely unwound

(Isozaki, Hiraoka, *et al.*, 1992; Okabe *et al.*, 1992). In the SmC^*_A phase subjected to an electric field the optical plane is perpendicular to the field, as shown in Fig. 17(f). No tilt is visible, which indicates that the structure is in an unwound anticlinic state. The SmC^*_{FI2} phase was found to exhibit the same behavior as the SmC^*_A phase with varying field, although the helix unwinding occurs at a much lower electric field compared to the field in the SmC^*_A phase, as shown in Fig. 17(g) (Okabe *et al.*, 1992). The antiferroelectric behavior was the reason that the SmC^*_{FI2} phase was at first named the AF or SmC^*_{AF} phase (Okabe *et al.*, 1992). For this phase Isozaki, Fujikawa, *et al.* (1992) suggested an antiferroelectric structure based on the Ising model, where the tilt direction changes every two layers and the repeating unit consists of four layers.

The structure of the SmC^*_{FI1} phase, first called the SmC^*_γ phase, was recognized in 1990 from its novel conoscopic figures under an applied electric field, as shown in Fig. 17(h) (Gorecka *et al.*, 1990). The conoscopic figure of this phase is quite unusual: a large tilt in the major axis of the optical indicatrix occurs perpendicular to the field direction, and biaxiality with the optical plane parallel to the field direction arises. If we confine ourselves to the Ising model for simplicity, a plausible model is as follows: The ratio of the molecular tilts in opposite senses is far from unity, so that finite polarization remains uncanceled and the molecule responds by reorientation toward the field direction (Gorecka *et al.*, 1990). Then what is the ratio of molecules tilting in opposite senses? To solve this problem, Takezoe, Lee, Ouchi, Fukuda, *et al.* (1991) considered the twisting power in the SmC^*_{FI1} phase (Lee, Ouchi, *et al.*, 1990). It was known that helix handedness in the SmC^*_A phase is always opposite to that in the SmC^* phase (Lee, Ouchi, *et al.*, 1990; Li *et al.*, 1991; Yamamoto *et al.*, 1992). Since the suggested Ising SmC^*_{FI1} structure consists of synclinic (ferroelectric) and anticlinic (antiferroelectric) neighboring layers, the twisting power in the SmC^*_{FI1} can be determined by the ratio of the twisting powers at the SmC^*-like and SmC^*_A-like interfaces. This assumption leads to the following simple relation:

$$\frac{1}{p(SmC^*_{FI1})} = \frac{F}{p(SmC^*)} + \frac{1-F}{p(SmC^*_A)}, \tag{1}$$

where p is the helical pitch or wavelength of the selective reflection band in the respective phases and F is the fraction of the parallel-tilted, i.e., *synclinic*, layers. Using the value of p in each phase, F was estimated to be 0.3. Therefore, the ratio of the synclinic and anticlinic layers was concluded to be 3:7. Since SmC^*_{FI1} is a thermally stable phase, the structure should have a periodic regular structure with a rather short length. The simplest ratio satisfying this condition is 1:2 with a repeating unit of three layers (Takezoe, Lee, Ouchi, Fukuda, *et al.*, 1991). In this way, the three-layered model of SmC^*_{FI1} appeared. The triple hysteresis loop (Lee, Chandani, *et al.*, 1990), the five-step electro-optic response (Hiraoka, Taguchi, *et al.*, 1990), the intermediate apparent tilt angle (Hiraoka, Chandani, *et al.*, 1990), and the dielectric constant (Fukui *et al.*, 1990; Hiraoka, Taguchi, *et al.*, 1990) between SmC^* and SmC^*_A also supported this structural model. Although later considerations did not support the intuitive path to it, the three-layered structure of the ferrielectric SmC^*_{FI1} phase really exists and was experimentally confirmed (Mach *et al.*, 1999).

As mentioned, the repeating units of one (SmC^*), two (SmC^*_A), three (SmC^*_{FI1}), and four (SmC^*_{FI2}) layers were conclusively reported for these four phases at least on the basis of the Ising model. The theoretical basis of these model structures was confirmed by an axially next nearest-neighbor interaction model including third neighbor interaction (Yamashita and Miyazima, 1993). In contrast, Čepič and Žekš (1995) and Roy and Madhusudana (1996) developed a discrete phenomenological model, leading to essentially a clock model, i.e., the tilt azimuthal angle makes one turn in three and four layers for SmC^*_{FI1} and SmC^*_{FI2} with a slight incommensurability due to chirality. This model was supported by resonant x-ray diffraction measurements by Mach *et al.* (1998). However, the intermediate model structures, deformed Ising or deformed clock models, were finally experimentally evidenced by optical properties (Akizuki *et al.*, 1999), ellipsometry (Johnson *et al.*, 2000; Fera *et al.*, 2001), detailed analysis of the resonant x-ray data (Johnson *et al.*, 2000; Matkin *et al.*, 2001), dynamic light scattering (Konovalov *et al.*, 2001), optical rotatory power (Muševič and Škarabot, 2001; Shtykov *et al.*, 2001), specular x-ray reflection (Fera *et al.*, 2001), and so on. The details will be discussed in the following.

III. THE SEARCH FOR INTERNAL STRUCTURES OF MULTILAYER PHASES

A. The crystallographic unit cell

After the investigation of the chiral polar phases, around the end of the 1990s, it was widely accepted that apart from the synclinic-ferroelectric SmC^* phase and the anticlinic-antiferroelectric SmC^*_A phase, three more distinct phases—the SmC^*_{FI1}, the SmC^*_{FI2}, and the SmC^*_α phases—exist, as mentioned previously. However, the situation was far from being clear. The basic repeating unit cell of these phases was still a subject of speculation based on indirect evidence. The structure of the unit cell in the intermediate phases, i.e., the two phases which appear between the SmC^* and the SmC^*_A phases, was still unsolved; some insisted that they could be described by an Ising model and others that the structures are more consistent with the clock model. Moreover, some researchers claimed that in their systems a larger number of intermediate phases could be identified (Fukuda *et al.*, 1994). Even for the most studied prototype antiferroelectric material MHPOBC, the ferroelectric nature of the phase identified as SmC^* by the Tokyo group was still questioned.

The first unambiguous proof that the SmC^*_{FI2}, SmC^*_{FI1}, and SmC^*_A phases have unit cells of four, three, and two

layers, respectively, came in 1998 from a resonant x-ray scattering experiment (Mach *et al.*, 1998, 1999). Conventional x-ray measurements allow for the studies of density modulation along the layer-normal direction only and are not sensitive to the orientation of the tilt direction in the layers. The transition between intermediate phases is generally not detectable by this method unless changes in the layer thickness are seen at the phase transition temperature. This can be related to small discontinuity of the tilt angle or to a change in the molecular interdigitation between layers (Hamplova *et al.*, 2003). The difference between phases could also be detected if electron densities at layer boundaries (in the Ising model synclinic and anticlinic) are appreciably different and thus signals of a superlattice become visible. Such a signal, related to the three-layer structure, was reported for the SmC^*_{FI1} phase by careful x-ray studies using a strong synchrotron source (Fernandes *et al.*, 2006).

Unlike the conventional x-ray method, resonant x-ray detection, when the beam energy is tuned to the absorption edge of one of the atoms present in molecular structure, usually sulfur, selenium, or bromine, is sensitive to the distribution of this particular atom in the crystal structure (Dmitrienko, 1983). In other words, the scattered beams from consecutive layers do not interfere destructively and the superlattice structure becomes visible in the x-ray diffraction (Fig. 18). The additional signals appear as satellites of the main reflection, with wave vector

$$q = q_0\left(l \pm \frac{m}{n}\right), \tag{2}$$

where $m=1$ (first-order peak) or 2 (second-order peak), n is the number of layers forming the unit cell of the phase, $q_0=2\pi/d$ is the reciprocal vector of main reflection, d is the layer thickness, and l takes the values 0, ±1, ±2.

For the preliminary resonant x-ray studies the mesogenic material 10TBBB1M7, containing a sulfur atom in the mesogenic core, was chosen. For this material Mach *et al.* demonstrated that indeed in the SmC^*_A phase, apart from the nonresonant signal, corresponding to the layer spacing, additional peaks related to double-layer periodicity exist [Figs. 18(d) and 18(e)]. They also reported that in the temperature range of the SmC^*_{FI1} and SmC^*_{FI2} phases, signals related to three- and four-layer periodicities were found, respectively [Figs. 18(b) and 18(c)]. On the other hand, in the SmC^*_α phase modulation of several layers was detected, incommensurate with the layer thickness [Fig. 18(a)]. The polarizations and intensities of the superlattice signals seemed to agree with a clock model. For the clocklike structure in an experiment in which the incident x-ray beam is σ polarized (polarized in the plane perpendicular to the plane containing the incident and the scattered beam), the first-order peaks ($m=1$) should be π polarized (polarized parallel to the plane containing the incident and the scattered beam) and the second-order peaks ($m=2$) should be σ polarized, as indeed was found in experiments. The Ising model predicts σ-polarized signals for the first-order reflections. The clocklike structure of the two intermediate phases was further supported by careful nonresonant x-ray measurements, where no subharmonics of the main periodicity in any of the studied compounds were observed (Fera *et al.*, 2001), suggesting that all interlayer boundaries in SmC^*_{FI2} and SmC^*_{FI1} phases are indeed identical, as predicted by the model. However, it soon turned out that although resonant x-ray studies showed correctly the superlattice periodicity of the intermediate phases, the arguments about their internal structure were premature.

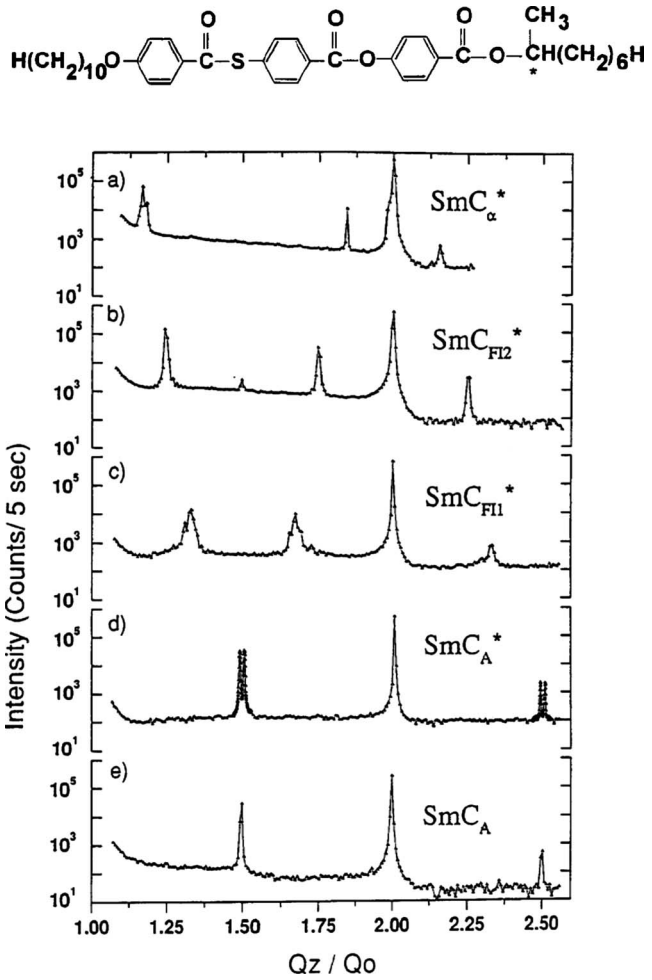

FIG. 18. X-ray intensity scans in (a)–(d) the indicated phases of the (R) enantiomer and (e) the racemic 10OTBBB1M7. Additional signals related to the layer superstructure appear, apart from the second harmonic of the signal related to the layer structure, $q_z/q_0=0$. From Mach *et al.*, 1998.

The suggested clock model was inconsistent with the results of optical studies. Short helical structures should be optically uniaxial with the optical axis along the layer normal, as the dielectric tensor components describing properties of the structure in the direction perpendicular to the layer normal (in-plane components) are equal. Thus, the samples observed along the layer-normal direction (for example, free-standing films) should have zero birefringence. The optical rotatory power should

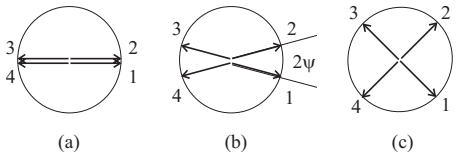

FIG. 19. Considered director projections on the smectic layer for the SmC^*_{FI2} phase: (a) Ising structure, (b) distorted structure, and (c) clock structure. The distortion ψ is measured with respect to the tilt direction in the Ising structure.

also be negligible, as the helical modulation of the tilt direction with the period of the modulation extending over only a few smectic layers is much shorter than the wavelength of the incident light. In contrast to these predictions, films drawn in the SmC^*_{FI1} and SmC^*_{FI2} phases show pronounced birefringence (Fig. 21); thus optical studies strongly suggested that the structure of intermediate phases—the SmC^*_{FI1} and the SmC^*_{FI2} phases—is either Ising-like (although this was excluded by former x-ray studies) or should be described by a new, different model. The best candidates were hybrid structures between the Ising-like and clock structures—called distorted clock structures. The question was how one could determine the distortion ψ from the clock or Ising structure (Figs. 19 and 20).

The biaxiality of the sample resulting from the distortion from the clock structure can be measured quantitatively by optical ellipsometry. Using this technique Johnson *et al.* (2000) concluded that the structures of the SmC^*_{FI1} and SmC^*_{FI2} phases are actually much closer to the Ising than to the clock model. For the MHPBC material the distortion ψ from the uniplanar Ising structure in the SmC^*_{FI2} phase is only about 5° (instead of 45° for the four-layer clock structure) (Fig. 19) and in the SmC^*_{FI1} phase it is only about 30° (instead of 60° for the three-layer clock structure) (Fig. 20).

Measurements of optical rotatory power were also proved to be useful for the detection of clock distortion (Akizuki *et al.*, 1999; Muševič and Škarabot, 2001; Shtykov *et al.*, 2001; Čepič *et al.*, 2002). According to the modified de Vries' equation (de Vries, 1951) the optical rotatory power depends on the anisotropy of the in-plane components of the dielectric tensor, calculated for a single crystallographic unit cell, and the effects of the longer *optical helix* due to the rotation of this unit cell in space (Fig. 21, top inset). In the SmC^*, SmC^*_A, SmC^*_{FI1}, and SmC^*_{FI2} phases the optical helix can be detected

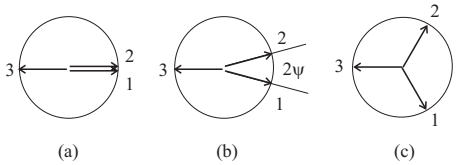

FIG. 20. Considered director projections on the smectic layer for the SmC^*_{FI1} phase: (a) Ising structure (b), distorted structure, and (c) clock structure. The distortion ψ is measured with respect to the tilt direction in the Ising structure

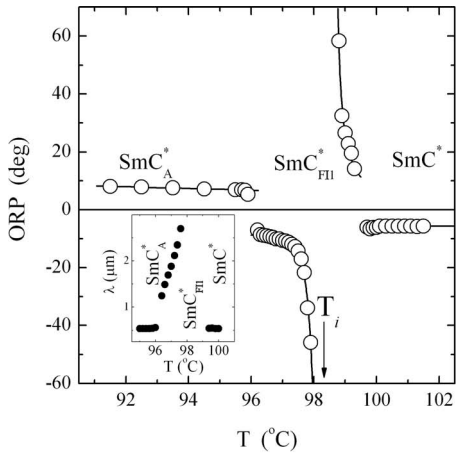

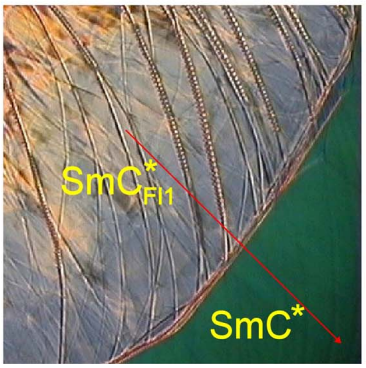

FIG. 21. (Color online) Optical rotary power and selective reflection for HHBBMz compound. The temperature dependence of the optical rotatory power and selective reflection wavelength (inset); note that within the temperature range of the SmC^*_{FI1} phase helix-twist inversion takes place (top) for the material 12 HHBBMz (Dzik *et al.*, 2005). Textures of SmC^*_{FI1} and SmC^* phases in free suspended film samples were observed between crossed polarizers, subject to a temperature gradient (the arrow indicates the direction of increasing temperature). In SmC^* the color of selective reflection is visible (dark lower right corner, green online), in SmC^*_{FI1} at the temperature at which the optical helix becomes unwound clear birefringence colors appear (bright upper left region, blue online) (bottom).

from the selective reflection of the incident light in some cases if the optical helix is in the range of the visible or the near infrared light wavelengths. If the period of the optical helix, the pitch, is in the range of the visible or infrared light wavelengths, it can also be measured in planar samples as the distance between dechiralization lines (Brunet and Williams, 1978; Glogarova *et al.*, 1983). From information about the pitch and the optical rotatory power, the in-plane components of the dielectric tensor and thus the distortion ψ from the Ising structure can be estimated. Because the optical rotatory power is related to the anisotropy of the dielectric tensor of the single crystallographic unit cell, it should be maximal for the uniplanar Ising structure and zero for the ideal clock model. Using optical rotatory power measurements it was deduced that for 10OTBBB1M7, i.e., the compound used for the first resonant x-ray measurements (Mach *et*

al., 1999), the distortion from the uniplanar structure is not larger than 10° in both SmC^*_{FI1} and SmC^*_{FI2}; distortion less than 10° in the SmC^*_{FI1} phase was also found for MHPOBC (Muševič and Škarabot, 2001). Some materials might even have an ideal planar structure (Dzik *et al.*, 2005). Moreover, it was shown that the distortion angle is nearly temperature independent (Brimicombe *et al.*, 2007).

In summary, taking into account results of the ellipsometry and the optical rotatory power measurements, it became evident that neither the SmC^*_{FI1} nor the SmC^*_{FI2} phase could possibly have the simple clock structure. Only the measurements of the SmC^*_α phase seemed to be consistent with the clock structure as in this phase negligible optically rotatory power was found (Muševič and Škarabot, 2001) and optical uniaxiality was confirmed.

Reports about optical studies stimulated further x-ray investigations. During the years 2001 and 2002 some reports appeared that provided additional evidence for more detailed description of the intermediate phase structures by high resolution resonant x-ray method (Cady *et al.*, 2001; Hirst *et al.*, 2002). The calculation of the tensorial form factors by Levelut and Pansu showed that in phases with an additional optical helix, superimposed on the basic few-layered structure, both first- and second-order resonant signals should be additionally split and observed at

$$q = q_0\left[l \pm m\left(\frac{1}{n} + \frac{d}{p}\right)\right], \tag{3}$$

where p is the pitch length (Levelut and Pansu, 1999). The splitting is larger for shorter pitches. While the intensities of the second-order signal $m=2$, split due to the helix, should always be equal, the intensities of the split first order $m=1$ signals are more complex. The intensity ratio for these signals departs quickly from 1, as the basic crystallographic unit becomes distorted from the clock structure and for the ideal Ising structure one of the signals disappears. For the SmC^*_{FI2} phase in MHDDOPTCOB, by comparing the intensities of peaks positioned near $1.25q_0$ and $1.75q_0$, Cady *et al.* (2001) deduced that the structure is almost Ising-like and the distortion is only about 10° from the Ising uniplanarity and nearly temperature independent. Similar results were obtained soon after for a few other materials having SmC^*_{FI2} and SmC^*_{FI1} phases (Wang *et al.*, 2006).

Finally, after some years of intensive research, consistency between the optical and x-ray results was obtained. The SmC^*_{FI2} and SmC^*_{FI1} phases have a basic crystallographic unit cell of four and three layers, respectively, in which the tilt directions in smectic layers form a strongly distorted clock structure (Figs. 19 and 20). Additionally, a secondary long-wavelength periodicity, the optical helix, is formed. Only SmC^*_α has a few-layered clock structure (Fig. 22). In the following years other properties of the phases also became more understandable.

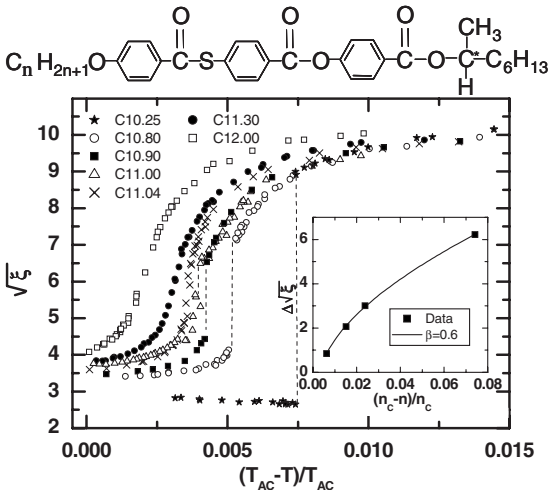

FIG. 22. Evolution of the pitch at the SmC^*-SmC^*_α phase transition for mixtures of compounds with $n=10$ and 11. The jump in the pitch at the phase transition (inset) decreases with decreasing concentration of the $n=11$ homolog in the mixture. The studied system shows the evolution from first-order to overcritical behavior. From Liu *et al.*, 2006.

B. Secondary helical modulation of the phases

For nearly all compounds the twist sense of the optical helix changes in the SmC^*-SmC^*_A and also in the SmC^*_{FI2}-SmC^*_{FI1} phase transitions (Čepič *et al.*, 2002; Lagerwall *et al.*, 2006). This is consistent with constant chiral nearest-neighbor interlayer interactions in the system (see Sec. IV). However, in a number of materials the sense of the helical-modulation sign reverses within one of the phases. The helical-modulation inversion occurs in SmC^*_A in MHPOBC but in many other materials it happens in one of the intermediate phases, although the temperature range of these phases is usually very narrow. Due to the strong temperature dependence of the optical helix length in the vicinity of the helix sense inversion the texture changes are rather violent. The behavior was sometimes misinterpreted as an additional phase transition (Nguyen *et al.*, 1994). On the other hand, the helical modulation does not reverse at the transition from the SmC^* to the SmC^*_α phase. The two phases seem to have similar structure except that the pitch in SmC^*_α is very short, below the resolution of microscopic observations. Its length can be determined only by the resonant x-ray method. Gleeson and Hirst (2006) measured the helical pitch in SmC^*_α in different materials and found a pitch ranging from 5 to 54 layers (Mach *et al.*, 1999). With a few assumptions the length of the helical modulation can also be estimated from ellipsometric data. The pitch is usually incommensurate with the smectic layer and can be as tight as 3.5 layers (Cady *et al.*, 2002; Wang *et al.*, 2006; Liu *et al.*, 2007). The short pitch in the SmC^*_α phase can also be estimated by the comparison of Friedel fringes which appear due to the changes of the propagating light ellipticity and the wedge fringes in free surface drops of liquid crystals. For the four-layer structure of the SmC^*_α phase, the phase

difference between tilts in neighboring layers is exactly $\pi/2$ and phase retardation for the two polarizations of light does not appear. Therefore the structure seen by light has no chiral properties and the continuous change of the structure through the $\pi/2$ phase difference gives rise to a peculiar behavior of the period of the Friedel fringes (Laux *et al.*, 1999, 2000).

As the temperature is lowered and the system approaches the transition to the SmC* phase the pitch greatly increases. The evolution between SmC^*_α and SmC* phases can be either discontinuous (Ema *et al.*, 2000; Cady *et al.*, 2002) or continuous (Liu *et al.*, 2006). Since both phases have the same symmetry the system can be considered as an analog to the gas-liquid system. The order parameter for this transition is the helical pitch, which can evolve continuously beyond the critical end point. The existence of such a critical end point for the SmC*-SmC^*_α phase transition was shown by Liu *et al.* (2006). In the vicinity of the critical point the dependence of the jump in the pitch is described by a mean-field critical exponent close to 0.5.

C. Polarity of multilayer phases

The tilted phases have more or less distinct polar properties, which can be explained by a distorted clock model. Both the two-layered SmC^*_A phase and the distorted four-layered SmC^*_{FI2} phase have compensated electric polarization in the crystallographic unit cell and thus they have antiferroelectric properties. The SmC* and smectic SmC^*_α are ferroelectric, as their crystallographic unit cell is just a single electrically polarized layer; the SmC^*_{FI1} phase with its three-layered structure and only partially compensated polarization is ferrielectric.

The polar properties of the phases are easily distinguished by the dielectric response using dielectric spectroscopy. Fluctuations of polarization with the wave vector $q=0$ (thus homogeneous in space) can be followed by this method (Merino *et al.*, 1996; Panarin *et al.*, 1998).

The dielectric response in the SmC* and SmC^*_α phases is dominated by the Goldstone mode, which should be more properly called the helix-distortion mode (Fajar *et al.*, 2002; Douali *et al.*, 2004). This mode is related to collective movements of the molecules on the tilt cone (azimuthal mode) which also affect the polarization vector's direction. The amplitude of these fluctuations is smaller and the relaxation time is shorter for shorter helical pitches. This is the reason why the dielectric response in the SmC* phase is much stronger and has much lower relaxation frequency than the mode observed in the SmC^*_α phase.

In the antiferroelectric phases, the SmC^*_A and SmC^*_{FI2} phases, the dielectric response is at least one order of magnitude weaker than in the ferroelectric SmC* and SmC^*_α phases. There are two main collective fluctuations which contribute to the dielectric response (Parry-Jones and Elston, 2002). A mode with higher relaxation frequency appears due to antiphase azimuthal tilt angle

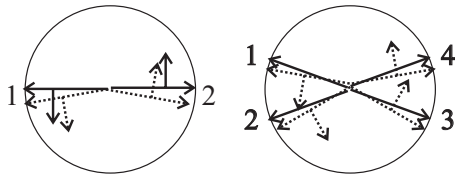

FIG. 23. Polar azimuthal antiphase modes in the antiferroelectric (a) SmC^*_A and (b) SmC^*_{FI2} phases. Note that polarization is perpendicular to the tilt (marked by small arrows). When the structure is deformed due to the fluctuations (dashed arrows) the polarization in the unit cell does not cancel out.

fluctuations (Fig. 23) in which the antiferroelectric structure of the crystallographic unit cell is distorted. The lower-frequency mode is usually attributed to helix distortion. This mode is visible due to the small noncompensated polarization in the crystallographic unit cell (Lagerwall, 2005; Dolganov and Zhilin, 2008).

The dielectric response in the SmC^*_{FI1} phase is much stronger than in the antiferroelectric SmC^*_A phase but weaker than in the ferroelectric SmC* phase (Figs. 24 and 25). Its characteristic feature is a broad distribution of mode relaxation frequencies usually in the range of 10 Hz–1 kHz. The polydisperse character of the dielectric response suggests that, apart from antiphase azimuthal tilt angle changes disturbing the three-layered equilibrium structure and the helix-distortion mode, some other mechanism might also contribute strongly to the dielectric response in the same frequency window. The candidate could be movements of boundaries between domains of differently oriented polarizations of the three-layered unit cell (Miyachi *et al.*, 1994) (see Fig. 40 in Sec. IV). Such an origin of the dielectric response is supported by the strong influence of surface interactions on the dielectric response and the history of electric field application to the sample (Miyachi *et al.*, 1994). Generally, in all phases, in addition to the described azimuthal modes related to the changes of the polarization direction in the smectic layers, amplitude modes, related to the changes of the tilt angle magnitude and thus polarization (due to the tilt-polarization coupling) in the layers, also contribute to the dielectric response. However, this contribution is weak except in the vicinity of the phase transition to the nontilted SmA phase (Bourny *et al.*, 2000).

The difference in the polarity of phases is also shown in their electro-optical response (Panarin *et al.*, 1997). While in ferroelectric phases application of an electric field reorients polarizations along the helix continuously and the threshold for the switching is nearly negligible, in antiferroelectric phases the switching usually takes place in two steps: initially the unwinding of the helical structure occurs and at higher electric fields the antiferroelectric order transforms to ferroelectric order with the polarization oriented parallel to the electric field (Parry-Jones and Elston, 2001). The threshold electric field necessary to break antiferroelectric interactions and impose the ferroelectric structure is of the same order of magnitude for the SmC^*_{FI2} and SmC^*_A phases and

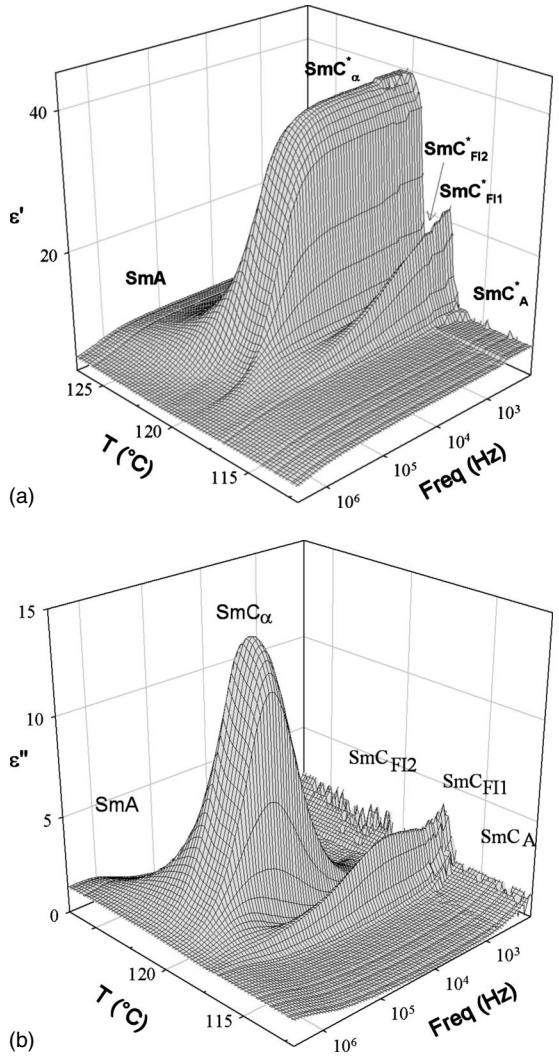

FIG. 24. Temperature-frequency dependence of (left) real and (right) imaginary parts of dielectric permittivity for MHPOBC with high optical purity (showing SmA, SmC^*_α, SmC^*_{FI2}, SmC^*_{FI1}, and SmC^*_A). Note that the antiferroelectric phases SmC^*_A and SmC^*_{FI2} have much weaker dielectric response than SmC^*_α and SmC^*_{FI1}. From Gorecka *et al.*, 2002.

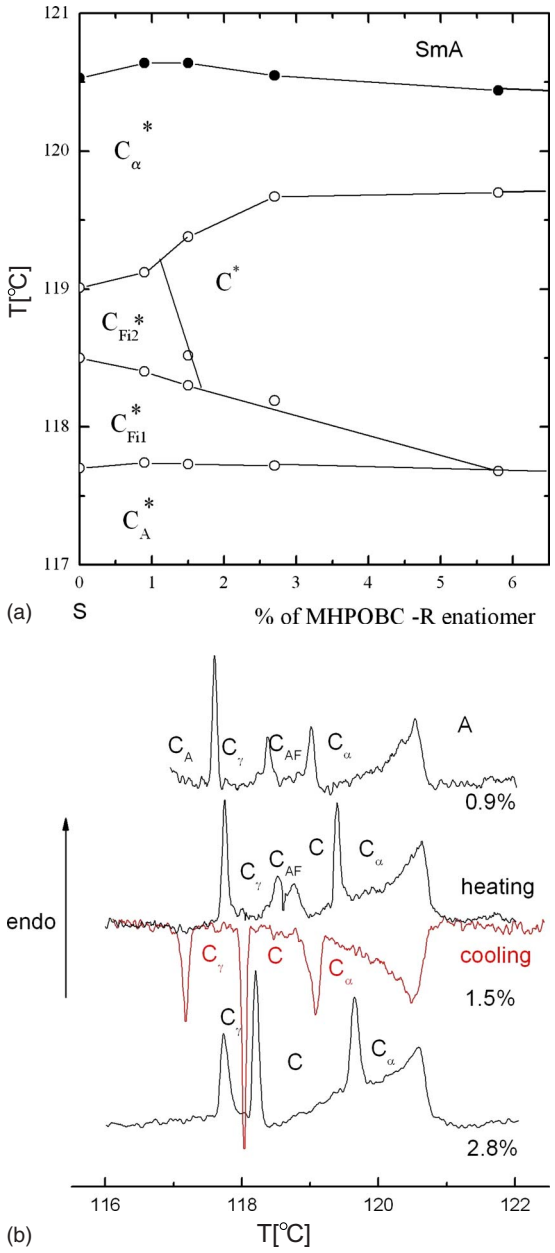

FIG. 25. (Color online) Phase diagram and corresponding differential calorimetric scans. (Left) Phase diagram for MHPOBC showing the influence of optical purity on the subphase sequence. (Right) Differential Scanning calorimetry scans for the mixtures of different optical purity. From Gorecka *et al.*, 2002.

decreases on approach to the ferroelectric SmC* phase. In the SmC^*_A phase, the induction of the synclinic structure by application of an electric field (or temperature) is visible in thin cells as characteristic stripes propagating in the sample in the direction parallel to the smectic layers. The velocity at which the stripes propagate is proportional to the strength of the applied field. The stripes were described as solitary waves resulting from strong coupling of the layers (Li *et al.*, 1995; Bahatt *et al.*, 2001). In the SmC^*_{FI1} phase the structural changes are also stepwise when an electric field is applied. At lower fields the helical modulation unwinds; as the field increases the structural changes from the three-layered ferrielectric structure to the ferroelectric structure occur.

Generally the helical pitch in the SmC^*_α phase is so short that its switching often mimics the antiferroelectric behavior—the helically modulated structure with very short pitch rapidly unwinds and rewinds if the polarization is measured using triangular voltage dependence (Lagerwall, 2005). The same behavior, i.e., tristable switching, was observed even in the SmC* phase with an ultrashort pitch (Itoh *et al.*, 1997).

D. Temperature sequence of phases

Unlike to the SmC^*_α-SmC* phase transition, which can be continuous or discontinuous, the other phases appear by first-order transitions (Ema *et al.*, 2000), except for some unusual systems with a critical end point for the

SmC^*-SmC_A^* phase transition (Song *et al.*, 2008). As the temperature is lowered the most general sequence is SmC_α^*-SmC^*-SmC_{FI2}^*-SmC_{FI1}^*-SmC_A^*. In some systems some phases might be missing or be metastable; however, as the temperature is lowered it is generally observed that the crystallographic unit cell of phase structures shortens from many layers in the SmC_α^* phase to four layers in the SmC_{FI2}^* phase, to three layers in the SmC_{FI1}^* phase, and finally to two layers in the SmC_A^* phase. While the SmC and SmC_A phases are observed in racemic mixtures or in nonchiral materials, SmC_α^*, SmC_{FI1}^*, and SmC_{FI2}^* are found only in systems with high optical purity (Fukuda *et al.*, 1994). In most systems the enantiomeric excess has a dramatic influence on the observed phase sequence. For example, in the prototype material MHPOBC it was found that in samples of high optical purity the phase sequence SmC_α^*-SmC_{FI2}^*-SmC_{FI1}^*-SmC_A^* is observed, while in a slightly racemized sample the antiferroelectric SmC_{FI2}^* phase disappears and the ferroelectric SmC^* phase appears in the same temperature window. The phase sequence of the slightly racemized sample is SmC_α^*-SmC^*-SmC_{FI1}^*-SmC_A^* (Gorecka *et al.*, 2002), as reported by the first studies of this system (Chandani, Gorecka, *et al.*, 1989). This solved the long-lasting controversy of some reporting antiferroelectric properties (Li *et al.*, 1996; Sako *et al.*, 1996; Jakli, 1999) for the phase below the SmC_α^* phase and other ferroelectric properties for presumably the same phase (Chandani, Gorecka, *et al.*, 1989; Gorecka *et al.*, 1990).

Although shortening of the crystallographic unit cell seems to be the most common situation as the temperature is lowered, it should be mentioned that in some materials the SmC_{FI1}^* phase (Laux *et al.*, 2000) or the SmC_{FI2}^* phase (Wang *et al.*, 2006, 2009) interferes between the SmC_α^* and SmC^* phases. In some systems a reentrant phenomenon is observed where the phase sequence SmC^*-SmC_A^*-SmC^* (Kašpar *et al.*, 2001; Pociecha *et al.*, 2001) appears. Recently a SmC_α^*-SmC_{FI1}^*-SmC^* phase sequence was also reported (Sandhya *et al.*, 2008) and even SmC_{FI2}^*-SmC^*-SmC_{FI2}^* reentrancy in some mixtures (McCoy *et al.*, 2008) was detected.

It should also be mentioned that some claim (Isozaki, Hiraoka, *et al.*, 1992; Chandani *et al.*, 2005; Emelyanenko *et al.*, 2006; Panov *et al.*, 2007) that they are able to detect more than five tilted smectic *C*-type phases (e.g., with the unit cell larger than four smectic layers) in some materials or mixtures. However, these additional phase transitions are detected indirectly, for example, as small, nearly experimental-resolution-limited, jumps in the thickness of the film made of the material. Only very recently six-layer structure was confirmed by resonant x-ray experiment in narrow temperature window between SmC_α and SmC_{FI2} phases (Wang *et al.*, 2010).

The three- and four-layered phases were also found to be stable in device geometry. It was proved that an electric-field-induced transition from the structure of the intermediate three- or four-layered phase to the ferroelectric SmC^* structure occurs in thin glass cells. One can imagine that application of a sufficiently high electric field stabilizes the SmC^* phase. Extensive studies on the electric-field-induced phase transition have been made by study of the dielectric response under a bias field (Hiraoka, Taguchi, *et al.*, 1990; Panarin *et al.*, 1997) and the apparent tilt angle (Hiraoka *et al.*, 1991) conoscopy (Isozaki, Hiraoka, *et al.*, 1992; Fukuda *et al.*, 1994), induced polarization (Hou *et al.*, 1997; Panarin *et al.*, 1997), pyroelectric (Shtykov *et al.*, 2001), and resonant x-ray diffraction (Jaradat *et al.*, 2008) measurements. A particularly interesting result is the field-induced sequential transition SmC_{FI2}^*-SmC_{FI1}^*-SmC^*. This transition behavior is found in *E-T* phase diagrams determined by other experimental methods (Isozaki, Hiraoka, *et al.*, 1992; Fukuda *et al.*, 1994; Shtykov *et al.*, 2001), as shown in Figs. 26(a) and 26(b). Recently Jaradat *et al.* showed that in some materials the four-layered structure undergoes a transition to the three-layered structure at weaker fields before the SmC^* phase occurs (Jaradat *et al.*, 2008). They used resonant x-ray diffraction and found that a diffraction peak at $q/q_0=2/3$ disappeared and instead $q/q_0=3/4$ emerged on application of a field. The predicted *E-T* diagram is similar to those determined by conoscopy and pyroelectric measurements.

E. Present understanding of phase structures

After two decades of intensive studies the picture of all five definitely confirmed phases is finally consistent. The results obtained by a number of complementary techniques proved that the crystallographic unit cells of the SmC^*, SmC_A^*, SmC_{FI1}^*, and SmC_{FI2}^* phases consist of one, two, three, and four layers. The structure within the basic unit of the SmC_{FI1}^* and SmC_{FI2}^* phases is neither clocklike nor Ising, but it has properties of both. Most measurement showed that distortion from the clock model is rather high; apparently the tendency for a uniplanar structure is pronounced in these systems. The orientation of the basic unit cell additionally slowly rotates along the layer normal giving an additional long optical helix. Moreover, it turns out that the SmC_α^* and SmC^* phases are structurally identical, differing only quantitatively in the length of the helical pitch, which is sometimes even smaller than five (Liu *et al.*, 2007) smectic layers in the SmC_α^* phase.

Now the question arises as to the molecular interactions at the origin of these structures.

IV. THEORETICAL MODELING OF PHASES AND PHASE SEQUENCES

An old joke says: a theorist is a person whom nobody believes except himself; an experimentalist is a person whom everybody believes except himself. Following this joke one might think that a theoretical understanding of newly discovered phenomena is not of much importance. It could wait for the maturity of the problem when an extensive set of experimental results would al-

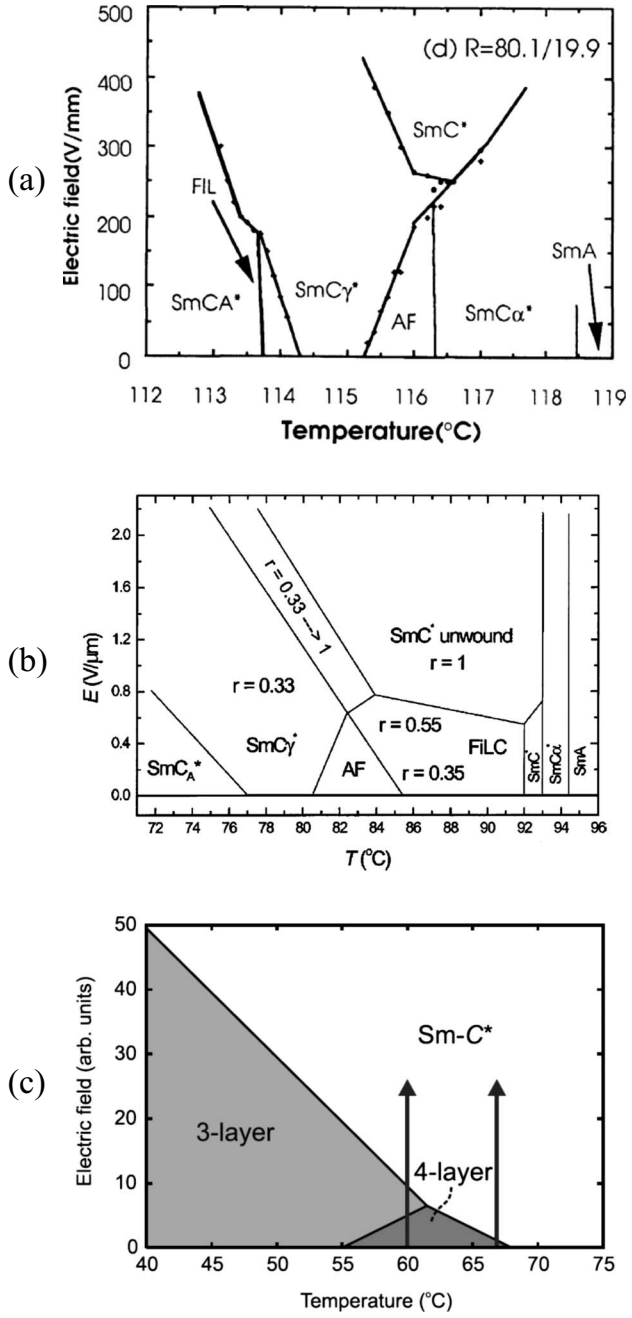

FIG. 26. *E-T* phase diagrams proposed by (a) conoscopy in slightly racemized (R:S=90:10) TFMH-PBC (Fukuda *et al.*, 1994), (b) pyroelectricity in 12OF1M7 (Shtykov *et al.*, 2001), and (c) resonant x-ray diffraction (Jaradat *et al.*, 2008). In (b) *r* is a parameter expressing polar strength, 1 for SmC* and 0 for SmC_A^*.

low for control of the model at the early stage of its development. However, theorists do not share this opinion. The first theories appear almost always immediately after the discovery of a new phenomenon. This was true for antiferroelectric liquid crystals. Various groups, many of them having experience with the theoretical modeling of ferroelectric liquid crystals, became interested in the new materials immediately. Some of the models developed from proposed structures, while the others independently predicted structures that nobody

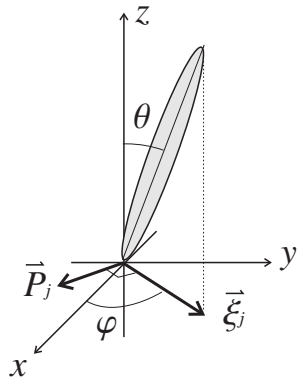

FIG. 27. Tilt $\vec{\xi}_j$ and polarization $\vec{P}_j$ order parameters presented schematically for an average molecule in the *j*th layer.

except the authors believed in. Surprisingly, a few of these predictions were later confirmed by experimental observations, but some are still in their ghostlike form.

The reader wants to know what we theoretically understand today and what can he or she apply for understanding of his or her experimental results. Therefore the theoretical section is organized as follows: We begin with the two most widely used models. The continuous model can be used for understanding of the two phases with less complex structure—the SmC* and the SmC_A^* phase. It is especially useful for the analysis of intralayer structures in displays. The discrete model is more general as it allows for experimentally consistent structures of all observed phases as described in Sec. III.E. The discrete model makes a bridge between microscopic interactions and phenomenological coefficients and gives reasons for the phase sequence dependence on optical purity. Therefore this model is discussed in detail. In addition, we present an overview of other models and approaches for modeling of antiferroelectric liquid crystals.

A. Continuous model

The first theoretical model of the antiferroelectric liquid crystals was proposed almost immediately after their discovery (Orihara and Ishibashi, 1990). Orihara and Ishibashi constructed a theory that was based on the bilayer structure of the antiferroelectric SmC_A^* phase. They assumed that bilayer periodicity is an essential property of these systems and they introduced four two-dimensional order parameters, an approach that had proven successful in a number of studies of antiferroelectric and antiferromagnetic crystalline systems (Kittel, 1951). They introduced two two-dimensional order parameters (Fig. 27) $\vec{\xi}_j$ and $\vec{P}_j$, which are the property of the layer,

$$\vec{\xi}_j = \{n_{jx}n_{jz}, -n_{jy}n_{jz}\},$$
$$\vec{P}_j = \{P_{jx}, P_{jy}\}, \tag{4}$$

and four two-dimensional order parameters as their combinations,

$$\vec{\xi}_{f,j} = \tfrac{1}{2}(\vec{\xi}_{2j+1} + \vec{\xi}_{2j}) \approx \vec{\xi}_f(z),$$

$$\vec{\xi}_{a,j} = \tfrac{1}{2}(\vec{\xi}_{2j+1} - \vec{\xi}_{2j}) \approx \vec{\xi}_a(z),$$

$$\vec{P}_{f,j} = \tfrac{1}{2}(\vec{P}_{2j+1} + \vec{P}_{2j}) \approx \vec{P}_f(z), \tag{5}$$

$$\vec{P}_{a,j} = \tfrac{1}{2}(\vec{P}_{2j+1} - \vec{P}_{2j}) \approx \vec{P}_a(z).$$

The order parameters with the subscript f are nonzero in the ferroelectric SmC^* phase, and order parameters with the subscript a are zero. The opposite is true in the antiferroelectric SmC^*_A phase, where the f parameters are zero and the a parameters are nonzero. As they explicitly describe ferroelectric or antiferroelectric properties of the structure, they are called the ferroelectric (f) and the antiferroelectric (a) tilt and polarization. Although layer order parameters abruptly change from layer to layer, the sum and the difference of order parameters in neighboring layers vary slowly along the layer normal. This allows for the treatment of the order parameters as continuous variables. The free energy was constructed from terms allowed by symmetry considerations. It has a similar form to the Pikin-Indebom free energy for ferroelectric liquid crystals (Pikin and Indebom, 1978). The free energy for the antiferroelectric liquid crystal system is expressed with both types of order parameters with additional coupling terms. Here,

$$\begin{aligned} G = {} & \frac{1}{2}\tilde{a}_a\xi_a^2 + \frac{1}{4}b_a\xi_a^4 + \frac{1}{2}\tilde{a}_f\xi_f^2 + \frac{1}{4}b_f\xi_f^4 + \frac{1}{2}\gamma_1\xi_a^2\xi_f^2 \\ & + \frac{1}{2}\gamma_2(\vec{\xi}_a\cdot\vec{\xi}_f)^2 + \lambda_a(\vec{\xi}_a\times\vec{P}_a) + \lambda_f(\vec{\xi}_f\times\vec{P}_f) \\ & + \frac{1}{2\chi_a}P_a^2 + \frac{1}{2\chi_f}P_f^2 + \frac{1}{2}\tilde{\kappa}_a\left(\frac{\partial\vec{\xi}_a}{\partial z}\right)^2 + \frac{1}{2}\tilde{\kappa}_f\left(\frac{\partial\vec{\xi}_f}{\partial z}\right)^2 \\ & - \tilde{\delta}_a\left(\vec{\xi}_a\times\frac{\partial\vec{\xi}_a}{\partial z}\right)_z - \tilde{\delta}_f\left(\vec{\xi}_f\times\frac{\partial\vec{\xi}_f}{\partial z}\right)_z \\ & + \mu_a\left(\vec{P}_a\times\frac{\partial\vec{\xi}_a}{\partial z}\right)_z + \mu_f\left(\vec{P}_f\times\frac{\partial\vec{\xi}_a}{\partial z}\right)_z. \end{aligned} \tag{6}$$

The first two terms describe the anticlinic ordering of the tilt and the next two terms its synclinic ordering. Terms with coefficients γ_1 and γ_2 give the couplings between the ferroelectric and antiferroelectric tilt order parameters. The parameters λ_a and λ_f give "piezoelectric" couplings of the ferroelectric polarization with the ferroelectric tilt and the antiferroelectric polarization with the antiferroelectric tilt, respectively. The next two terms present the electrostatic contributions of the ferroelectric and antiferroelectric dipolar orderings. The terms with κ_a and κ_f give the energy contributions of elastic deformations of both tilt order parameters. Chiral interactions between molecules in neighboring layers are given by the terms with parameters δ_a and δ_f. In a description of the order parameter within these terms a z component with a zero value is formally added to the initially two-dimensional order parameter, which allows for the correct description of the chiral term using the cross product. The flexoelectric inductions of the ferroelectric and antiferroelectric polarizations are given by the terms μ_f and μ_a, respectively. The temperature-dependent coefficients are

$$\tilde{a}_a = \alpha_a(T - T_a),$$

$$\tilde{a}_f = \alpha_f(T - T_f) \tag{7}$$

and T_a and T_f are the temperatures where the anticlinic and synclinic tilts would appear without the presence of the piezoelectric, elastic, and other interactions. To describe the phase sequence which is always found in antiferroelectric liquid crystals, where the antiferroelectric phase is the phase stable within the lowest temperature range, the temperature T_a should be lower than the temperature T_f.

In order to obtain stable solutions the free energy has to be minimized with respect to all four order parameters. The bilinear coupling of the polarizations with the tilt allows for a straightforward elimination of the polarizations, and the free energy obtains a much simpler form,

$$\begin{aligned} G = {} & \frac{1}{2}a_a\xi_a^2 + \frac{1}{4}b_a\xi_a^4 + \frac{1}{2}a_f\xi_f^2 + \frac{1}{4}b_f\xi_f^4 + \frac{1}{2}\gamma_1\xi_a^2\xi_f^2 \\ & + \frac{1}{2}\gamma_2(\vec{\xi}_a\cdot\vec{\xi}_f)^2 + \frac{1}{2}\kappa_a\left(\frac{\partial\vec{\xi}_a}{\partial z}\right)^2 + \frac{1}{2}\kappa_f\left(\frac{\partial\vec{\xi}_f}{\partial z}\right)^2 \\ & - \delta_a\left(\vec{\xi}_a\times\frac{\partial\vec{\xi}_a}{\partial z}\right)_z - \delta_f\left(\vec{\xi}_f\times\frac{\partial\vec{\xi}_f}{\partial z}\right)_z, \end{aligned} \tag{8}$$

where the parameters are renormalized as

$$a_a = \tilde{a}_a - \chi_a\lambda_a^2, \quad a_f = \tilde{a}_f - \chi_f\lambda_f^2,$$

$$\delta_a = \tilde{\delta}_a + \chi_a\lambda_a\mu_a, \quad \delta_f = \tilde{\delta}_f + \chi_f\lambda_f\mu_f, \tag{9}$$

$$\kappa_a = \tilde{\kappa}_a - \chi_a\mu_a^2, \quad \kappa_f = \tilde{\kappa}_f - \chi_f\mu_f^2.$$

Orihara and Ishibashi (1990) neglected the terms that considered derivatives of the tilt order parameters and therefore limited the analysis to nonmodulated structures. Žekš and Čepič later analyzed possible structures and their stability if elastic and chiral interactions are not neglected and found phases that were helically modulated (Žekš and Čepič, 1993). A year later the same structures were found by Lorman *et al.* independently (Lorman *et al.*, 1994). Recently, the model was also analyzed in regions of coefficient values where such simple modulated structures are not stable and an incommensurate modulated structure was found (Čepič and Žekš, 2007).

We now describe the structures allowed by the continuous model. The experimental observations have shown homogeneous order with helical modulation but no higher periodicities in samples. Therefore, the constant amplitude approximation seems reasonable and the magnitude of both order parameters is considered as constant, θ_a and θ_f. In addition, a simple helical modu-

lation with only one wave vector q is also included in the trial solution (ansatz) as well as a general but fixed phase difference φ_0 between the ferroelectric and antiferroelectric order parameters in structures where both order parameters exist. We call solutions of this type simply modulated phases in the following as they are described by a single wave vector of modulation q:

$$\vec{\xi}_a = \theta_a\{\cos qz, \sin qz\},$$
$$\vec{\xi}_f = \theta_f\{\cos(qz+\varphi_0), \sin(qz+\varphi_0)\}. \tag{10}$$

Using Eq. (10) the free energy adopts a simpler form

$$G = \tfrac{1}{2}(a_a - 2\delta_a q + \kappa_a q^2)\theta_a^2 + \tfrac{1}{4}b_a\theta_a^4 + \tfrac{1}{2}(a_f - 2\delta_f q + \kappa_f q^2)\theta_f^2 + \tfrac{1}{4}b_f\theta_f^4 + \tfrac{1}{2}\gamma_1\theta_a^2\theta_f^2 + \tfrac{1}{2}\gamma_2\theta_a^2\theta_f^2(\cos\varphi_0)^2. \tag{11}$$

Minimization of the free energy (11) is rather simple. Five different structures are stable depending on the values of the model coefficients: One solution describes the nontilted SmA phase. There are four different solutions that describe helically modulated phases with only one period of modulation and one solution with a more complex structure where the competition between two different favorable periods of modulation results in a solitonlike structure not commensurate either with the layer thickness or with either of the two favorable periods. In the following, the short description of solutions is given.

1. The nontilted SmA phase

The trivial solution of the free-energy minimization equations is stable when both θ_a and θ_f are zero. It is stable at the highest temperatures and it develops to one of the two tilted structures, the SmC* or the SmC_A^* phase, below the transition temperature. The dynamical properties of the system (Žekš *et al.*, 1991) reveal the character of the phase below SmA. In all nontilted systems having tilted phases at lower temperatures two types of tilt fluctuations exist—synclinic and anticlinic. The fluctuation that has the lower frequency and condenses at higher temperature defines the nature of the tilted phase below the SmA phase. If the synclinic fluctuations have lower frequency, the ferroelectric SmC* phase becomes stable as the temperature decreases and the antiferroelectric SmC_A^* phase becomes stable if the anticlinic fluctuation is the one with the lower frequency.

2. The simply modulated SmC* phase

For certain sets of model coefficients and a certain range of temperatures, the stable solution requires that θ_a is zero and θ_f is nonzero. The structure is recognized as the structure of the ferroelectric SmC* phase predicted by Meyer and synthesized by his co-workers already in 1974 (Meyer *et al.*, 1975). The molecules in each layer are tilted by θ_f, which increases with decreasing temperature and the structure is helically modulated with the wave vector $q_f = \delta_f/\kappa_f$, which is temperature independent. The temperature independence of the wave vector q_f is actually not consistent with experiments, but inclusion of higher-order chiral terms can account for this inconsistency. We do not discuss this detail, as our attempt is to discuss only the main features of the simplest possible continuous model.

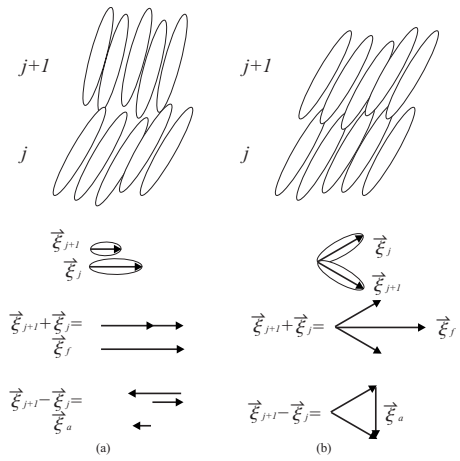

FIG. 28. In the ferrielectric $\mathrm{SmC}_{\mathrm{SM}}^*$ phase both order parameters, $\vec{\xi}_f$ and $\vec{\xi}_a$, are nonzero. (a) For $\gamma_2<0$ the order parameters are parallel, molecules are tilted within the same plane, but the magnitude of the tilt differs in odd and even layers. (b) For $\gamma_2>0$ the order parameters $\vec{\xi}_f$ and $\vec{\xi}_a$ are perpendicular. The magnitude of molecular tilts is equal in all layers; however, the directions of tilts in odd and even layers are at an angle.

3. The simply modulated SmC_A^* phase

The solution where θ_a is nonzero and θ_f is zero describes the antiferroelectric phase with the wave vector of helicoidal modulation $q_a = \delta_a/\kappa_a$. The temperature region of its stability depends on the choice of the temperature T_a and the ratio of the model coefficients b_a/b_f. As both transition temperatures T_f and T_a and the values of the fourth-order coefficients b_f and b_a define the general phase sequence, the model also describes simple ferroelectric systems where the antiferroelectric phase does not develop.

4. The two simply modulated ferrielectric $\mathrm{SmC}_{\mathrm{SM}}^*$ phases

The model also allows for two phases with one wave-vector modulation and both order parameters different from zero. The phase difference φ_0 between the two order parameters is well defined only in these structures. The minimization of the free energy with respect to φ_0 allows for two different structures. The uniplanar structure is characterized by having the ferroelectric and antiferroelectric order parameters in the same plane ($\varphi_0 = 0$ or π), so all layers are tilted to the same plane defined by the layer normal and the tilt [Fig. 28(a)]. It is stable for negative values of the coefficient γ_2.

For positive values of the coefficient γ_2 the structures where the ferroelectric $\vec{\xi}_f$ and antiferroelectric $\vec{\xi}_a$ order parameters lie in two mutually perpendicular planes ($\varphi_0 = \pm\pi/2$) are stable. The solution presents the struc-

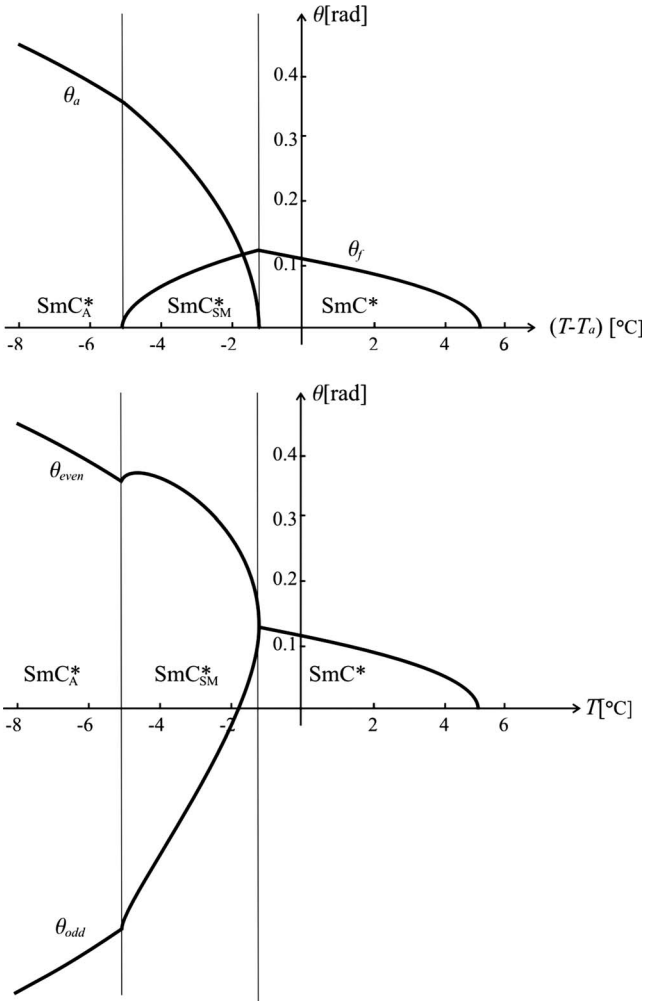

FIG. 29. Tilt dependence on temperature for $\gamma_2<0$. (Top) The temperature dependence of the ferroelectric $\vec{\xi}_f$ and the antiferroelectric $\vec{\xi}_a$ order parameters for $\gamma_2<0$. (Bottom) Corresponding tilts in even and odd smectic layers. The negative sign of the tilt magnitude in the odd layers means the tilt is in the opposite direction to the tilt in even layers.

ture where the tilts in neighboring layers have the same magnitude but their directions are at an angle [Fig. 28(b)]. The temperature development of both order parameters has the same form for both structures,

$$\theta_a^2 = \frac{(a_f - 2\delta_f q + \kappa_f q^2)\gamma - (a_a - 2\delta_a q + \kappa_a q^2)\beta_f}{\beta_a\beta_f - \gamma^2},$$
$$\theta_f^2 = \frac{(a_a - 2\delta_a q + \kappa_a q^2)\gamma - (a_f - 2\delta_f q + \kappa_f q^2)\beta_a}{\beta_a\beta_f - \gamma^2}, \quad (12)$$

where $\gamma = \gamma_1 + \gamma_2 \cos\varphi_0$ and the wave vector q is the result of the free-energy minimization. The temperature range of phase stability lies between the stability range of the ferroelectric and antiferroelectric phases, providing the model parameter γ_2 is large enough to bind the directions of both order parameters (Figs. 29–31).

Although these two structures were ruled out as candidates for the structure of the SmC^*_γ phase by the first direct resonant x-ray observations, the structure of the

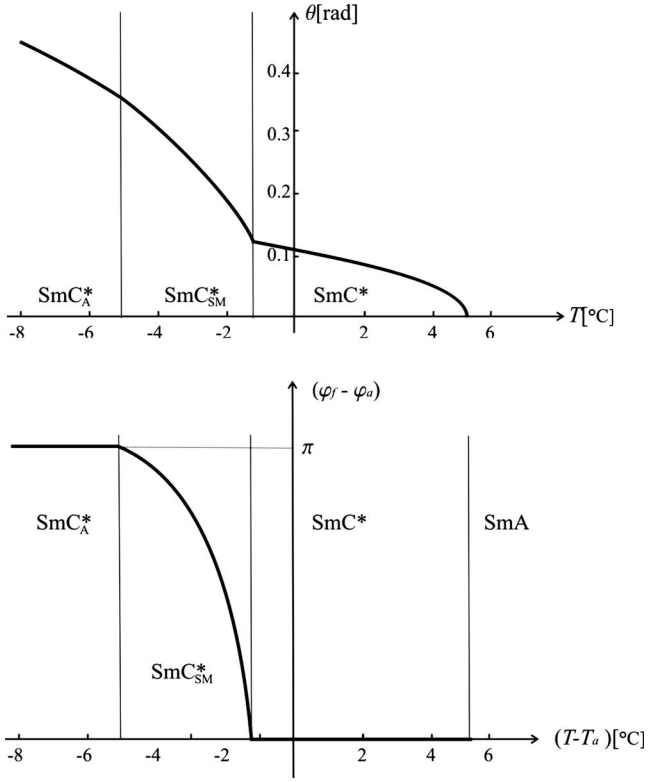

FIG. 30. Tilt dependence on temperature for $\gamma_2>0$. (Top) The temperature dependence of the ferroelectric $\vec{\xi}_f$ and antiferroelectric $\vec{\xi}_a$ order parameters for $\gamma_2>0$. (Bottom) Corresponding angle between directions of the tilts in even and odd smectic layers.

unwound ferrielectric SmC^*_{SM} phase for the coupling $\gamma_2>0$ develops if an electric field is applied to the antiferroelectric SmC^*_A phase.

5. The incommensurate SmC^*_{IC} phase

The phase sequence depends on the choice of model coefficients. Comparison to experiments gives the theo-

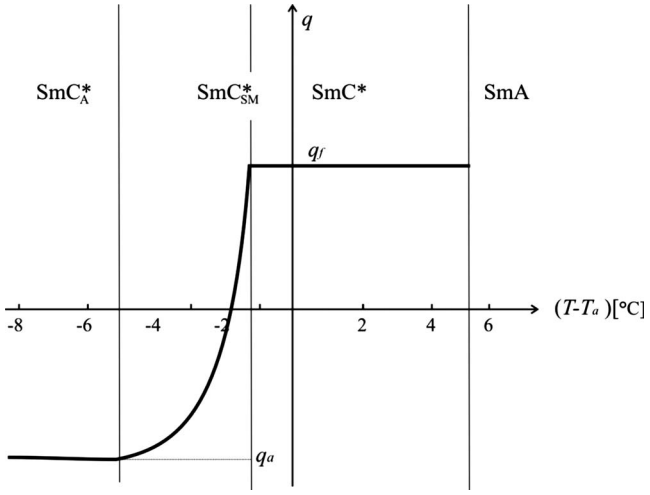

FIG. 31. Temperature dependence of the wave vector q for the simple modulation is qualitatively equal for both signs of γ_2.

rist a hint about the magnitudes and signs of the coefficients. Therefore the space of model coefficients is usually analyzed in order to find conditions for which different phases are stable (Žekš and Čepič, 1993; Lorman *et al.*, 1994; Olson *et al.*, 2002; Hamaneh and Taylor, 2004). However, detailed analysis of the model coefficients space revealed another curiosity: only simply modulated structures cannot be stable for any set of model coefficients.

A consideration can give us a hint. Imagine the system which could be described by the negligible coupling $\gamma_2 = 0$. This condition means that the ferroelectric order parameter $\vec{\xi}_f$ does not influence the antiferroelectric order parameter $\vec{\xi}_a$ even if both of them exist. Therefore they form two independent generally different helices, the ferroelectric and the antiferroelectric ones, guided by the competition in chiral and elastic properties expressed by considering the two order parameters independently. If the coupling in the system is weak, the system solves the frustration between two different helices by formation of domains with a single wave vector separated by domains where the order parameters flip from one relative orientation to the opposite one. Although the problem was pointed out long ago (Žekš and Čepič, 1993) a more detailed analysis with solutions obtained within the constant amplitude approximation was performed only recently (Čepič and Žekš, 2007). However, the structure allowed by the model seems not a candidate for any real structure found in antiferroelectric liquid crystals, and it can be considered as one of the ghostlike solutions, possibly applicable in completely different systems (Pociecha *et al.*, 2003).

The continuous model and its structures have a few important flaws. First, the high-temperature phase, the SmC^*_α phase, which often develops through a continuous transition from the nontilted SmA phase, could not be reproduced within this model. The higher-temperature tilted phase is always either the SmC^* phase or the SmC^*_A phase. Other structures become stable only at lower temperatures where the tilt is already present. Second, the resonant x-ray scattering experiments have shown that two distinctly different intermediate phases exist, the SmC^*_{FI2} phase with four-layer periodicity and the SmC^*_{FI1} phase with three-layer periodicity. Reproduction of both phases within the continuous model would require introduction of many new order parameters. The required number of independent tilt and polar order parameters is the same as the basic periodicity of the phase. The number of coupling terms between these order parameters that enter the free energy is even higher, making theoretical equations extremely hard to manage. Finally, the resonant x-ray method has shown that of the four different structures allowed by the continuous model only the SmC^* and the SmC^*_A phases are consistent with experiments. Therefore this model cannot satisfy expectations.

The model is still useful for consideration of various phenomena within these two phases: the structures formed in the cell, under the application of an electric field (Parry-Jones and Elston, 2001), where the electric field induces the structure of the unwound bilayer ferrielectric phase, the structure of defects, and more. Whenever one faces a situation where it is expected that the order parameters (ferroelectric, antiferroelectric, or both) do not change significantly at distances comparable to the molecular length or the layer thickness, the continuous approach is the most appropriate.

B. Simple clock model

Limitations of the continuous model having the form (6) are quoted at the end of the previous section. So, is it possible to construct free energy which allows for additional structures without introducing new order parameters?

In the following we shall present an alternative approach to the continuous modeling of antiferroelectric liquid crystals—the discrete model. We discuss two variants of discrete modeling: the simple clock and the distorted clock models.

The basic idea of the discrete approach is as follows:

- The interlayer and intralayer interactions are considered separately.
- Instead of elastic deformations which allow for gradual changes of order parameters only, abrupt and significant changes of order parameters from layer to layer are allowed.
- Elastic deformations are not written in derivatives but as couplings of order parameters in neighboring layers.
- Interactions with more distant layers than neighboring layers are taken into account.

Orihara and Ishibashi (1990) had sown the seed for the discrete approach using the continuous model. Soon after publication of the continuous model for antiferroelectric liquid crystals Sun *et al.* published the analysis of interlayer interactions (Sun *et al.*, 1993) that led to the proposed form of the model (6). They wrote expressions for elastic and chiral terms in the form of differences between tilt order parameters in neighboring layers up to the distance to the next-nearest neighbors. These expressions were the basis of terms that phenomenologically express interlayer interactions within the discrete description of the free energy. Their analysis showed that the continuous description is allowed only in systems in which next-nearest layers prefer parallel (synclinic) tilt directions. However, they did not consider the other possibility: the favorable orientation of tilts in the next-nearest layers as anticlinic.

Favorable anticlinicity in next nearest layers introduces frustration into the system. Favorable ferroelectric or antiferroelectric order, even a combination of both of them, as present in solutions of the continuous model, is always in contradiction with anticlinicity in the next-nearest layers. In all solutions of the continuous model tilts in next-nearest layers are parallel [Figs. 32(a)–32(c)].

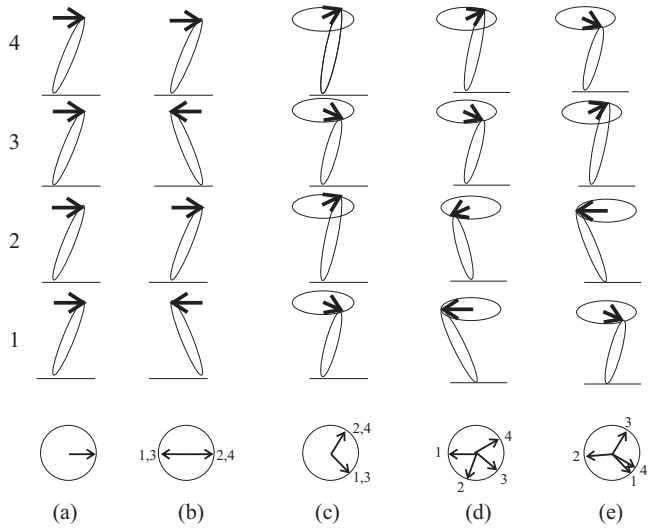

FIG. 32. For favorable anticlinic tilts in neighboring layers all bilayer structures (a)–(c) are disfavored. The short helix allows for the reduction of frustration as the neighboring layer slightly deviates from the favorable (d) synclinicity or (e) anticlinicity; however, the next-nearest layers slightly deviate from the favorable anticlinicity.

The system can suppress frustration by modulation of the order parameters from layer to layer. The tilt order parameter can vary in magnitude, in direction, or in both. If variation of the magnitude were important, the x-ray measurements should have shown variations of the smectic layer thickness. No such observations have been reported so far. Therefore we conclude that structures with amplitude variation are not present at least not in bulk. The next possibility is variation of the tilt direction. Ising models, which will be discussed later, assumed that the tilt is bound to one plane defined by the layer normal and the tilt direction. Such structures are said to be uniplanar (Rovšek *et al.*, 2000). This assumption means that tilts in neighboring layers can be either parallel (the difference in tilt directions in neighboring layers, also called the phase difference, is equal to zero) or antiparallel (the phase difference is equal to π).

In addition, there are two questions that need to be answered if one wants to pursue the uniplanar structures for the missing SmC^*_α phase:

- What is the origin of the uniplanar constraint? Observations of properties of ferroelectric and antiferroelectric phases did not reveal any reasons for the constraint of the tilt to one plane only.
- How can the transition from the nontilted SmA phase to SmC^*_α be continuous, as experimentally observed? If the structure of the phase leads to different interactions between neighboring layers because interfaces can be both parallel, both antiparallel, or combined and therefore the magnitude of the tilt in these layers should differ, the phase could develop only through a discontinuous phase transition from the nontilted SmA phase or at lower temperatures in bulk samples.

As the two questions cannot be answered satisfactorily one should discuss a last possibility: how to avoid or at least lessen the competition between favorable interactions with nearest and next-nearest layers: the out-of-plane tilt modulation. The argument is the following. A structure where the directions of tilts in neighboring layers form a large angle can result in an angle close to π in the next-nearest layers [Figs. 32(d) and 32(e)]. Put simply, if the system "pays" in nearest layers by not having exactly parallel or antiparallel tilts, it benefits by the tilts being almost antiparallel or at least far from parallel in the next-nearest layers. As a final effect, the free energy of the structure can be lower than the free energy of structures formed in the uniplanar way.

This understanding of structures is essentially different from that of the continuous approach. The large angle of a few tenths of degrees formed by tilt directions in neighboring layers contradicts the concept of elastic energy connected to small changes of order parameter from layer to layer. Although the change of the tilt direction from layer to layer is already included in the continuous model, it could still be considered as an internal structure within the crystallographic unit cell of two layers.

Another question concerns interlayer interactions which do not significantly decrease with distance. But if interactions between nearest layers originate in different interactions that have opposite effects they may cancel out, at least partially. If so, the interactions with next-nearest layers may become comparable to interactions with nearest layers. This possibility for the structure was first reported by Čepič and Žekš (1995). The microscopic origin of the interaction will be discussed later in Sec. IV.C when the reader will already be acquainted with the model coefficients and their effects on the structure.

The free energy in its simplest form that includes the considerations above consists of a few terms only and is expressed in tilt order parameters. Tilt order parameters (Fig. 27) are a layer property and are allowed to vary significantly from layer to layer. Due to the significant changes allowed, the classical expression for the elastic energy is replaced by a phenomenologically expressed direct interaction between layers in a form that allows large changes of direction from layer to layer. The interactions are separated to intralayer interactions and interlayer interactions extending to the next- and next-next-nearest layers. Each layer interacts with the layers above and below itself. The free energy is then

$$G_j = \tfrac{1}{2}\alpha_0(T - T_0)\vec{\xi}_j^2 + \tfrac{1}{4}b_0\vec{\xi}_j^4 + \tfrac{1}{4}a_1(\vec{\xi}_{j+1}\cdot\vec{\xi}_j + \vec{\xi}_j\cdot\vec{\xi}_{j-1}) + \tfrac{1}{4}f_1(\vec{\xi}_j\times\vec{\xi}_{j+1} + \vec{\xi}_j\times\vec{\xi}_{j-1})_z + \tfrac{1}{16}a_2(\vec{\xi}_j\cdot\vec{\xi}_{j+2} + \vec{\xi}_j\cdot\vec{\xi}_{j-2}). \quad (13)$$

The first two terms, rewritten from the continuous model, comprise interactions between molecules from the same layer and account for the main tilt dependence on the temperature. The subscript zero denotes the interactions within the same layer. The third term a_1 describes the achiral interaction between the nearest-

neighboring layers. The subscript 1 reminds the reader that the interactions considered are in the first-neighboring layer. In its simplest bilinear form it can only account for favorable anticlinicity ($a_1>0$) or synclinicity ($a_1<0$). The term f_1 describes the chiral interactions with nearest-neighboring layers. The sign of the coefficient depends on the handedness of the sample, i.e., on the enantiomeric excess. It is zero for racemic mixtures. Although chiral interactions are in general considered as very weak, one is not allowed to exclude them, as experiments clearly show the large influence of optical purity on structures and phase sequences. The last term a_2 gives achiral interlayer interactions to the second neighboring layers. It might favor synclinicity ($a_2<0$), which is a required condition for the formation of bilayer primitive cells. If anticlinicity is favored ($a_2>0$), competition between nearest-layer and next-nearest-layer interactions takes place. For strong enough competition ($a_2>|a_1|$), the new structure with large angles between tilt directions in neighboring layers becomes stable [Figs. 32(d) and 32(e)].

As in the continuous model, we search for a solution with constant magnitude of the tilt in all layers, consistent with the uniform layer thickness reported by x-ray observations (Isozaki, Hiraoka, *et al.*, 1992). For the simplest structure we assume that the angle between tilt directions in neighboring layers is constant as well,

$$\vec{\xi}_j = \theta\{\cos(j\alpha+\varphi_0),\sin(j\alpha+\varphi_0)\}, \tag{14}$$

where θ is the magnitude of the tilt, α is the phase difference, φ_0 is the angle the tilt in the zeroth layer forms with the arbitrary direction in space chosen as a coordinate axis, and j runs over all layers in the sample. The free energy (13) adopts the form

$$G_j = \tfrac{1}{2}\alpha_0(T-T_0)\theta^2 + \tfrac{1}{4}b_0\theta^4 + \tfrac{1}{2}a_1\theta^2\cos\alpha + \tfrac{1}{2}f_1\theta^2\sin\alpha + \tfrac{1}{8}a_2\theta^2\cos 2\alpha. \tag{15}$$

If one neglects the chiral interaction, the minimization of the free energy with respect to the phase difference α leads to three different tilted structures. Conditions for their stability are simple,

$$\begin{aligned} &\mathrm{SmC}^*: && \frac{a_1}{a_2} \leqslant -1, \quad \alpha = 0, \\ &\mathrm{SmC}_A^*: && \frac{a_1}{a_2} \geqslant 1, \quad \alpha = \pi, \\ &\mathrm{SmC}_\alpha^*: && -1 < \frac{a_1}{a_2} < 1 \quad \alpha = \arccos\left(-\frac{a_1}{a_2}\right). \end{aligned} \tag{16}$$

Two structures present in the continuous model can easily be recognized. The solution with $\alpha=0$ presents a structure with synclinic neighboring layers of the SmC phase. The solution with $\alpha=\pi$ presents a structure with anticlinic neighboring layers of the SmC_A phase. Both structures can be found in racemic mixtures; due to the absence of chirality, polarization is not present and only clinicity can be observed. With inclusion of the weak chiral term, the phase difference is distorted from 0 or π for an angle δ,

$$\delta = \pm\frac{f_1}{|a_1|+a_2}, \tag{17}$$

where the positive sign gives the deviation from 0 for the ferroelectric structure and for positive f_1, while the negative sign gives the deviation from π for the antiferroelectric structure and for the positive sign of f_1. Therefore the helical modulations have opposite signs in the chiral ferroelectric SmC* and antiferroelectric SmC_A^* phases of the same material, as is consistent with experimental observations.

The third structure is helically modulated even in the absence of chirality and the period of modulation extends over a few layers only. The modulation is not the result of the chiral interactions and is, in the absence of chiral terms, doubly degenerate. If chiral interactions are present, the degeneracy is lifted and the helical modulation has only one sense defined by the chirality of the molecules. This was suggested as a possible structure for the SmC_α^* phase. It is consistent with experimental observations: the molecules are tilted, due to the sublight wavelength pitch of the helical modulation the optical properties do not reveal optical rotatory power or other indications of the helical modulation such as selective reflection, and the properties are due to averaging effects similar to the properties of the SmA phase. The phase can be stable in the temperature window below the nontilted SmA phase and can evolve continuously from SmA. Direct resonant x-ray scattering experiments have confirmed this helicoidally modulated structure of the SmC_α^* phase with pitch extending over a few layers only (Mach *et al.*, 1998, 1999). Later detailed measurements in various systems have shown that the pitch in the SmC_α^* phase can have any incommensurate values including very small values close to three layers (Liu *et al.*, 2007) as well as rather large values around 20 layers (Johnson *et al.*, 1999).

Before direct resonant x-ray observations were made the short-pitch model for the SmC_α^* phase was not widely accepted. However, there were some indirect indications that the suggested structure could allow for an explanation of the oscillating behavior of the difference between the ordinary and extraordinary refraction indices as temperature decreases found in the free-standing film in the SmC_α^* phase (Bahr *et al.*, 1995; Schlauf *et al.*, 1999) (Fig. 33, top). The reasoning is the following. The free-standing film consisting of a few tenths of layers is thick enough that helices of the short-pitch SmC_α^* phase develop. When the pitch is commensurate with a number of film layers, the average optical indicatrix is uniaxial with the axis along a layer normal. If the pitch is not commensurate, the remnant part of the helix contributes to the biaxiality of the indicatrix and to the difference between the largest and smallest refraction indices. This difference is measured ellipsometrically. The film is oriented using a small electric field perpendicular to the layer normal, which defines the eigendirections of

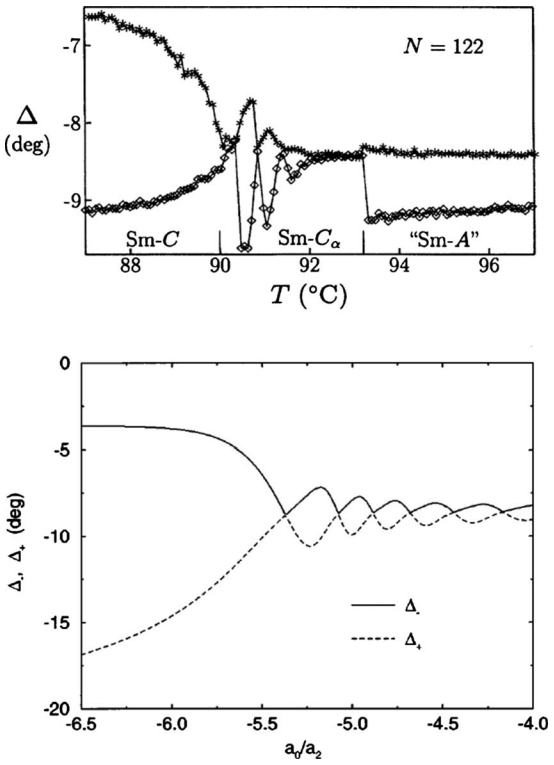

FIG. 33. Comparison of theoretical analysis and experimental observations of phase retardation. (Top) The measurement of the phase retardation between the ordinary and the extraordinary ray for a freestanding film consisting of 122 layers in the SmC^*_α phase. From Bahr *et al.*, 1995. (Bottom) The calculation of the phase difference based on the theoretical model of the SmC^*_α phase for the same number of layers. From Rovšek *et al.*, 1996.

the optical indicatrix. The oblique light perpendicular to the electric-field direction is incident on the film and the phase difference between the ordinary and extraordinary rays is measured for two opposite directions of the electric field. The oscillating behavior of the phase difference indicates the increase and the decrease of the birefringence as the temperature decreases due to the temperature dependence of the helical pitch length and its consequent remnant part (Rovšek *et al.*, 1996).

The model was further developed to account for the whole phase sequence and the microscopic origin of the values and signs of the model coefficients was discussed (Žekš and Čepič, 1998; Škarabot *et al.*, 1998). To account for the whole phase sequence of MHPOBC including the SmC^*_α and SmC^*_γ phases within one model and a single set of model coefficients, the discrete model was merged with the continuous one rewritten in a discrete form. The idea was the following: the continuous model successfully reproduced three of the phases, the SmC^*, the SmC^*_A, and the SmC^*_γ between them. What was missing was the phase between the SmC^* and the SmA, which was now occupied with the short-pitch structures proposed by the discrete model (Čepič and Žekš, 1995).

The discrete form of the continuous model is obtained by inserting definitions of the ferroelectric and antiferroelectric order parameters (5) in the free energy (6) as discussed by Sun *et al.* (1993). The coupling of the ferroelectric and antiferroelectric order parameters expressed in layer order parameters suggested another term which describes the biquadratic coupling between neighboring layers,

$$\tfrac{1}{4} b_Q (\xi_j \cdot \xi_{j+1})^2. \tag{18}$$

Here the model coefficient b_Q can be positive, favoring perpendicular orientation of tilts in neighboring layers, or negative, favoring parallel or antiparallel orientation of tilts in neighboring layers. A positive value of b_Q leads to a new form of frustration even when $a_2 < 0$ and interactions between next-nearest layers favor synclinicity. It was shown that electrostatic quadrupolar interactions lead to a positive sign of b_Q (Čepič and Žekš, 2007). If the coefficient a_1 changes sign from negative to positive and a_2 from positive to negative as temperature decreases, the phase sequence found in MHPOBC can be reproduced. However, the structure proposed for the SmC^*_γ phase by the continuous model was soon ruled out by direct structural observations (Mach *et al.*, 1998); therefore the combinations of the two models was recognized as incorrect.

The structures with short pitch are also called clock structures, following the well-known model from solid-state physics (Chaikin and Lubensky, 1995), and also from the pictures of the structures, since the bird's-eye view of the set of molecules representing the average molecule in the layer are reminiscent of a clock hand at various hours [Figs. 19(c) and 20(c)]. Therefore, the same observation that unambiguously proved the existence of large changes in direction from layer to layer; i.e., the short-pitch helical structure for the SmC^*_α phase, ruled out the bilayer model of ferrielectric SmC^*_γ or as it is called the SmC^*_{FI1} phase. The structures suggested for the intermediate phases by resonant x-ray investigations were clock structures of commensurate numbers of layers (three and four), which seemed the most simple and consistent with the resonant x-ray data.

C. Origin of interactions

In the model presented above we discussed the effects of different terms and the signs of model coefficients. However, we have not discussed the origin of the terms and their coefficients, why signs are positive or negative, and why they change with temperature. All interactions were simply described as effective interactions expressed in tilts. Each term that appears in the free energy (13) has its origin in intermolecular interactions.

The first two terms originate in van der Waals attractive interactions and repulsive steric interactions between molecules in neighboring layers. Both coefficients include the essential competition between the entropic desire for disorder and the best packing to reduce voids between molecules within the same layer. The expression is the same as in the continuous model (Pikin and

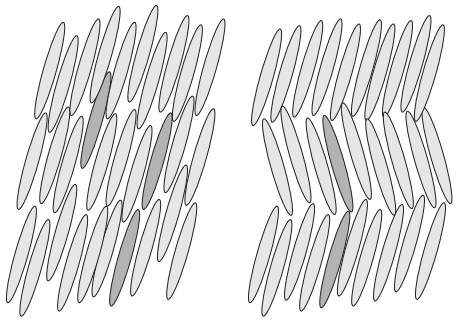

FIG. 34. The schematic presentation of microscopic origins for bilinear interactions between nearest layers. (a) Molecules that diffuse through layers promote the same direction of the tilt. (b) Distances between parts of the molecules in neighboring layers are shorter for anticlinic orientation than for synclinic.

Indebom, 1978), but in continuous models the contribution to the free energy is not separated into intralayer and interlayer interactions.

The achiral interlayer interactions given by the coefficient a_1 have three different sources. The molecular diffusion or partial interpenetration between neighboring layers promotes parallel tilts in interacting layers as hard molecular cores cannot bend and adapt to different directions of tilts in neighboring layers [Fig. 34(a)]. As diffusion is the consequence of entropic effects it is reasonable to expect that this contribution decreases with decreasing temperature. The contribution is present in chiral samples and racemic mixtures and as it favors parallel ordering in neighboring layers it contributes negatively to the coefficient a_1.

Molecules in neighboring layers are attracted by van der Waals forces as well. It was shown (Bruinsma and Prost, 1994) that the anisotropic properties of layers do not influence interlayer interactions if layers possess an ideal liquid order, i.e., without any positional correlations between molecules. This is valid for van der Waals attraction as well as for electrostatic interactions. Therefore, the tilt orientation should not be affected by the van der Waals and electrostatic interactions between layers. However, in any material the ideal positionally noncorrelated disorder is never realized. At least some positional correlations can be expected even for molecules in neighboring layers, but if this is the case, then for long molecules one has to consider that distances between parts of molecules are very different and the closer parts feel a stronger attraction [Fig. 34(b)]. The antiparallel ordering of positionally correlated molecules becomes more favorable as the effective distances between parts of the interacting molecules become shorter. The contribution seems not to change significantly with decreasing temperature and as it favors antiparallel order it contributes positively to the coefficient a_1.

The last contribution to a_1 has an achiral symmetry but is present in chiral samples only. The tilt induces polarization which is proportional to the tilt of chiral molecules. Therefore the tilted chiral molecules possess effective dipole moment perpendicular to the tilt and these dipoles interact electrostatically. Although the dipoles from neighboring layers if they are oriented along the layer do not interact in the absence of positional correlations (Bruinsma and Prost, 1994), it was shown that if simple positional correlations are assumed antiparallel dipoles are favored (Čepič and Žekš, 1997). As the polarization is perpendicular to the tilt and its direction is defined by the molecular chirality, the favorable antiparallel orientation of dipoles is transferred to the favorable antiparallelism of the tilt. The interaction is also not significantly influenced by the temperature. Because of its favored antiparallelism it contributes positively to a_1.

Now we can see that as the temperature decreases, the negative contribution to the a_1 term decreases, the coefficient may become very small and even change sign. The reasoning is consistent with the experimental observation that antiferroelectric SmC_A^* is always stable at the lowest temperature in the phase sequence.

The molecular interpenetration, i.e., diffusion, does not contribute to the interactions in the next-nearest layers. As one can assume at least weak positional correlations to the next-nearest layers we are left with two contributions mentioned before that both favor antiparallel ordering. From this it seems that it is natural that the coefficient a_2 is always positive. However, only antiferroelectric liquid crystals are materials where the interactions to nearest layers become weak enough and frustrating competition between them takes place.

We now spend a few words on the chiral interaction given by the f_1 term. This term is the discrete form of the usual Lifshitz term in the continuous model (Pikin and Indebom, 1978). As mentioned, this is not the only interaction that depends on chirality. The piezoelectric coupling between the tilt and the polarization is of chiral origin as well. However, the origin of the f_1 term is the van der Waals interactions. Various molecular bonds and their polarizability contribute to these. If the molecule is chiral, then the van der Waals field around the molecule reflects its chiral symmetry. Another chiral molecule found in this field therefore adopts an orientation which due to chirality is not strictly parallel or antiparallel to the molecule that is the source of the van der Waals field. Since the chiral center is not a large part of the molecule it seems that the direct chiral interaction given by the f_1 term is weak. As the effect of the term favors nonparallelism of molecules, it influences the magnitude of the phase difference α. This influence is probably small but cannot be separated from the influences of other interactions, at least not in the SmC_α^* phase. However, the important effect is that chiral interactions lift the degeneracy between left- and right-handed helical modulations.

D. Distorted clock model

The resonant x-ray measurements posed a new question for theoretical understanding. What is the reason

for lock in to three and four layers? Are there any interactions present in the system that extend over longer range than next nearest layers? The nature of interactions discussed previously unfortunately did not give any reasons for interactions of longer range. Therefore it seems that one has to consider the effect of polarization in the free energy explicitly. The free energy has to include the chiral piezoelectric coupling to make the effect of chirality more transparent. Interlayer polar interactions should be taken into account as well. As the studies of odd-even number of layers effects in free-standing racemic ferroelectric liquid crystalline films revealed the possible importance of the flexoelectric interactions (Andreeva *et al.*, 1999), one should consider them. The flexoelectric interaction is not of chiral origin and can be significant for systems formed of any incompletely symmetric molecules. The flexoelectric term

$$\mu\left(\vec{P}\cdot\frac{\partial\vec{\xi}}{\partial z}\right) \tag{19}$$

was always considered as unimportant in continuous models, but for large changes of the tilt direction it is not necessarily so. The discrete form of the free energy including polarization explicitly is (Čepič and Žekš, 2001)

$$\begin{aligned} G_j = {} & \tfrac{1}{2}\alpha_0(T-T_0)\xi_j^2 + \tfrac{1}{4}\beta_0\xi_j^4 + c_p(\vec{\xi}_j\times\vec{\eta}_j)_z + \tfrac{1}{2}b_0\vec{\eta}_j^2 \\ & + \tfrac{1}{4}a_1(\vec{\xi}_j\cdot\vec{\xi}_{j+1}+\vec{\xi}_j\cdot\vec{\xi}_{j-1}) + \tfrac{1}{4}f_1(\vec{\xi}_{j+1}\times\vec{\xi}_j+\vec{\xi}_j\times\vec{\xi}_{j-1}) \\ & + \tfrac{1}{4}b_1(\vec{\eta}_j\cdot\vec{\eta}_{j+1}+\vec{\eta}_j\cdot\vec{\eta}_{j-1}) + \tfrac{1}{2}\mu\vec{\eta}_j\cdot(\vec{\xi}_{j+1}-\vec{\xi}_{j-1}). \end{aligned} \tag{20}$$

In this expression the order parameter η was introduced in order to lift the confusion about the polarization origin. The polarization appears due to the ordering of molecules that have a shape with geometric polar symmetry (Čepič and Žekš, 2001) given by the order parameter η. The polarization of the layer is directly proportional to the ordering of geometric dipoles,

$$\vec{P}_j = P_0\vec{\eta}_j. \tag{21}$$

The polarization P_0 depends on the molecular properties and is hidden in the piezoelectric coefficient c_p. (Čepič and Žekš, 2001) were to reduce the confusion about the origin of the polar ordering: it is not the electrostatic interactions but mainly van der Waals and steric interactions. Because the electrostatic polarization within the layer is directly proportional to the extent of the geometric polar ordering, one calls the order parameter $\vec{\eta}$ simply the *polarization*. The interactions between the layer polarizations extend to more distant layers, at least to the next-nearest layers. However, it was shown (Emelyanenko and Osipov, 2003) that flexoelectric interactions have similar effects as dipolar interactions to the next-nearest layers, but they are expected to be more important. Therefore we limit electrostatic interactions to the same layer and to nearest layers only (b_0 and b_1). The coefficients are both positive. b_0 is positive because the polarization is not the primary order parameter and b_1 is positive because dipolar interactions favor antiparallel ordering of dipoles. The coefficients of terms expressed in tilts (a_1,f_1) include only steric (diffusion) and van der Waals interactions.

The flexoelectric interaction includes the fact that the direction of the tilt in the layers above and below the considered layer influences hindered molecular rotation and consequently induces polarization in the layer. The flexoelectric term μ is written in a discrete form; here the difference in tilts above and below is coupled to the polarization. In the expression for the free energy the interactions with the next-nearest layers expressed in tilts are neglected as well, as it is expected that the van der Waals interactions to the next-nearest layers are of the same magnitude as or even smaller than the dipolar direct interactions.

The elimination of the polarization revealed some interesting facts. All terms expressed in polarizations $\vec{\eta}_j$ can be written in the matrix form

$$G_P = \eta\cdot\underline{C}\cdot\xi + \tfrac{1}{2}\eta\cdot\underline{B}\cdot\eta. \tag{22}$$

Here η and ξ are $2N$-dimensional vectors of the form

$$\begin{aligned} \eta &= \{\eta_{1x},\ldots,\eta_{jx},\ldots,\eta_{Nx},\eta_{1y},\ldots,\eta_{jy},\ldots,\eta_{Ny}\}, \\ \xi &= \{\xi_{1x},\ldots,\xi_{jx},\ldots,\xi_{Nx},\xi_{1y},\ldots,\xi_{jy},\ldots,\xi_{Ny}\}. \end{aligned} \tag{23}$$

The matrix $\underline{B}$ couples polarization in the same layer and between the neighboring layers. It is a $2N$-dimensional three-diagonal matrix and is composed from two N-dimensional tridiagonal matrices $\tilde{\underline{B}}$,

$$\begin{bmatrix} \tilde{\underline{B}} & 0 \\ 0 & \tilde{\underline{B}} \end{bmatrix}, \tag{24}$$

with elements having the form

$$\begin{aligned} B_{j,j} &= b_0, \\ B_{j,j\pm1} &= B_{j\pm1,j} = \tfrac{1}{2}b_1. \end{aligned} \tag{25}$$

The matrix $\underline{C}$ is the antisymmetric matrix composed of two different N-dimensional matrices $\tilde{\underline{C}}$ and $\tilde{\underline{M}}$ as

$$\begin{bmatrix} \tilde{\underline{M}} & \tilde{\underline{C}} \\ -\tilde{\underline{C}} & \tilde{\underline{M}} \end{bmatrix}, \tag{26}$$

where the elements of the matrices are

$$\begin{aligned} \tilde{M}_{j,j\pm1} &= \pm\tfrac{1}{2}\mu, \\ \tilde{C}_{j,j} &= c_p. \end{aligned} \tag{27}$$

The minimization of Eq. (20) with respect to the polarization η leads to the set of linear equations

$$\eta = -\underline{B}^{-1}\underline{C}\xi, \tag{28}$$

where $\underline{B}^{-1}$ is an inverse matrix of the five-diagonal matrix $\underline{B}$. With this solution, the part of the free energy [Eq. (20)] that gives interlayer interactions can be written in the form

$$G_{\mathrm{int}} = \frac{1}{2}\sum_j \left(\sum_k \tilde{a}_k (\vec{\xi}_j \cdot \vec{\xi}_{j+k}) + \tilde{f}_k (\vec{\xi}_j \times \vec{\xi}_{j+k})_z \right). \tag{29}$$

This expression clearly shows that after elimination one can find interactions extending over more distant neighboring layers. They are indirect, a consequence of induced polarizations due to the tilt variation, i.e., the flexoelectric effect. If the interactions decrease significantly with increasing distance, one can safely keep only achiral and chiral coefficients of smaller k. As a first guess as to how many distant layers should contribute, the experimentally shown basic periods of the primitive cell (three and four layers) were used. k was limited to three in achiral and to two in chiral terms. These limits were chosen because the four-layer structure of the $\mathrm{SmC}^*_{\mathrm{FI2}}$ phase could be the consequence of the interactions with next-nearest layers and the three-layer structure of the $\mathrm{SmC}^*_{\mathrm{FI1}}$ phase seems to require interaction to third neighbors which favor synclinic orientation,

$$\tilde{a}_1 = a_1 + \left(\frac{c_p^2}{b_0} + \frac{1}{4}\frac{\mu^2}{b_0} \right)\left(\frac{b_1}{b_0} \right),$$

$$\tilde{a}_2 = \frac{1}{2}\frac{\mu^2}{b_0},$$

$$\tilde{a}_3 = -\frac{1}{8}\frac{\mu^2}{b_0}\left(\frac{b_1}{b_0} \right), \tag{30}$$

$$\tilde{f}_1 = f_1 - 2\frac{c_p \mu}{b_0},$$

$$\tilde{f}_2 = \frac{c_p \mu}{b_0}\left(\frac{b_1}{b_0} \right).$$

If interlayer interactions change with temperature, one can expect many phases, each stabilized within the temperature range where one or the other interaction is prevailing or the competition is strong. The negative sign of the achiral third-nearest-neighbor interaction gives hope for limiting the period to three layers. The positive sign of the effective achiral interactions to the next nearest layers favors four-layer structures.

Some groups made detailed analyses of the phase diagrams in dependence of various model coefficients $\tilde{a}_k$ and $\tilde{f}_k$ (Čepič and Žekš, 2001; Olson *et al.*, 2002). They did not find a strict lock in of the periods but broadening of the regions where the period was close to three layers or close to four layers with coexistence of both. The effective interlayer coefficients $\tilde{a}_k$ and $\tilde{f}_k$ are not free to vary, but they depend on the original interlayer interactions, such as piezoelectric and flexoelectric effects and electrostatic dipolar interactions between nearest-neighboring and next-nearest-neighboring layers. Because they are not free to vary, many sets (values) of the coefficients $\tilde{a}_k$ and $\tilde{f}_k$ cannot be obtained using the discrete model coefficients c_p, μ, b_0, etc., which reasonably describe interlayer interactions. For example, as mentioned, all b coefficients have to be positive, as electrostatic dipolar interactions within the layer are not the origin of the polar ordered state, and between the layers the antiferroelectric order of dipoles is always favored (Čepič and Žekš, 1997).

1. Lock in to commensurate periods

Within the discrete model with temperature-dependent model coefficients one is able to reproduce something similar to the observed phase sequence. Semistabilized structures with periods around three and four layers can also be reproduced, especially if surface interactions are taken into account. However, consistency with experimental results could not be reached in this way. Clock structures, which are solutions of the model (20) and which are also suggested by the first resonant x-ray scattering results, could not explain the large optical rotatory power observed in the three- and four-layer phases. Additionally, it became clear that within the four-layered $\mathrm{SmC}^*_{\mathrm{FI2}}$ phase a reversal of the optical rotatory power sign appears very often, which indicates the possibility of helix reversal (Philip *et al.*, 1995). Careful studies revealed biaxial properties of films at the temperature where optical rotation vanishes (Fig. 35), clearly disallowing the simple symmetric clock structure (Čepič *et al.*, 2002).

Experimentalists (Akizuki *et al.*, 1999) proposed a modification of the clock model in which phase differences between neighboring layers are not the same. The clock structure is expected to be flattened [Figs. 19(b) and 20(b)] or distorted. Today these structures are called distorted clock structures in the literature. These structures allow for the biaxiality of the crystallographic unit cell and the consequent optical rotatory power of the helically modulated structures having three- and four-layer basic periods.

The interactions considered within the model (20) did not give any hints about a favorable "flattening" of the structure. What kind of interactions could possibly be the reason for the flat structures and the lock in?

The theoretical explanation followed from simpler although also interesting system (Pociecha *et al.*, 2001). The homologous series of *m*PIRn shows an interesting reentrant behavior (Fig. 36). The first phase that is stable below SmA upon cooling is the ferroelectric SmC^* phase which develops into the antiferroelectric SmC^*_A phase. Surprisingly, for short homologs the ferroelectric phase reenters. The only possible reason for the explanation of the phenomenon was a nonmonotonic temperature dependence of the interactions between nearest layers. However, the microscopic origin of the reentrance of the favorable synclinicity was not clear. It turned out that, in spite of the previous understanding, interlayer biquadratic coupling b_Q is not of electrostatic origin only, which requires b_Q to be positive (Čepič and Žekš, 1997), but interactions of geometric quadrupolar origin as well (Neal *et al.*, 1997) contribute negatively to the sign of the coefficient b_Q. The importance of geometric quadrupolar interactions is typical for lathlike

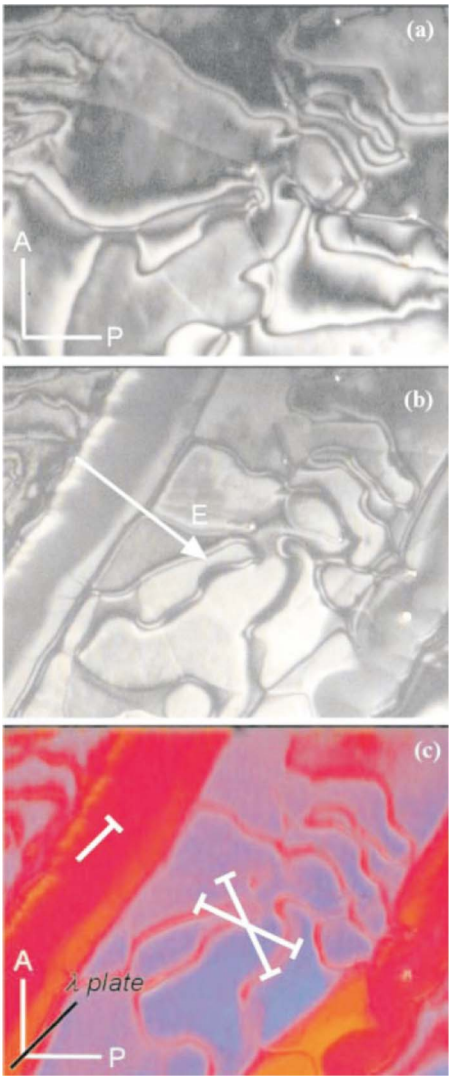

FIG. 35. (Color online) The one surface free film of the (R) enantiomer of 10TBBB1M7, the material studied by resonant x-ray scattering (Mach *et al.*, 1998). (a) At the temperature of the helix reversal in the SmC^*_{FI2} phase the film is clearly birefringent and (b) oriented in the electric field. (c) The film observation using a λ plate reveals the orientation of the larger and the smaller refraction indices. From Čepič *et al.*, 2002.

molecules where an additional ordering within the layer takes place (Žekš, 1984). If molecules order within the layer with short axes parallel [Fig. 37(a)], the system favors both the diffusion of molecules between the layers, which favors parallel ferroelectric ordering in neighboring layers [Fig. 37(b)], and shorter distances between parts of molecules, which favor antiparallel tilt ordering, i.e., the antiferroelectric structure [Fig. 37(c)] at the same time. The interaction can be described by

$$\tfrac{1}{4} b_Q (\xi_j \cdot \xi_{j+1})^2, \tag{31}$$

with a negative coefficient b_Q.

Addition of the term to the discrete model allowed for solutions whose periods and distortions were consistent with experimental observations; even better, as a result

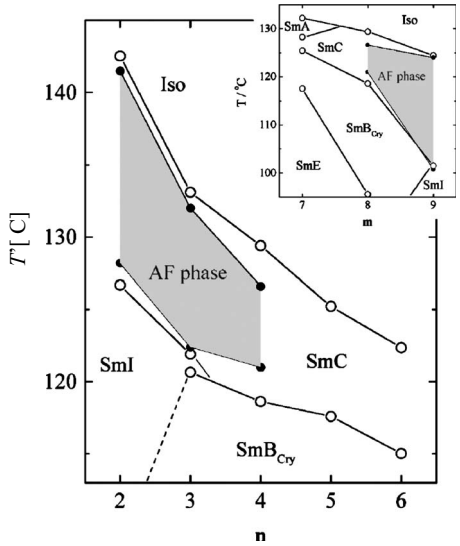

FIG. 36. Phase diagram of the homologous series 8PIRn in which the length of the alkyl chain attached to the chiral carbon atom is varied. Inset: Phase diagram for the homologous series *m*PIR4 in which the length of the achiral alkoxy chain is changed. In both cases a reentrant synclinic phase appears. From Pociecha *et al.*, 2001.

of the minimization the helix reversal within the four-layered SmC^*_{FI2} phase came out as an intrinsic property of the model (Čepič *et al.*, 2002) (Fig. 38).

Why are four- and three-layer structures stabilized when the geometric quadrupolar term is present? The favorable synclinicity or anticlinicity of the interaction strengthens the next-nearest achiral interactions which favor only one type of ordering, synclinic or anticlinic.

2. The four-layer SmC^*_{FI2} phase

As a hand-waving argument consider the formation of the four-layered structure from the point of energetic costs and benefits. For the special situation where a_1 is zero, a_2 and the quadrupolar b_Q interactions define the

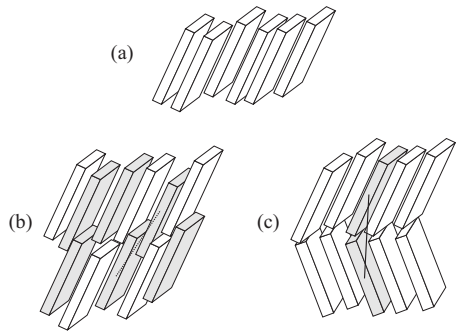

FIG. 37. The schematic presentation of microscopic origins for biquadratic interactions between nearest layers. (a) Lathlike molecules ordering within the layer. (b) Partial interlayer diffusion (gray molecules) favors synclinic ordering. (c) Intermolecular distances are on average shorter for the anticlinic ordering [solid line in (c)] as favored by van der Waals attraction than those for the synclinic ordering [dotted line in (b)].

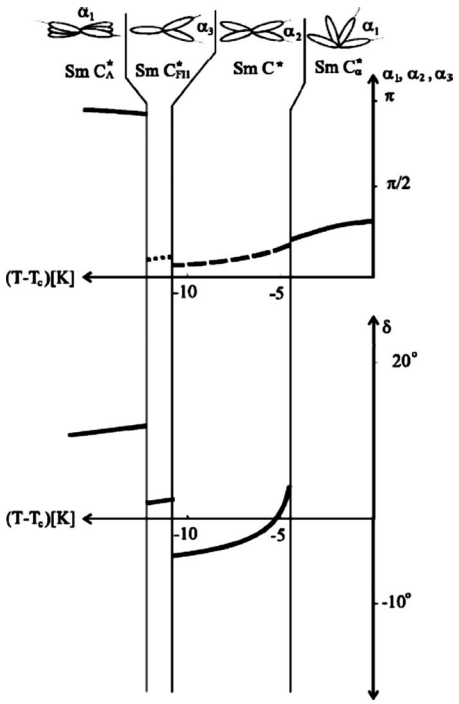

FIG. 38. Theoretical reproduction of the phase sequence observed in 10TBBB1M7. Evolution of the distortion ($\alpha_2=2\psi$ in the SmC^*_{FI2} and $\alpha_3=2\psi$ in the SmC^*_{FI1} phase) (top) and the phase difference δ between the neighboring repeating units in dependence on the temperature (bottom). From Čepič *et al.*, 2002.

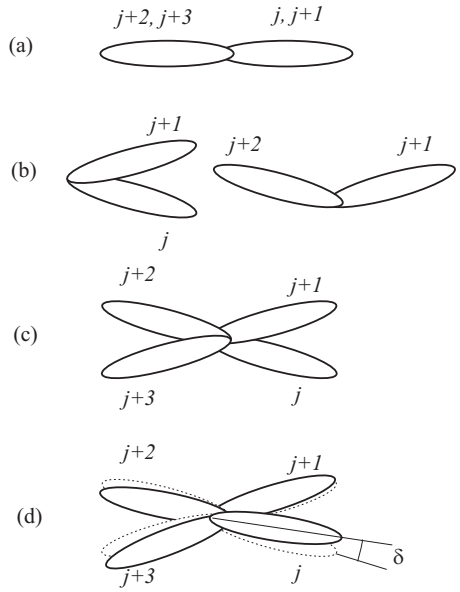

FIG. 39. Schematic presentation of the four-layer structure construction. (a) The four-layered structure is stable in systems with quadrupolar interactions ($b_Q<0$) and negligible achiral bilinear coupling between nearest layers ($\tilde{a}_1\approx 0$). (b) If the chiral interaction between neighboring layer, $\tilde{f}_1$, is not negligible, the synclinic pair (left) is distorted in the opposite direction to the anticlinic pair (right). (c) The consequence is a four-layered repeating unit if the chiral interaction $\tilde{f}_1$ is not negligible. (d) For non-negligible chiral interactions to more distant layers, $\tilde{f}_2$, the sum of the phase differences between neighboring layers over the repeating unit is not 2π.

structure, and the rest of the interactions we consider as negligible for a moment. The favorable structure is shown in Fig. 39(a) and consists of alternating synclinic and anticlinic neighboring layers. All layers are "happy" as the next-nearest neighbors are strictly anticlinic, which is favored by interactions with the next-nearest layers (a_2 positive). Nearest neighbors are happy as well. The relative structure is either synclinic or anticlinic, both structures favored by the quadrupolar coupling with b_Q negative. Now, switch on the chiral interaction given by f_1, which might be rather significant [see Eq. (30)] if the flexoelectric coupling μ is comparable to other terms. The parallelism of synclinic layers is distorted and the direction of the tilt in neighboring layers forms the angle 2ψ [Fig. 39(b), left]. The anticlinic pair is also distorted but in the opposite sense and the directions form an angle $\pi-2\psi$ [Fig. 39(b), right]. The structure has a periodicity of four layers and is strictly commensurate [Fig. 39(c)]. If interactions with more distant layers are negligible, the four-layered structure is commensurate without any additional modulations. However, chiral interactions with next nearest layers f_2 induce slight nonantiparallelism of tilts in next-nearest-neighboring layers and give rise to a helical modulation on a longer scale [Fig. 39(d)]. It is rather easy to find the set of model coefficients that gives the correct phase sequence, the optical helix reversal within the SmC^*_{FI2} phase, opposite helices in the SmC^* and SmC^*_A phases, as well as experimentally consistent phase differences between neighboring layers. However, a detailed analysis of values requires experimental data on the same material synthesized within the same procedure in one laboratory. Such an extensive and elaborate study on one single material is still missing to our knowledge. Therefore, for the time being the model coefficients are only tentative (Čepič *et al.*, 2002).

The four-layer structure of SmC^*_{FI2} differs in symmetry from the helical structure of the SmC^*_α, SmC^*, and SmC^*_A phases, which can all be described by one tilt and one phase difference. The distorted clock structure with a period of four layers has two different phase differences between neighboring layers, say α and β, which interchange. To find the regions where such a structure is stable, one has to consider contribution to the free energy of interfaces having both phase differences. The expected solution has the following form:

$$\vec{\xi}_{2j} = \theta\{\cos(j\alpha + j\beta), \sin(j\alpha + j\beta)\},$$
$$\vec{\xi}_{2j+1} = \theta\{\cos[(j+1)\alpha + j\beta], \sin[(j+1)\alpha + j\beta]\}, \quad (32)$$

and the free energy has to be averaged over two layers. This solution is generally not commensurate to four layers and can present the structure with any periodicity, even completely incommensurate ones. However, it turns out that the minimum of the free energy is obtained only when the sum $\alpha+\beta$ is close to π. A small

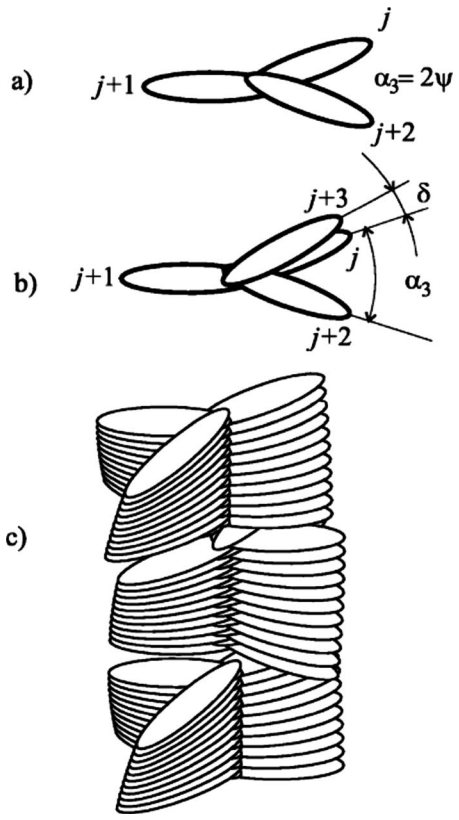

FIG. 40. Schematic presentation of the three-layer structure construction. (a) The three-layered structure is stable in systems with quadrupolar interactions ($b_Q<0$). (b) When the chiral interaction between nearest layers, $\tilde{f}_1$, is not negligible, the sum of the phase differences over the repeating unit is not 2π. (c) The soliton lattice is formed dynamically. From Čepič *et al.*, 2002.

deviation from π results in a long scale modulation observed in four-layer systems. At specific conditions, strict lock in exists, where the sum is exactly π and the structure is locked to exactly four layers. It is experimentally observed as the temperature where the optical rotatory power diverges and changes sign, where the free-standing films become biaxial within the temperature region of the SmC^*_{FI2} phase, and where the pitch of the optical modulation diverges. These changes are not accompanied by any other evidences of a phase transition such as differential scanning calorimetry peaks or similar. But because of this behavior this "commensurate" temperature was mistaken several times for a phase transition to a new phase.

3. The three-layer SmC^*_{FI1} phase

Similarly, the ansatz that considers three-layered structures also leads to a stable solution for certain choices of the model coefficients. From Fig. 40(a) one can see that this structure can be described by the sequence of three phase differences α, β, and γ, whose sum locks to approximately 2π in the three-layer structure. It turns out that for symmetry reasons only the solution where $\alpha=\gamma$ can be stable. The expected solution for the minimization is

$$\vec{\xi}_{3j} = \theta\{\cos(2j\alpha + j\beta), \sin(2j\alpha + j\beta)\},$$

$$\vec{\xi}_{3j+1} = \theta\{\cos[(2j+1)\alpha + j\beta], \sin[(2j+1)\alpha + j\beta]\}, \quad (33)$$

$$\vec{\xi}_{3j+2} = \theta\{\cos[2(j+1)\alpha + j\beta], \sin[2(j+1)\alpha + j\beta]\},$$

and the free energy has to be averaged over three layers.

The deviation of angles α and β from zero and π for both three- and four-layer phases is defined by chiral interactions, mainly by the combination of the flexoelectric and piezoelectric interactions that define the magnitudes of the $\tilde{f}_1$ and $\tilde{f}_2$ coefficients.

It seems that a solitonlike structure [Fig. 40(c)], where the direction of the polarization in the three-layer crystallographic unit cell reverses dynamically within domain walls, might give consistent explanations of the experimental observations (Čepič *et al.*, 2002).

The three-layer structure is of special interest for theorists. As pointed out by Dolganov *et al.* (2002, 2008), the symmetry of the phase also requires modulation of the tilt amplitude. Tilts in layers having phase differences with both neighboring layers closer to π should be larger than in layers having a phase difference with one of the neighboring layers closer to zero. The reason is that the phase appears in the region where nearest-layer interactions favor anticlinicity. The modulation of the tilt amplitude leads to the modulation of density and potential observability even by nonresonant x-ray diffraction. In fact, the predicted satellite peak (Dolganov *et al.*, 2002) was found only in the three-layer phase SmC^*_{FI1} (Fernandes *et al.*, 2006).

In the systems studied only structures with unit cells up to four layers have been undoubtedly experimentally confirmed, and discrete phenomenological modeling was able to reproduce them. We searched for minimal solutions for structures with a number of combinations having different phase differences, locking to various short-range periodicities. Unfortunately, we were not able to find stable structures of longer periodicities unless the periodicity in layers was already imposed by the period of the cycling boundary conditions (Emelyanenko and Osipov, 2003; Emelyanenko *et al.*, 2006). As mentioned before, the six-layer sturcture was found only recently (Wang *et al.*, 2010). The existence of the six-layer phase within the region of the SmC^*_α without imposture of periodic boundary conditions is theoretically studied at present.

4. Some additional interesting results of discrete modeling

The discrete modeling has some additional advantages over the continuous model. The restricted geometry in free-standing films that consist of a few layers only or have a distinctly different smectic order in only a few layers close to the surface than in the interior presents systems where the transition from the structures stabilized by surface interactions toward structures sta-

bilized by bulk interactions can be studied. Theoretical consideration of free-standing films revealed additional curiosities (Rovšek *et al.*, 2000) that were later also observed experimentally (Conradi *et al.*, 2004, 2005). Free-standing films seem ideal systems to study structures of phases and were used as such (Bahr and Fliegner, 1993a; Johnson *et al.*, 1999; Schlauf *et al.*, 1999). In free-standing films a significant fraction of the volume is exposed to interactions at the surfaces, which differ from the interactions in the interior of the film due to the missing interactions with neighboring layers or larger ordering due to the surface tension. This might have an important effect on the structure of the film as a whole, resulting in modulation of the tilt amplitude, not present in bulk phases and the consequent longitudinal flexoelectric effect (Andreeva *et al.*, 1999), as well as the existence of uniplanar phases similar to the first Ising-like structural models (Rovšek *et al.*, 2000).

Similarly, the analysis of the SmC^*_α structure in an external electric field using the discrete model has given few surprising results. The short-pitch structures do not behave like structures with longer periods of helical modulation where soliton type of unwinding (Benguigui and Jacobs, 1994; Kutnjak-Urbanc and Žekš, 1995) takes place. The period of the structure already locks to certain commensurate periods at low external fields forming devil's staircase transitions as the electric field increases (Fig. 41). At higher electric field the devil's staircase transforms to a harmless staircase where the period of helical modulations increases in periods of integer numbers of layers. Finally the unwinding that occurs at the critical field is always discontinuous in systems with achiral interactions between the next-nearest layers (Rovšek *et al.*, 2004).

The results might explain the steps found in apparent tilt angle during initial studies of antiferroelectric liquid crystals (Hiraoka *et al.*, 1991) and the behavior of phases in external electric fields, results which lead to Ising-like structural and theoretical models. Although the analysis has been done for the electric field, which couples polarization with the electric field linearly, one might speculate about similar behavior in the magnetic field, which couples with tilt quadratically. Measurements have shown that even unwinding of the long periods originating in weak interactions requires extremely high magnetic fields (Škarabot *et al.*, 2000), so one can hardly hope for unwinding of the short helix in the SmC^*_α phase by application of an external magnetic field. But the influences of surfaces can be in some circumstances considered as fields which couple with the tilt quadratically. As the period of the modulation changes as the temperature is lowered, the surface field can lead to a lock of certain commensurate periods and result in the observed steplike behavior of the SmC^*_α phase (Isozaki, Hiraoka, *et al.*, 1992) also as the temperature changes. These problems still wait for more detailed experimental and theoretical research.

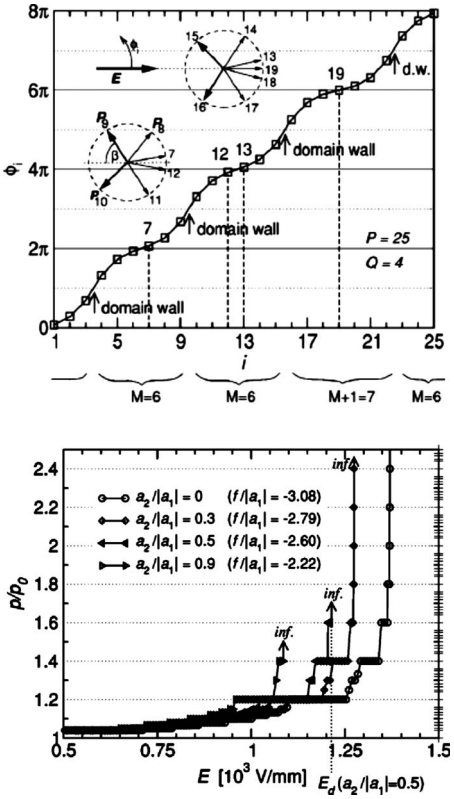

FIG. 41. Structural changes of the SmC^*_α phase in external electric field. (Top) Distorted helical structure in an external electric field. The pitch in the absence of the field extends over six layers; in the field the commensurate structure of four rotations in 25 layers is stable for the considered field. (Bottom) The structures are locked to commensurate ratios of distorted and nondistorted helices p/p_0 at lower electric field. At higher electric field helices lock to integer numbers of layers in the pitch p. From Rovšek *et al.*, 2004.

5. Discrete model with long-range interactions

In spite of successful results of discrete modeling having nearest-neighbor interactions only, Eq. (20) including the biquadratic term (31), theoretical curiosity still exists: is the biquadratic coupling the only possible origin of structures locked to commensurate periods or do other, maybe simpler, mechanisms exist, which could also allow for commensurate periods of longer ranges? One idea for possible long-range interactions, which might give rise to lock ins, was suggested by Bruinsma and Prost (1994). They showed that neither ordered dipoles nor van der Waals interactions lead to an interlayer interaction that favors some particular relative ordering of the tilt direction, providing that layers can be considered as ideal liquids without positional correlations of molecules in neighboring layers. However, thermally excited polarization waves result in the weak long range repulsion forces that were postulated within Ising models (Yamashita, 1996, 1997).

The idea of competition between short- and long-range interlayer interactions which result in structures locked to commensurate periods was considered by Hamaneh and Taylor (2004, 2005, 2007). They limited the

short-range interaction to neighboring layers only. The contribution to the free energy due to short-range interactions depends on the relative orientations of the tilt in neighboring layers. The most general form of this interaction is (Hamaneh and Taylor, 2007)

$$V_{\mathrm{sr}} = v_{\mathrm{sr}} \sum_l (\phi_{l+1} - \phi_l). \tag{34}$$

In their model the preferential angle formed by tilt in neighboring layers was considered,

$$V_{\mathrm{sr}} = - v_{\mathrm{sr}} \sum_l \cos(\phi_{l+1} - \phi_l - \alpha), \tag{35}$$

although they did not consider the origin of that preferred angle. In principle the angle can be a consequence of competing bilinear short-range interactions (Čepič and Žekš, 1995, 2001), especially when strong chiral interactions are present.

They proposed that interactions to more distant layers originate in bending fluctuations of smectic layers. They took into account the anisotropy of elastic constants for bending of smectic layers, which is a consequence of the anisotropic molecular tilt order in the smectic layer explicitly. The energy associated with bending of the smectic layer along the tilt direction is necessarily different from the energy for bending perpendicularly to the tilt. Therefore fluctuation in one direction is more favorable than in the other. The bending fluctuation contribution to the free energy is

$$f_l = \frac{1}{2}\left(k_x \frac{\partial^2 u_l}{\partial x_l^2} + k_y \frac{\partial^2 u_l}{\partial y_l^2} \right). \tag{36}$$

Here the x and y directions are considered parallel and perpendicular, respectively, to the tilt direction in the considered layer. As the normal modes contribute mostly at lower frequencies, the Debye-like approximation was used and integration of the contribution of different modes resulted in the simple form of the free energy

$$\mathcal{F} = - \frac{v}{Nd} \sum_l \cos(\phi_{l+1} - \phi_l - \alpha) - \eta J^2, \tag{37}$$

where v gives the mean-field strength of the short-range interactions, N is the number of layers, and d is the layer thickness. The new order parameter J is defined as

$$J = \frac{1}{N} \sum_l \cos 2\phi_l. \tag{38}$$

Here the direction in which the flattening occurs is chosen as direction x. The order parameter is zero for any structure where all directions are equivalently occupied. This is also valid for commensurate clocklike structures. However, if the phase ϕ_l occupies more directions closer to zero or π, this leads to a flattened structure and it is also more likely that the structure is commensurate. In general, one can also imagine structures that have an order parameter defined as in Eq. (38) equal to 1 and are not commensurate (for instance, a general Ising sequence extending over the whole sample without a unit cell). However, such structures do not present the minimum of the free energy. The mean-field interaction of the ordered systems given by η depends on the level of anisotropy [the ratio $(k_x - k_y)/(k_x + k_y)$], the magnitude of the average elastic constant, temperature, and layer thickness. The expression is rather complicated and details of its derivation are given by Hamaneh and Taylor (2004, 2005). The commensurate structures are likely to appear if the coefficient η is approximately equal to 1. Starting from the general experimental data for tilt angles, magnitudes of the switching external electric fields, layer polarizations, and layer thicknesses, they deduced that the value of η could be close to unity in some systems and therefore the mechanism is worth considering (Hamaneh and Taylor, 2004, 2005). They also calculated the range and strength of the entropy-induced interaction and showed that this interaction depends on the ratio of the two constants for bending a layer of tilted smectic liquid crystal along the tilt direction and perpendicular to it. They can be of a longer range for small ratios but they decay as an inverse third power of the interlayer distance. In addition to the structure with the longest unit cell of four layers found in the distorted clock model, they also found one additional commensurate structure with the unit cell extending over six layers.

6. Ising-like models

Another model that requires a potential that bounds tilts strongly into one plane formed by the molecular tilt and the layer normal was initiated by the first structures proposed for intermediate phases and the SmC^*_α phase. In these tentative structures the sequences of synclinic and anticlinic neighboring layers formed the basic repetitive unit of the structure. Structures with different periods that should transform one into another upon temperature changes and should in principle have various commensurate periods were considered as devil's staircase structures. Yamashita and Miyazima (1993) first attempted to explain devil's staircase structures, the temperature ranges of the stability, and their macroscopic properties using an Ising-like model. The main assumption of the Ising-like model(s) is the limitation of the tilt to one plane only—uniplanarity—consistent with early proposed structures (Isozaki, Hiraoka, *et al.*, 1992). The tilt plane is defined by the layer normal and the molecular tilt, and directions out of this plane are considered as prohibited or highly energetically disfavored. As this limitation leads to only two possible directions of the tilt and x-ray studies showed no variations of the layer thickness, a constant tilt amplitude was also assumed. The tilt order within the smectic layer was described by the Ising-type variable typical for a layer, where +1 means the tilt is in one direction and –1 in the opposite direction. Within these assumptions the free energy was written as (Yamashita, 1996, 1997)

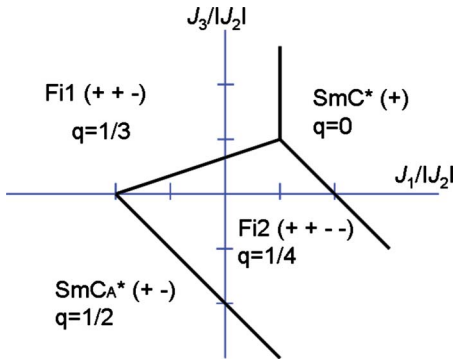

FIG. 42. (Color online) Possible stable structures allowed by the Ising model with interactions to the third-nearest-neighboring layers.

$$G = -J\sum_{(i,j)} s_i s_j - J_1\sum_i s_i s_{i+1} - J_2\sum_i s_i s_{i+2} - J_3\sum_i s_i s_{i+3}. \tag{39}$$

Here the first term gives the intermolecular interactions within the layer. The coefficient J_1 can be either positive, favoring ferroelectric structures, or negative, favoring antiferroelectric structures. The J_2 term introduces competition and is always considered as negative. The J_3 term is the most important for the stability of structures with periodicities of three layers.

The stability of the four phases is drawn in $(J_1/|J_2|, J_3/|J_2|)$ space in Fig. 42 (Yamashita and Miyazima, 1993), where q is given by n (number of waves in a period) divided by m (number of layers in a period). In the region of $J_1 \gg 0$, a ferroelectric phase ($q=0$, SmC*) is stabilized. When J_1 is negative, two possible orientations are possible: (1) an antiferroelectric phase ($q=1/2$, SmC_A^*) is stabilized for $J_3<0$ since the third-nearest neighbors always tilt in opposite directions; $\mathrm{SmC}_{\mathrm{FI1}}^*$ ($q=1/3$) is stabilized for $J_3>0$ since the third-nearest neighbors always tilt in the same direction. Near the origin (small J_1 and J_3 compared with J_2) $\mathrm{SmC}_{\mathrm{FI2}}^*$ ($q=1/4$) is stabilized since the next nearest neighbors always favor the opposite tilt. The phase diagram obtained in the form of a devil's flower (Chaikin and Lubensky, 1995) is shown in Fig. 43 (Yamashita, 1997). Apart from the structures with complicated q numbers, the order of the phase sequence, i.e., SmC^*-$\mathrm{SmC}_{\mathrm{FI2}}^*$-$\mathrm{SmC}_{\mathrm{FI1}}^*$-$\mathrm{SmC}_A^*$ was explained.

There was a problem in the construction of Ising-like models: the relation to the microscopic origins of the phenomenological coefficients. The origin of the restriction of the tilt to one plane was not known. In addition, more complicated terms, where many molecules contribute, required sophisticated statistical analysis with a number of assumptions. Yamashita tried to explain the microscopic origin (Yamashita, 1996) and to introduce the effect of breaking the tilt restriction (Tanaka and Yamashita, 2000) with only a limited success.

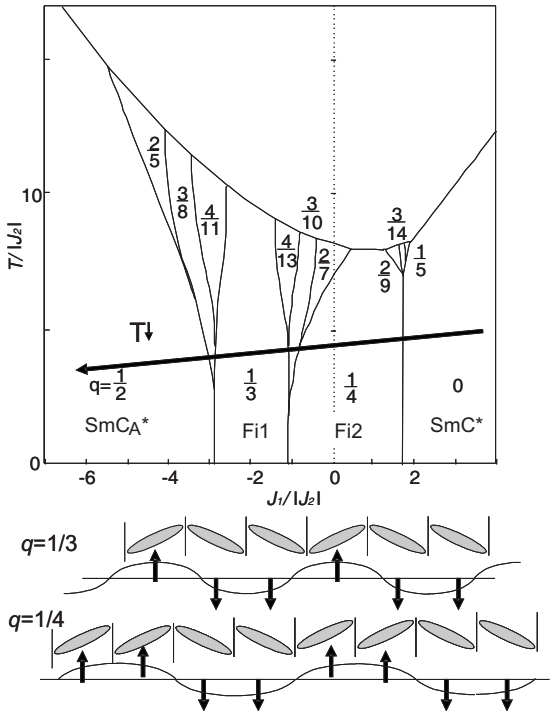

FIG. 43. Devil's flower, the phase diagram in dependence of the temperature allowed by the Ising model. The arrow indicates the path of the coefficient ratio which accounts for the four- and the three-layered structures.

E. Other theoretical approaches

Although Hamaneh and Taylor (2004, 2005) pointed out that a minor change in synthesis, like addition of one single group, changes the phase diagram of the sample drastically and therefore it is highly unlikely that intralayer and interlayer molecular interactions can be understood from first principles, theorists have not given up on determining how the model coefficients are related to molecular properties. Two approaches are known: the molecular statistical approach and computer simulations. The molecular statistical approach presents molecules as sources of multipole fields of different origins (Neal *et al.*, 1997; Emelyanenko and Osipov, 2003) and the free energy of a system is derived using statistical thermodynamics. In computer simulations interactions between molecules are modeled in more or less detail including molecular properties such as shape or the presence of dipoles, and the results of simulations give some information about the system behavior or even about some macroscopic properties which can be related to the phenomenological considerations and experimental results. Both approaches are discussed in the following; however, for more detail see the overview articles of Wilson (1997, 2007).

1. Molecular statistical approach

This is another powerful theoretical approach. Its purpose is to establish a relationship between the general macroscopic description discussed before and the intermolecular interactions at the microscopic level. Mol-

ecules are modeled as rigid biaxial molecules (Neal *et al.*, 1997; Osipov and Fukuda, 2000) with additional dipoles and/or quadrupoles; other properties can also be included. Usually only pair intermolecular interactions to the nearest molecules are considered. This approach starts from an effective potential, which is usually constructed from van der Waals attractive and repulsive interactions, electrostatic forces, and the like. The free energy is calculated as a statistical sum of contributions due to the intermolecular interactions. As effective potentials often depend on the state of order expressed in order parameters, the order parameters can be calculated from self-consistent equations, or the expression for the free energy can be obtained by expansion of its dependence for small values of the order parameters. In the latter case, the relation to phenomenological models of existing theories can be established; the importance of some terms in phenomenological theories was considered and the sign and even magnitude of the phenomenological model coefficients were calculated (Emelyanenko and Osipov, 2003). On the other hand, this treatment can also result in the construction of a Landau-type free energy for the system or in the introduction of new important terms in existing expressions for the free energy (Emelyanenko and Osipov, 2003). As the whole approach starts from basic molecular properties such as shape or dipoles, the results can be helpful in avoiding the trial and error approach during the process of organic synthesis as well as a hint for computer simulations.

2. Computer simulations

Molecules forming liquid crystals with tilted polar smectic phases consist of 100 or even more atoms, in some places bound with flexible rotatable bonds and having different polarizabilites, some of the bonds having nonuniform charge distributions leading to effectively electrostatic molecular dipoles or quadrupoles, and some of the connected groups being chiral. Such molecules generally possess a number of different conformations changing over the time span due to fluctuations or as a reaction to interactions with neighboring molecules. The molecules are generally large in comparison with intermolecular distances giving rise to a strong dependence of the interactions on the relative positions and orientations of the interacting molecules. All described properties give rise to changes of molecular behaviors on different time and length scales. For example, the changes of molecular conformations and vibrations are on the order of femtoseconds, but the formation of clusters near the phase transitions takes 10^6 longer. On the other hand, atomistic simulations that consider all atoms in the molecules and interactions between them can consider a few hundreds of molecules at most using advanced computers and techniques. But, for consideration of phase transitions one needs to consider hundreds of thousands or even a few millions of interacting molecules. It is highly unlikely that a single simulation can consider phenomena on both short and long time and length scales.

In spite of extensive work and rapidly developing computers, researchers have had to be satisfied with simulations for simpler systems, nematics and smectics, only. They were able to extract experimentally and theoretically consistent elastic and flexoelectric coefficients for nematics (Allen and Masters, 2001) and they modeled isotropic nematic and nematic smectic phase transitions (Care and Cleaver, 2005), but accurate densities of materials are still an open question. Molecular simulations of complex molecules forming complex phases are still at the beginning of their evolution (Maiti *et al.*, 2004). As phenomenological modeling uses hand-waving arguments for the signs of model coefficients leading to certain structures, the integration of these guessed interactions with computer simulations can lead to an understanding of the intermolecular interactions as well as serving as a hint to molecular design for better material properties for applications.

Computer simulations are of a few types. The simplest type is a spin model, where a molecule or groups of molecules is presented as vectors (spins) that interact with neighbors through a pair potential. Then random changes of orientations are applied on individual vectors and the energy is calculated as a criterion for the acceptance or rejection of the change. The degree of order is calculated with respect to the average vector direction. However, these types of model give only orientational order, no translations of molecules are possible, and therefore the model can only account for phase transitions where the orientational order changes.

The second class of models is called single-site coarse-grain molecular models. The interaction potentials are hard anisotropic potentials to which additional attractive parts can be added. Typical representatives of these types of models are models where molecules are modeled as hard spheroids, hard spherocylinders, or hard ellipsoids. The temperature does not influence the structures in hard models and therefore the models are more appropriate for lyotropic liquid crystals. The changes in order are induced by changes of density. Most models use Monte Carlo simulations where the criteria for hard potentials are rather simple. All positions that result in overlapping configurations are rejected. Thermotropic liquid crystals are better modeled by soft potentials, for example, the Gay-Berne potential (Gay and Berne, 1981). Here,

$$U_{ij} = 4\epsilon_0[\epsilon(\hat{u}_i,\hat{u}_j)]^{\nu}[\epsilon'(\hat{u}_i,\hat{u}_j,\hat{r}_{ij})]^{\mu} \times\left[\left(\frac{\sigma_0}{r_{ij}+\sigma(\hat{u}_i,\hat{u}_j,\hat{r}_{ij})+\sigma_0}\right)^{12} -\left(\frac{\sigma_0}{r_{ij}+\sigma(\hat{u}_i,\hat{u}_j,\hat{r}_{ij})+\sigma_0}\right)^{6}\right]. \quad (40)$$

Here repulsion is proportional to $1/r^{12}$ and attraction is proportional to $1/r^6$, where r is the distance between the two interacting molecules. The dependence on unit vectors $\hat{u}$ and $\hat{r}$ describes the dependence of the interactions

on orientations. The properties of the potential are adjusted by the constants ϵ_0 and σ_0. The model can be generalized for disklike, biaxial, or noncentrosymmetric molecules. It is also relatively easy to add dipoles or quadrupoles. For example, the addition of a longitudinal dipole in the molecular center or two off-center dipoles led to the formation of the tilted smectic.

The most demanding are the atomistic models that consider intermolecular interactions in detail. In these models the interatomic bonds in molecules are considered as flexible rotatable, bonds, conformations of molecules are allowed, etc. Although these models are the most realistic, the number of molecules that can be considered nowadays is still too small (up to 1000) and the life span of the simulations still too short to simulate phase transitions and other properties. However, all-atom simulations have shown that the populations of different complex molecular conformations differs in different phases (Cheung *et al.*, 2004). This result is important as it explains the surprising stability of various phases. The computing time could be shortened by the application of coarse-grain models, where molecules are usually modeled by a series of Gay-Berne potentials.

F. Discussion

All phenomenological models presented are still in use for consideration in different circumstances. Even strongly distorted clocklike structures are present in some systems, as shown by x-ray experiments (Gleeson and Hirst, 2006).

The continuous model is practical for consideration of systems where only the two simplest phases, the SmC^* and SmC^*_A phases, exist. It allows for the straightforward relation of model coefficients and macroscopic properties. It also allows for implementation of results from other solid systems in the liquid crystals due to the similarities of the models.

The clock model without biquadratic coupling proved itself effective close to the transition to the SmA phase where the biquadratic coupling is still weak. For more qualitative analysis the biquadratic coupling can safely be neglected. The model was also often used in its renormalized version where only interactions expressed in tilt vectors were used. The origin and limitations of the model coefficients describing initial interactions were sometimes overseen. A number of groups have considered their experimental results within this slightly poorer model and got many results consistent with experimental observations (Douali *et al.*, 2004). Various structural behaviors were found including the recent discovery of continuous evolution of the short pitch from few-layer pitches toward two layers (Liu *et al.*, 2007) as predicted by Čepič and Žekš (1996).

The distorted clock model with inclusion of the biquadratic term has also experienced a life of its own. The flexoelectric contribution was derived from microscopic origins that were an important contribution to the understanding of microscopic interactions (Emelyanenko and Osipov, 2004). Sometimes this model is also called the "Emelyanenko model"; however, it is the same as the clock model (Chandani *et al.*, 2005; Emelyanenko *et al.*, 2006).

Discrete modeling has proven its efficiency; however there are still a number of open problems that might be addressed by the discrete approach. There are still missing answers: how many commensurate structures exist with more than four layers in the unit cell? Do they form a distinct phase with a phase transition between them? Some have not found such stable structures (Jaradat *et al.*, 2008); others claim that they have, although it seems that their periodicities could also be the consequence of the cycling boundary conditions of short period used during the solution of minimization equations (Emelyanenko and Osipov, 2004; Emelyanenko *et al.*, 2006).

Another open question concerns the link or interplay between the continuous and the discrete approach. Within a layer one has to consider structure continuously; from layer to layer changes of the tilt directions can be large. How can both of the approaches be connected? Dynamics and stability have been theoretically and experimentally studied for simple helices. But analysis of dynamics of structures with three and four layers is still lacking. Theoretical analysis of films and comparison of predictions with experiments can reveal the influence of chiral and quadrupolar interactions on the evolution of uniplanar structures. Discrete modeling has been successfully applied for other systems (Pociecha *et al.*, 2003, 2006; Nishida *et al.*, 2006) and it is worth mentioning that it might be applied in all systems where structural changes can be large at short distances, i.e., on a tenth of a nanoscale.

There are also open questions with respect to other theoretical approaches. The link between computer simulations, the molecular statistical approach, and the phenomenological modeling will help the organic chemists in their search for materials with larger potentials for applications. As simple phenomenological modeling is less time demanding than some computer simulations, the hints one can get from structures formed by complex molecules modeled in computer simulations can also help to improve phenomenological models.

V. APPLICATIONS

As mentioned in Sec. II, the history of antiferroelectric liquid crystal research started in 1988 as a display application without knowledge of the molecular orientation or structure (Chandani *et al.*, 1988). At that time, many engineers were developing ferroelectric liquid crystal displays (FLCDs) using surface-stabilized states (Clark and Lagerwall, 1980). FLCDs were quite promising because of their many advantages for passive matrix addressing, such as fast response speed, the memory effect, and threshold behavior (Fig. 44). On the other hand, there were some drawbacks such as mechanical damage on alignment, low contrast ratio, and charge accumulation. Antiferroelectric liquid crystal displays (AFLCDs) were expected to solve these problems, as mentioned below. Hence extensive efforts toward devel-

FIG. 44. (Color online) Antiferroelectric liquid crystal display developed by DENSO.

oping AFLCDs have been made (Johno *et al.*, 1990; Yamada *et al.*, 1990; Yamamoto *et al.*, 1992).

The fundamental concept of AFLCDs is shown in Figs. 45 and 46. There are two bistable states for the apparent tilt angle in positive- and negative-field regions. We can use the two bistable states alternately, so that charge accumulation problems can be solved. The driving scheme is shown in Fig. 45 together with the transmittance change against an applied voltage (Fig. 46, right). Here crossed polarizers are located parallel to the smectic layer. The AF state gives a dark and the two ferroelectric states (F^+ and F^-) give bright views. The simplified driving voltage scheme (left) shows, at the beginning of each frame, the device is reset to AF by the termination of the field for a short period. If the first pulse (V_D) in addition to a bias voltage (V_0) is higher than the higher threshold voltage ($V_{\rm th}^H$), i.e., $V_0+V_D > V_{\rm th}^H$, either F^+ or F^- is realized depending on whether the field is positive or negative. On the other hand, if the first pulse V_D is low such that $V_0+V_D < V_{\rm th}^H$, the device remains in AF. By use of a bias voltage between the lower and higher threshold voltages $V_{\rm th}^L$ and $V_{\rm th}^H$, $V_{\rm th}^L < V_0 < V_{\rm th}^H$, we can always use two bistable states alternately. This leads to the advantage of no charge accumulation.

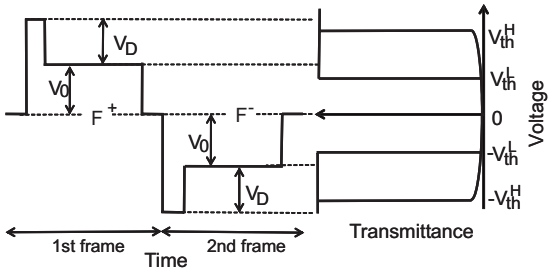

FIG. 45. Driving scheme for AFLCDs. On the right-hand side, optical response (transmittance vs applied voltage) is shown. Simplified driving scheme is shown on the left. The short period of 0 V at the first stage of each frame resets the system to the AFLC state. The first (high or low) pulse V_D in addition to the bias voltage V_0 selects for the antiferroelectric or ferroelectric state.

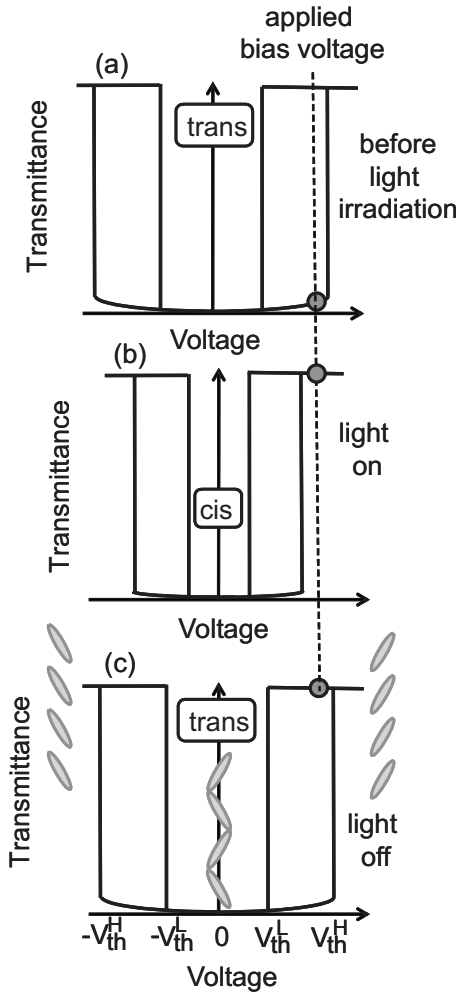

FIG. 46. Principle of spatial light modulator using antiferroelectric liquid crystals with photoisomerizable molecules. The threshold voltage shift is associated with *trans-cis* isomerization by light irradiation. Dark and bright (off and on) states can be switched under a bias voltage.

The response time is as fast as in FLCDs, in the range between microseconds and milliseconds depending on the applied field and temperature. The viewing angle characteristics are as good as in FLCDs since the switching occurs essentially within the plane parallel to the substrates. As for the mechanical shock problems, a self-recovery effect was demonstrated; the deformed layer structure is recovered during the switching (Itoh *et al.*, 1991). However, the recovery is not perfect, so that the low-contrast problem still remains. In addition, there is another essential problem in the contrast ratio in AFLCDs. As shown in Fig. 45, transmittance leakage occurs when $V_{\rm th}^H$ is approached, due to the pretransition from the SmC_A^* to the SmC^* state. Such problems bringing about low contrast ratio were solved by materials development.

DENSO presented a prototype display in 1997, as shown in Fig. 44. However, AFLCDs as well as FLCDs had lots of problems: (1) weakness to mechanical dam-

age due to the existence of smectic layer structures, (2) smectic layer rotation on application of an electric field (Ozaki *et al.*, 1994; Nakayama *et al.*, 1995), (3) temperature dependence of physical parameters such as tilt angle and viscosity, (4) rather low contrast ratio, and so on. These are not problems in nematic liquid crystal displays (NLCDs). In addition, the development of NLCDs rapidly solved various problems such as the switching speed and viewing angle (Kim and Song, 2009). For these reasons, DENSO could not commercialize AFLCDs.

Antiferroelectric liquid crystal materials with a tilt angle near 45° have a special optical property, i.e., the anticlinic molecular orientation between neighboring layers gives isotropy at least when viewed from the normal direction. Such a material was first reported in 1976 [MHTAC (Figs. 1 and 2)], although it was not identified as an antiferroelectric phase at that time. Robinson *et al.* (1997, 1998) also reported such materials. More recently, Drzewinski *et al.* (Drzewinski *et al.*, 1999; Dabrowski, 2000) synthesized partially fluorinated compounds with a high tilt angle near 45°. D'Have, Dahlgren, *et al.* (2000) and D'Have, Rudquist, *et al.* (2000) used these materials to measure the optical performance associated with the SmC_A^*-SmC^* field-induced phase transition. They showed that a homogeneously aligned SmC_A^* cell becomes uniaxial with the optical axis perpendicular to the cell normal when the tilt angle is 45° and actually showed an excellent dark state in the absence of a field. Because of the isotropy around the cell-normal direction, the darkness does not depend on the layer-normal direction. This means that surface alignment treatment is not necessary. Although the advantages of using 45° antiferroelectrics are clear, displays using such materials are still far from being commercial.

The AFLCDs mentioned above are of passive matrix addressing type and are bistable devices essentially for black-and-white displays. For full-color images, display of gray levels is indispensable. To realize a full-color display as in Fig. 44, spatial and/or temporal multiplexing is necessary. Otherwise, continuous brightness change has to be achieved by other techniques. For this purpose, polymer-stabilized AFLCDs were examined (Strauss and Kitzerow, 1996). Another display mode that is called V-shaped switching and is capable of displaying gray levels was proposed by Inui *et al.* (1996). Although extensive effort has been made from basic and application approaches, we do not describe the details since there is still discussion as to whether the performance is based on a ferroelectric, ferrielectric, or antiferroelectric phase (Matsumoto *et al.*, 1999; Park *et al.*, 1999; Rudquist *et al.*, 1999).

Another possible application is as a spatial light modulator. Spatial light modulators are key for information processing. Actually liquid crystal panels behave as spatial light modulators, by which a lot of information is transformed electrically into a two-dimensional image. They can be addressed optically; parallel optical information processing becomes possible. Applications are to wide-image encryption and motive object extraction using digital image processing, noise removal, pattern recognition using spatial frequency filtering, stereo display, and image reconstruction using holograms (optical phase conjugation). Thus, it is a promising technology. The material is composed of an antiferroelectric liquid crystal doped with photoisomerizable compounds such as azobenzene. The device performance is based on the change in the threshold voltage by photoisomerization of azobenzene, as shown in Fig. 46. When the homogeneously aligned AFLC cells are irradiated with uv light, the photochromic molecules are excited from *trans* to *cis* [from (a) to (b) in Fig. 46]. This photoisomerization slightly distorts the orientation around the dye molecules and effectively decreases the order parameter, resulting in a decrease of the transition temperature (Moriyama *et al.*, 1993). This transition temperature decrease brings about a decrease of the threshold voltage for the field-induced antiferroelectric-ferroelectric phase transition. If the cell is under dc bias voltage just below V_{th}^H, the transition occurs from the antiferroelectric to the ferroelectric state on light irradiation. The ferroelectric state is memorized under the bias voltage after the light irradiation is turned off because of the bistability [Fig. 46(c)]. It is easy to return to the antiferroelectric state by termination of the bias voltage for a short period.

A response time of about 30 ms was reported on irradiation of a 10 mW Ar laser without focusing. The transmittance can be controlled by either the light power or the light pulse duration. From a microscope observation, it was found that the gray level recording is based on the area ratio of the antiferroelectric and ferroelectric domains but not an intermediate state. On irradiation, ferroelectric domains grow along the layer direction (Kajita *et al.*, 1993). Therefore the spatial resolution of the image construction is higher along the smectic layer-normal direction, i.e., at least several tens of micrometers, than the layer direction. Improvements in performance such as the response time can be made by properly choosing the liquid crystals and photochromic compounds.

VI. CONCLUSIONS AND OPEN QUESTIONS

Antiferroelectric liquid crystals are systems formed by elongated chiral molecules ordered in smectic layers, which possess a variety of phases with different macroscopic properties. The specific systems are the results of the interplay of various interactions always present when systems are formed of more or less complex molecules. Three basic intermolecular interactions always compete with the entropic move toward disorder. The van der Waals attractive interactions favor the shortest possible intermolecular distances. As the molecules are large (a few nanometers) in comparison with intermolecular distances between neighboring centers of masses, the attraction cannot be modeled by simple forms of van der Waals attractions between centers of masses. The attraction, which is the consequence of the interactions between induced dipoles in different bonds within the

molecules, depends significantly on the distances between parts of different molecules, which can generally be much larger or much smaller than the distances between molecular centers of masses. Therefore the molecular shape has an important role in the formation of the nanostructures present in antiferroelectric liquid crystals. As close packing competes, on the other hand, with steric or excluded volume interactions and the electrostatic interactions because molecules have a significant dipole moment, the final structure is formed due to the delicate balance between the interactions and entropic tendency. These complex interactions are responsible for the fact that antiferroelectric materials are rarer than ferroelectric ones.

Although the present understanding of these systems is approaching maturity, many phenomena are still not well understood. Therefore an overview of the experimental results and the problems they cause for understanding of structures and properties can provide ideas for the solution of future problems studied in these systems. Even more useful, the polar properties can be created in other systems where molecules or parts of molecules also have a complicated enough structure to allow the construction of a polar vector associated with the orientation of certain molecular properties. One example is application of the knowledge acquired in the modeling of antiferroelectric liquid crystals to explanation of DNA structure. The shape of the parts of DNA molecules can be described by the direction of the dyadic axis, which has all the properties of polarization except the significant electrostatic polarization associated with the zigzag shape in tilted chiral smectics. Because parts of the molecule are also chiral, they exhibit the range of phenomena typical for antiferroelectric liquid crystals (Lorman and Podgornik, 2005; Manna *et al.*, 2007). The experimental methods and theoretical reasoning can also be applied in rather similar achiral polar systems, where polar packing is granted due to the specific bananalike molecular shape (Roy and Madhusudana, 1997; Čepič *et al.*, 1999; Nishida *et al.*, 2006; Niigawa *et al.*, 2007).

This paper gives an overview of the indications that later led to the discovery of antiferroelectric liquid crystals. The methods of identification developed at that time are still crucial for the recognition of phases today. The five different tilted phases discussed in this paper range from the ferroelectric SmC^* phase to the antiferroelectric SmC^*_A phase with the basic repeating unit extending over two layers, and three rather complex phases which have longer basic repeating units. Two of them, which develop directly above the antiferroelectric SmC^*_A phase, the three-layered SmC^*_{FI1} phase and the four-layered SmC^*_{FI2} phase, have distinct ferrielectric and antiferroelectric properties. The SmC^*_α phase, which develops in the temperature region directly below the SmA phase where the tilt is still small, is helically modulated with a very short pitch extending over a few smectic layers only. Thorough experimental studies accompanied by theoretical modeling led to the consistent model of the system that is accepted nowadays.

A number of details are still open questions worthy of study. We quote a few of them which are more or less related to our work. Some experimental observations still await explanation. The softening of the polar mode in an external electric field in the antiferroelectric SmC^*_A phase (Dzik *et al.*, 2005) is an interesting question. The behavior of structures with more layers in the basic repeating unit in external fields, such as an electric field or the influence of surfaces, is also an interesting problem. The predicted devil's and harmless staircase behaviors of the SmC^*_α phase (Rovšek *et al.*, 2004) are also a difficult experimental problem. A detailed study of the polarization in the layer due to the combination of the flexoelectric and piezoelectric effects (Čepič *et al.*, 2002) and the consequent nonperpendicularity of the tilt and polarization within the layer in more complex structures is still lacking. Although the phase diagram is theoretically quite well understood, the dependence of the general phase diagram on interlayer interactions was only partially reproduced (Vaupotič and Čepič, 2005). The influence of the quadrupolar coupling probably significantly influences the formation of the devil's staircase in an external electric field. Another interesting question concerns the effects of chirality. Does chirality affect only polarization and interlayer chiral interactions or does it also affect other properties such as the flexoelectric interaction or even intermolecular interactions within the layer? How do the positions of chiral groups affect intermolecular interactions in general (Dierking, 2005)?

The potential of antiferroelectric liquid crystals for application is probably not sufficiently appreciated nowadays. As technology has solved a number of problems in the construction and efficiency of displays working on the basis of nematic liquid crystals (Kim and Song, 2009), development of the displays using new and more complex materials is not of such importance at the moment. However, complex structures found in antiferroelectric liquid crystals offer multiple memory states, fast responses, and interesting optical properties that can also be useful in the future in different applications we are not able to imagine at present.

Last, complex antiferroelectric liquid crystalline systems provide an area where scholars can learn various experimental methods, phenomenological modeling based on description of various types of order; they can study the influence of anisotropic and chiral properties and the combination of them both. Studies of behavior in restricted geometries such as Langmuir-Blodget or free-standing films can provide an understanding of the crossover behavior from two- to three-dimensional systems. The experiences gained can be efficiently used in a number of studies in soft matter such as biological systems. The understanding of effects of competing mechanisms can be used almost everywhere.

GLOSSARY

SmA The nontilted or orthogonal smectic phase. This describes its basic property that the elongated molecules are oriented perpendicular to the layer and parallel to the layer

normal; the molecules are not tilted. This phase is the highest temperature smectic phase in the liquid crystalline phase sequence.

SmC* The usual ferroelectric synclinically tilted phase. The structure is helicoidally modulated and the pitch extends over 100 and more layers. Due to the polarization in the layers the structure is susceptible to an external electric field. Originally, the structure was named SmC^*_β as it appeared below the SmC^*_α phase.

SmC^*_α Phase in which the elongated molecules are tilted and the layers are polar. The structure is helicoidally modulated but the period of modulation is short and can extend from a few layers up to a few tenths of layers. The phase always appears directly below the nontilted SmA phase.

SmC^*_A The antiferroelectric anticlinically tilted phase. Due to the opposite tilts in neighboring layers, the polarizations have opposite directions in neighboring layers as well. The polarizations cancel out over two layers and the system behaves antiferroelectrically. The structure is helically modulated, forming a double helix, which extends over 100 and more layers. The phase usually appears as the lowest temperature phase in the phase sequence of the SmC*-type phases.

SmC^*_{FI1} Structure with a three-layer periodicity. The tilt directions in neighboring layers form alternatively two different angles α and β, and $2\alpha+\beta\approx 2\pi$. The polarizations do not cancel out over three layers and the structure behaves ferrielectrically. Deviation from the three-layer basic periodicity results in a long helicoidal modulation extending over a few hundred layers. When discovered, the structure was named SmC^*_γ as it appeared below the SmC^*_β phase.

SmC^*_{FI2} The structure with a four-layer periodicity. The tilt directions in neighboring layers form two different angles α and β, and $2\alpha+2\beta \approx 2\pi$. Because the polarizations cancel out over four layers the structure is antiferroelectric, although the subscript FI2 recalls the historical consideration of the phase as ferrielectric. Deviation from the four-layer basic periodicity results in a long helicoidal modulation extending over a few hundred layer. In some papers the phase is called SmC^*_{AF} as it is antiferroelectric.

ACKNOWLEDGMENTS

The authors acknowledge Damian Pociecha and Nataša Vaupotič for many stimulating discussions and careful reading of the paper. The financial support of Slovenian Ministry of Higher Education, Science, and Technology to research Program No. P1-0055 is acknowledged.

REFERENCES

Akizuki, T., K. Miyachi, Y. Takanishi, K. Ishikawa, H. Takezoe, and A. Fukuda, 1999, Jpn. J. Appl. Phys., Part 1 **38**, 4832.
Allen, M. P., and A. J. Masters, 2001, J. Mater. Chem. **11**, 2678.
Andreeva, P. O., V. K. Dolganov, C. Gors, R. Fouret, and E. I. Kats, 1999, Phys. Rev. E **59**, 4143.
Bahatt, N., S. Zhang, S. Keast, M. Neubert, and C. Rosenblatt, 2001, Phys. Rev. E **63**, 062703.
Bahr, C., and D. Fliegner, 1993a, Phys. Rev. Lett. **70**, 1842.
Bahr, C., and D. Fliegner, 1993b, Ferroelectrics **147**, 1.
Bahr, C., D. Fliegner, C. Booth, and J. Goodby, 1994, Europhys. Lett. **26**, 539.
Bahr, C., D. Fliegner, C. J. Booth, and J. W. Goodby, 1995, Phys. Rev. E **51**, R3823.
Bailey, C., and A. Jákli, 2007, Phys. Rev. Lett. **99**, 207801.
Benguigui, L., and A. E. Jacobs, 1994, Phys. Rev. E **49**, 4221.
Bock, H., and W. Helfrich, 1995, Liq. Cryst. **18**, 707.
Bourny, V., A. Fajar, and H. Orihara, 2000, Phys. Rev. E **62**, R5903.
Brimicombe, P., N. Roberts, S. Jaradat, C. Southern, S. Wang, C. Huang, E. DiMasi, R. Pindak, and H. Gleeson, 2007, Eur. Phys. J. E **23**, 281.
Bruinsma, R., and J. Prost, 1994, J. Phys. II **4**, 1209.
Brunet, M., and C. Williams, 1978, Ann. Phys. **3**, 137.
Cady, A., D. A. Olson, X. F. Han, H. T. Nguyen, and C. C. Huang, 2002, Phys. Rev. E **65**, 030701(R).
Cady, A., *et al.*, 2001, Phys. Rev. E **64**, 050702(R).
Care, C. M., and D. J. Cleaver, 2005, Rep. Prog. Phys. **68**, 2665.
Čepič, M., E. Gorecka, D. Pociecha, B. Žekš, and H. T. Nguyen, 2002, J. Chem. Phys. **117**, 1817.
Čepič, M., and B. Žekš, 1995, Mol. Cryst. Liq. Cryst. **263**, 61.
Čepič, M., and B. Žekš, 1996, Liq. Cryst. **20**, 29.
Čepič, M., and B. Žekš, 1997, Mol. Cryst. Liq. Cryst. **301**, 221.
Čepič, M., and B. Žekš, 2001, Phys. Rev. Lett. **87**, 085501.
Čepič, M., and B. Žekš, 2007, Ferroelectrics **349**, 21.
Čepič, M., B. Žekš, and J. Mavri, 1999, Mol. Cryst. Liq. Cryst. **328**, 47.
Chaikin, P. M., and T. Lubensky, 1995, *Principles of Condensed Matter Physics* (Cambridge University Press, Cambridge).
Chandani, A. D. L., E. Gorecka, Y. Ouchi, H. Takezoe, and A. Fukuda, 1989, Jpn. J. Appl. Phys., Part 2 **28**, L1265.
Chandani, A. D. L., T. Hagiwara, Y. Suzuki, Y. Ouchi, H. Takezoe, and A. Fukuda, 1988, Jpn. J. Appl. Phys., Part 2 **27**, L729.
Chandani, A. D. L., Y. Ouchi, H. Takezoe, A. Fukuda, K. Terashima, K. Furukawa, and A. Kishi, 1989, Jpn. J. Appl. Phys., Part 2 **28**, L1261.
Chandani, A. D. L., N. M. Shtykov, V. P. Panov, A. V. Emelyanenko, A. Fukuda, and J. K. Vij, 2005, Phys. Rev. E **72**, 041705.
Chandrasekhar, S., 1977, *Liquid Crystals* (Cambridge University Press, Cambridge).
Cheung, D. L., S. J. Clark, and M. R. Wilson, 2004, J. Chem. Phys. **121**, 9131.
Cladis, P., and H. R. Brand, 1993, Liq. Cryst. **14**, 1327.
Clark, N. A., and S. T. Lagerwall, 1980, Appl. Phys. Lett. **36**, 899.

Conradi, M., M. Čepič, M. Čopič, and I. Muševič, 2004, Phys. Rev. Lett. **93**, 227802.
Conradi, M., M. Čepič, M. Čopič, and I. Muševič, 2005, Phys. Rev. E **72**, 051711.
Dabrowski, R., 2000, Ferroelectrics **243**, 1.
de Gennes, P. G., and J. Prost, 1993, *The Physics of Liquid Crystals* (Clarendon, Oxford).
de Vries, H., 1951, Acta Crystallogr. **4**, 219.
D'Have, K., A. Dahlgren, P. Rudquist, J. Lagerwall, G. Andersson, M. Matuszczyk, S. T. Lagerwall, R. Dabrowski, and W. Drzewinski, 2000, Ferroelectrics **244**, 115.
D'Have, K., P. Rudquist, S. T. Lagerwall, H. Pauwels, W. Drzewinski, and R. Dabrowski, 2000, Appl. Phys. Lett. **76**, 3528.
Dierking, I., 2005, J. Phys.: Condens. Matter **17**, 4403.
Dmitrienko, V. E., 1983, Acta Crystallogr., Sect. A: Found. Crystallogr. **39**, 29.
Dolganov, P. V., and V. M. Zhilin, 2008, Phys. Rev. E **77**, 031703.
Dolganov, P. V., V. M. Zhilin, V. E. Dmitrienko, and E. I. Kats, 2002, JETP **76**, 498.
Dolganov, P. V., V. M. Zhilin, V. K. Dolganov, and E. I. Kats, 2008, JETP **87**, 253.
Douali, R., C. Legrand, V. Laux, N. Isaert, G. Joly, and H. T. Nguyen, 2004, Phys. Rev. E **69**, 031709.
Drzewinski, W., K. Czuprynski, R. Dabrowski, and M. Neubert, 1999, Liq. Cryst. **328**, 401.
Dzik, E., J. Mieczkowski, E. Gorecka, and D. Pociecha, 2005, J. Mater. Chem. **12**, 1255.
Ema, K., M. Kanai, H. Yao, Y. Takanishi, and H. Takezoe, 2000, Phys. Rev. E **61**, 1585.
Emelyanenko, A. V., A. Fukuda, and J. K. Vij, 2006, Phys. Rev. E **74**, 011705.
Emelyanenko, A. V., and M. A. Osipov, 2003, Phys. Rev. E **68**, 051703.
Emelyanenko, A. V., and M. A. Osipov, 2004, Phys. Rev. E **70**, 021704.
Fajar, A., H. Murai, and H. Orihara, 2002, Phys. Rev. E **65**, 041704.
Fera, A., R. Opitz, W. H. D. Jeu, B. I. Ostrovskii, D. Schlauf, and C. Bahr, 2001, Phys. Rev. E **64**, 021702.
Fernandes, P., P. Barois, E. Grelet, F. Nallet, J. W. Goodby, M. Hird, and J. S. Micha, 2006, Eur. Phys. J. E **20**, 81.
Fukuda, A., Y. Takanishi, T. Isozaki, K. Ishikawa, and H. Takezoe, 1994, J. Mater. Chem. **4**, 997.
Fukui, M., H. Orihara, A. Suzuki, Y. Ishibashi, Y. Yamada, N. Yamamoto, K. Mori, K. Nakamura, Y. Suzuki, and I. Kawamura, 1990, Jpn. J. Appl. Phys., Part 2 **29**, L329.
Fukui, M., H. Orihara, Y. Yamada, N. Yamamoto, and Y. Ishibashi, 1989, Jpn. J. Appl. Phys., Part 2 **28**, L849.
Furukawa, K., K. Terashima, M. Ichihashi, S. Saitoh, K. Miyazawa, and T. Inukai, 1988, Ferroelectrics **85**, 451.
Galerne, Y., and L. Liebert, 1989, in Abstract Book of Second International Conference Ferroelectric Liquid Crystals, edited by K. Kawarabayashi and A. Ukawa (unpublished), p. O27.
Galerne, Y., and L. Liebert, 1990, Phys. Rev. Lett. **64**, 906.
Gay, J. G., and B. J. Berne, 1981, J. Chem. Phys. **74**, 3316.
Gleeson, H., and L. S. Hirst, 2006, ChemPhysChem **7**, 321.
Glogarova, M., L. Lejček, J. Pavel, U. Janovec, and F. Fousek, 1983, Mol. Cryst. Liq. Cryst. **91**, 309.
Goodby, J., and E. Chin, 1988, Liq. Cryst. **3**, 1245.
Goodby, J. W., J. S. Patel, and E. Chin, 1992, J. Mater. Chem. **2**, 197.
Gorecka, E., A. D. L. Chandani, Y. Ouchi, H. Takezoe, and A. Fukuda, 1990, Jpn. J. Appl. Phys., Part 1 **29**, 131.
Gorecka, E., D. Pociecha, M. Čepič, B. Žekš, and R. Dabrowski, 2002, Phys. Rev. E **65**, 061703.
Gorecka, E., D. Pociecha, J. Mieczkowski, J. Matraszek, D. Guillon and B. Donnio, 2004, J. Am. Chem. Soc. **126**, 15946.
Gorecka, E., D. Pociecha, N. Vaupotič, M. Čepič, K. Gomola, and J. Mieckowski, 2008, J. Mater. Chem. **18**, 3044.
Hamaneh, M. B., and P. L. Taylor, 2004, Phys. Rev. Lett. **93**, 167801.
Hamaneh, M. B., and P. L. Taylor, 2005, Phys. Rev. E **72**, 021706.
Hamaneh, M. B., and P. L. Taylor, 2007, Phys. Rev. E **75**, 011703.
Hamplova, V., A. Bubnov, M. Kašpar, V. Novotna, D. Pociecha, and M. Glogarova, 2003, Liq. Cryst. **30**, 627.
Harris, W. F., 1970, Philos. Mag. **22**, 949.
Heppke, G., P. Kleineberg, D. Loetzsch, S. Mery, and R. Shashidhar, 1993, Mol. Cryst. Liq. Cryst. **231**, 257.
Hiji, N., A. D. L. Chandani, S. Nishiyama, Y. Ouchi, H. Takezoe, and A. Fukuda, 1988, Ferroelectrics **85**, 99.
Hiraoka, K., A. D. L. Chandani, E. Gorecka, Y. Ouchi, H. Takezoe, and A. Fukuda, 1990, Jpn. J. Appl. Phys., Part 2 **29**, L1473.
Hiraoka, K., A. Taguchi, Y. Ouchi, H. Takezoe, and A. Fukuda, 1990, Jpn. J. Appl. Phys., Part 2 **29**, L103.
Hiraoka, K., Y. Takanishi, K. Skarp, H. Takezoe, and A. Fukuda, 1991, Jpn. J. Appl. Phys., Part 2 **30**, L1819.
Hiraoka, K., Y. Takanishi, H. Takezoe, A. Fukuda, T. Isozaki, Y. Suzuki, and I. Kawamura, 1992, Jpn. J. Appl. Phys., Part 1 **31**, 3394.
Hirst, L. S., *et al.*, 2002, Phys. Rev. E **65**, 041705.
Hori, K., 1983, Mol. Cryst. Liq. Cryst. **100**, 75.
Hou, J., J. Schacht, F. Giesselman, and P. Zugenmaier, 1997, Liq. Cryst. **22**, 401.
Inui, S., N. Iimura, T. Suzuki, H. Iwane, K. Miyachi, Y. Takanishi, and A. Fukuda, 1996, J. Mater. Chem. **6**, 71.
Inukai, T., K. Furukawa, K. Terashima, S. Saito, M. Isogai, T. Kitamura, and A. Mukoh, 1985, in Abstract Book of Japan Domestic Liquid Crystal Meeting, Kanazawa, edited by K. Kawarabayashi and A. Ukawa (unpublished), p. 172 (in Japanese).
Isozaki, T., T. Fujikawa, H. Takezoe, A. Fukuda, T. Hagiwara, Y. Suzuki, and I. Kawamura, 1992, Jpn. J. Appl. Phys., Part 2 **31**, L1435.
Isozaki, T., K. Hiraoka, Y. Takanishi, H. Takezoe, A. Fukuda, Y. Suzuki, and I. Kawamura, 1992, Liq. Cryst. **12**, 59.
Itoh, K., M. Johno, Y. Takanishi, Y. Ouchi, H. Takezoe, and A. Fukuda, 1991, Jpn. J. Appl. Phys., Part 1 **30**, 735.
Itoh, K., Y. Takanishi, J. Yokoyama, K. Ishikawa, H. Takezoe, and A. Fukuda, 1997, Jpn. J. Appl. Phys., Part 2 **36**, L784.
Jakli, A., 1999, J. Appl. Phys. **85**, 1101.
Jákli, A., D. Krüerke, H. Sawade, and G. Heppke, 2001, Phys. Rev. Lett. **86**, 5715.
Jaradat, S., P. Brimicombe, C. Southern, S. Siemianowski, E. DiMasi, M. Osipov, R. Pindak, and H. F. Gleeson, 2008, Phys. Rev. E **77**, 010701.
Johno, M., K. Itoh, J. Lee, Y. Ouchi, H. Takezoe, A. Fukuda, and T. Kitazume, 1990, Jpn. J. Appl. Phys., Part 2 **29**, L107.
Johnson, P. M., D. A. Olson, S. Pankratz, T. Nguyen, J. Goodby, M. Hird, and C. C. Huang, 2000, Phys. Rev. Lett. **84**, 4870.
Johnson, P. M., S. Pankratz, P. Mach, H. T. Nguyen, and C. C.

Huang, 1999, Phys. Rev. Lett. **83**, 4073.
Kajita, J., T. Moriyama, Y. Takanishi, K. Ishikawa, H. Takezoe, and A. Fukuda, 1993, Ferroelectrics **149**, 237.
Kašpar, M., V. Hamplova, V. Novotna, M. Glogarova, and D. Pociecha, 2001, Liq. Cryst. **28**, 1203.
Kelker, H., 1988, Mol. Cryst. Liq. Cryst. **165**, 1.
Kim, K. H., and J. K. Song, 2009, NPG Asia Mater. **1**, 29.
Kittel, C., 1951, Phys. Rev. **82**, 729.
Kishikawa, K., S. Nakahara, Y. Nishikawa, S. Kohmoto, and M. Yamamoto, 2005, J. Mater. Chem. **127**, 2565.
Koike, M., Y. Chu-Chen, Y. Liu, H. Tsuchiya, M. Tokita, S. Kawauchi, H. Takezoe, and J. Watanabe, 2007, Macromolecules **40**, 2524.
Konovalov, D., H. T. Nguyen, M. Čopič, and S. Sprunt, 2001, Phys. Rev. E **64**, 010704.
Kutnjak-Urbanc, B., and B. Žekš, 1995, Phys. Rev. E **51**, 1569.
Lagerwall, J. P. E., F. Gisselman, and M. Osipov, 2006, Liq. Cryst. **33**, 625.
Lagerwall, J. P. F., 2005, Phys. Rev. E **71**, 051703.
Laux, V., N. Isaert, V. Faye, and H. T. Nguyen, 2000, Liq. Cryst. **27**, 81.
Laux, V., N. Isaert, G. Joly, and H. T. Nguyen, 1999, Liq. Cryst. **26**, 361.
Laux, V., N. Isaert, H. T. Nguyen, P. Cluseau, and C. Destrade, 1996, Ferroelectrics **179**, 25.
Lee, J., A. D. L. Chandani, K. Itoh, Y. Ouchi, H. Takezoe, and A. Fukuda, 1990, Jpn. J. Appl. Phys., Part 1 **29**, 1122.
Lee, J., Y. Ouchi, H. Takezoe, A. Fukuda, and J. Watanabe, 1990, J. Phys.: Condens. Matter **2**, SA271.
Levelut, A. M., C. Germain, P. Keller, L. Liebert, and J. Billard, 1983, J. Phys. (France) **44**, 623.
Levelut, A. M., and B. Pansu, 1999, Phys. Rev. E **60**, 6803.
Li, J., H. Takezoe, and A. Fukuda, 1991, Jpn. J. Appl. Phys., Part 1 **30**, 532.
Li, J., X. Wang, E. Kangas, P. Taylor, C. Rosenblatt, Y. Suzuki, and P. Cladis, 1995, Phys. Rev. B **52**, R13075.
Li, J. F., E. A. Shack, Y. K. Yu, X. Y. Wang, C. Rosenblatt, M. E. Neubert, S. S. Keats, and H. Gleeson, 1996, Jpn. J. Appl. Phys., Part 2 **35**, L1608.
Link, D. R., J. E. Maclennan, and N. A. Clark, 1996, Phys. Rev. Lett. **77**, 2237.
Link, D. R., J. E. Maclennan, and N. A. Clark, 2001, Phys. Rev. Lett. **86**, 4975.
Liu, Z. Q., B. K. McCoy, S. T. Wang, R. Pindak, W. Caliebe, P. Barios, P. Fernandes, H. T. Nguyen, C. S. Hsu, S. Wang, and C. C. Huang, 2007, Phys. Rev. Lett. **99**, 077802.
Liu, Z. Q., S. T. Wang, B. K. McCoy, A. Cady, R. Pindak, W. Caliebe, K. Takekoshi, K. Ema, H. T. Nguyen, and C. C. Huang, 2006, Phys. Rev. E **74**, 030702.
Lorman, V., and R. Podgornik, 2005, Europhys. Lett. **69**, 1017.
Lorman, V. L., A. A. Bulbitch, and P. Toledano, 1994, Phys. Rev. E **49**, 1367.
Mach, P., R. Pindak, A. M. Levelut, P. Barois, H. T. Nguyen, H. Baltes, M. Hird, K. Toyne, A. Seeda, J. W. Goodby, C. C. Huang, and L. Furenlid, 1999, Phys. Rev. E **60**, 6793.
Mach, P., R. Pindak, A. M. Levelut, P. Barois, H. T. Nguyen, C. C. Huang, and L. Furenlid, 1998, Phys. Rev. Lett. **81**, 1015.
Maiti, P. K., Y. Lansac, M. A. Glaser, and N. A. Clark, 2004, Phys. Rev. Lett. **92**, 025501.
Manna, F., V. Lorman, R. Podgornik, and B. Žekš, 2007, Phys. Rev. E **75**, 030901(R).
Matkin, L. S., S. J. Watson, H. F. Gleeson, R. Pindak, J. Pitney, P. M. Johnson, C. C. Huang, A. M. L. P. Barois, G. Srajer, J. Pollmann, J. W. Goodby, and M. Hird, 2001, Phys. Rev. E **64**, 021705.
Matsumoto, T., A. Fukuda, M. Johno, Y. Motoyama, T. Yui, S.-S. Seomun, and M. Yamashita, 1999, J. Mater. Chem. **9**, 2051.
McCoy, B., Z. Liu, S. Wang, L. Pan, S. Wang, H. Nguyen, R. Pindak, and C. Huang, 2008, Phys. Rev. E **77**, 061704.
Merino, S., M. R. de la Fuente, Y. Gonzlez, M. A. P. Jubindo, B. Ros, and J. A. Purtolas, 1996, Phys. Rev. E **54**, 5169.
Meyer, R., 1977, Mol. Cryst. Liq. Cryst. **40**, 33.
Meyer, R. B., L. Libert, L. Strzelecki, and P. Keller, 1975, J. Phys. (France) **36**, L69.
Miyachi, K., M. Kabe, K. Ishikawa, H. Takezoe, and A. Fukuda, 1994, Ferroelectrics **147**, 147.
Moriyama, T., J. Kajita, Y. Takanishi, K. Ishikawa, H. Takezoe, and A. Fukuda, 1993, Jpn. J. Appl. Phys., Part 2 **32**, L589.
Muševič, I., and M. Škarabot, 2001, Phys. Rev. E **64**, 051706.
Muševič, I., B. Žekš, M. Čopič, M. Wittebrood, T. Rasing, H. Orihara, and Y. Ishibashi, 1993, Phys. Rev. Lett. **71**, 1180.
Nakayama, K., H. Moritake, M. Ozaki, and K. Yoshino, 1995, Jpn. J. Appl. Phys., Part 2 **34**, L1599.
Neal, M. P., A. J. Parker, and C. M. Care, 1997, Mol. Phys. **91**, 603.
Nguyen, H. T., J. V. Rouillon, P. Cluzeau, G. Sigaud, C. Destrade, and N. Isaert, 1994, Liq. Cryst. **17**, 571.
Niigawa, Y., K. Nishida, W. J. Kim, S. K. Lee, S. Heo, J. G. Lee, F. Araoka, Y. Takanishi, K. Ishikawa, K.-T. Kang, M. Čepič, and H. Takezoe, 2007, Phys. Rev. E **76**, 031702.
Niori, T., T. Sekine, J. Watanabe, T. Furukawa, and H. Takezoe, 1996, J. Mater. Chem. **6**, 1231.
Nishida, K., M. Čepič, W. J. Kim, S. K. Lee, S. Heo, J. G. Lee, Y. Takanishi, K. Ishikawa, K.-T. Kang, J. Watanabe, and H. Takezoe, 2006, Phys. Rev. E **74**, 021704.
Okabe, N., Y. Suzuki, I. Kawamura, T. Isozaki, H. Takezoe, and A. Fukuda, 1992, Jpn. J. Appl. Phys., Part 2 **31**, L793.
Olson, D. A., X. F. Han, A. Cady, and C. C. Huang, 2002, Phys. Rev. E **66**, 021702.
Orihara, H., and Y. Ishibashi, 1990, Jpn. J. Appl. Phys., Part 2 **29**, L115.
Osipov, M. A., and A. Fukuda, 2000, Phys. Rev. E **62**, 3724.
Ouchi, Y., T. Shingu, H. Takezoe, A. Fukuda, E. Kuze, M. Koga, and N. Goto, 1984, Jpn. J. Appl. Phys., Part 2 **23**, L660.
Ozaki, M., H. Moritake, K. Nakayama, and K. Yoshino, 1994, Jpn. J. Appl. Phys., Part 2 **33**, L1620.
Panarin, Y., O. Kalinovskaya, and J. Vij, 1998, Liq. Cryst. **25**, 241.
Panarin, Y. P., O. Kalinovskaya, J. K. Vij, and J. W. Goodby, 1997, Phys. Rev. E **55**, 4345.
Panov, V., J. K. Vij, Yu. P. Panarin, C. Blanc, and V. Lorman, 2007, Phys. Rev. E **75**, 042701.
Park, B., S.-S. Seomun, M. Nakata, M. Takahashi, Y. Takanishi, K. Ishikawa, and H. Takezoe, 1999, Jpn. J. Appl. Phys., Part 1 **38**, 1474.
Parry-Jones, L. A., and S. J. Elston, 2001, Phys. Rev. E **63**, 050701.
Parry-Jones, L. A., and S. J. Elston, 2002, J. Appl. Phys. **92**, 449.
Philip, J., J. R. Lalanne, J. P. Marcerou, and G. Sigaud, 1995, Phys. Rev. E **52**, 1846.
Pikin, S. A., and V. L. Indebom, 1978, Usp. Fiziol. Nauk **21**, 487.
Pociecha, D., M. Čepič, E. Gorecka, and J. Mieczkowski, 2003, Phys. Rev. Lett. **91**, 185501.

Pociecha, D., E. Gorecka, M. Čepič, N. Vaupotič, and W. Weissflog, 2006, Phys. Rev. E **74**, 021702.
Pociecha, D., E. Gorecka, M. Čepič, N. Vaupotič, B. Žekš, D. Kardas, and J. Mieczkowski, 2001, Phys. Rev. Lett. **86**, 3048.
Robinson, W. K., C. Carboni, P. S. Kloess, W. P. Perkins, and H. J. Coles, 1998, Liq. Cryst. **25**, 301.
Robinson, W. K., P. S. Kloess, C. Carboni, and H. J. Coles, 1997, Liq. Cryst. **23**, 309.
Rovšek, B., M. Čepič, and B. Žekš, 1996, Phys. Rev. E **54**, R3113.
Rovšek, B., M. Čepič, and B. Žekš, 2000, Phys. Rev. E **62**, 3758.
Rovšek, B., M. Čepič, and B. Žekš, 2004, Phys. Rev. E **70**, 041706.
Roy, A., and N. V. Madhusudana, 1996, Europhys. Lett. **36**, 221.
Roy, A., and N. V. Madhusudana, 1997, Europhys. Lett. **39**, 021704.
Rudquist, P., *et al.*, 1999, J. Mater. Chem. **9**, 1257.
Sako, T., Y. Kimura, R. Hayakawa, N. Okabe, and Y. Suzuki, 1996, Jpn. J. Appl. Phys., Part 2 **35**, L114.
Sandhya, K. L., J. K. Song, Yu. P. Panarin, J. K. Vij, and S. Kumar, 2008, Phys. Rev. E **77**, 051707.
Scherowsky, G., and X. H. Chen, 1994, Liq. Cryst. **17**, 803.
Schlauf, D., C. Bahr, and H. T. Nguyen, 1999, Phys. Rev. E **60**, 6816.
Shtykov, N. M., J. K. Vij, and H. T. Nguyen, 2001, Phys. Rev. E **63**, 051708.
Škarabot, M., R. Blinc, I. Muševič, A. Rastegar, and T. Rasing, 2000, Phys. Rev. E **61**, 3961.
Škarabot, M., M. Čepič, B. Žekš, R. Blinc, G. Heppke, A. V. Kityk, and I. Muševič, 1998, Phys. Rev. E **58**, 575.
Song, J.-K., A. Fukuda, and J. K. Vij, 2008, Phys. Rev. E **78**, 041702.
Strauss, J., and H.-S. Kitzerow, 1996, Appl. Phys. Lett. **69**, 725.
Sun, H., H. Orihara, and Y. Ishibashi, 1993, J. Phys. Soc. Jpn. **62**, 2706.
Takanishi, Y., K. Hiraoka, V. K. Agrawal, H. Takezoe, A. Fukuda, and M. Matsushita, 1991, Jpn. J. Appl. Phys., Part 1 **30**, 2023.
Takanishi, Y., H. Takezoe, A. Fukuda, H. Komura, and J. Watanabe, 1992, J. Mater. Chem. **2**, 71.
Takanishi, Y., H. Takezoe, A. Fukuda, and J. Watanabe, 1992, Phys. Rev. B **45**, 7684.
Takanishi, Y., H. Takezoe, M. Johno, T. Yui, and A. Fukuda, 1993, Jpn. J. Appl. Phys., Part 1 **32**, 4605.
Takezoe, H., A. D. L. Chandani, E. Gorecka, Y. Ouchi, and A. Fukuda, 1989, in Abstract Book of Second International Conference Ferroelectric Liquid Crystal, edited by K. Kawarabayashi and A. Ukawa (unpublished), p. P108.
Takezoe, H., A. D. L. Chandani, J. Lee, E. Gorecka, Y. Ouchi, A. Fukuda, K. Terashima, K. Furukawa, and A. Kishi, 1989, in Abstract Book of Second International Conference Ferroelectric Liquid Crystal, edited by K. Kawarabayashi and A. Ukawa (unpublished), p. O26.
Takezoe, H., K. Kishikawa, and E. Gorecka, 2006, J. Mater. Chem. **16**, 2412.
Takezoe, H., J. Lee, A. D. L. Chandani, E. Gorecka, Y. Ouchi, and A. Fukuda, 1991, Ferroelectrics **114**, 187.
Takezoe, H., J. Lee, Y. Ouchi, and A. Fukuda, 1991, Mol. Cryst. Liq. Cryst. **202**, 85.
Tanaka, S., and M. Yamashita, 2000, Ferroelectrics **245**, 209.
Terentjev, E. M., M. A. Osipov, and T. J. Sluckin, 1994, J. Phys. A **27**, 7047.
Vaupotič, N., and M. Čepič, 2005, Phys. Rev. E **71**, 041701.
Wang, S., L. Pan, B. K. McCoy, S. T. Wang, R. Pindak, H. T. Nguyen, and C. C. Huang, 2009, Phys. Rev. E **79**, 021706.
Wang, S., L. Pan, R. Pindak, Z. Q. Liu, H. T. Nguyen, and C. C. Huang, 2010, Phys. Rev. Lett. **104**, 027801.
Wang, S. T., Z. Q. Liu, B. K. McCoy, R. Pindak, W. Caliebe, H. T. Nguyen, and C. C. Huang, 2006, Phys. Rev. Lett. **96**, 097801.
Wilson, M. R., 1997, J. Chem. Phys. **107**, 8654.
Wilson, M. R., 2007, Chem. Soc. Rev. **36**, 1881.
Yamada, Y., N. Yamamoto, K. Mori, K. Nakamura, T. Hagiwara, Y. Suzuki, I. Kawamura, H. Orihara, and Y. Ishibashi, 1990, Jpn. J. Appl. Phys., Part 1 **29**, 1757.
Yamamoto, N., Y. Yamada, N. Koshobu, K. Mori, K. Nakamura, H. Orihara, Y. Ishibashi, Y. Suzuki, and I. Kawamura, 1992, Jpn. J. Appl. Phys., Part 1 **31**, 3186.
Yamashita, M., 1996, J. Phys. Soc. Jpn. **65**, 2122.
Yamashita, M., 1997, Mol. Cryst. Liq. Cryst. **303**, 153.
Yamashita, M., and S. Miyazima, 1993, Ferroelectrics **148**, 1.
Yen, C.-C., M. Tokita, B. Park, H. Takezoe, and J. Watanabe, 2006, Macromolecules **39**, 1313.
Žekš, B., 1984, Mol. Cryst. Liq. Cryst. **114**, 259.
Žekš, B., R. Blinc, and M. Čepič, 1991, Ferroelectrics **122**, 221.
Žekš, B., and M. Čepič, 1993, Liq. Cryst. **14**, 445.
Žekš, B., and M. Čepič, 1998, Proc. SPIE **3318**, 68.